CropWatch Bulletin

QUARTERLY REPORT ON GLOBAL CROP PRODUCTION

Monitoring Period: October 2015 - January 2016

February 4, 2016
Vol. 16, No. 1 (total No. 100)

Institute of Remote Sensing and Digital Earth
Chinese Academy of Sciences

February 2016

Institute of Remote Sensing and Digital Earth (RADI), Chinese Academy of Sciences
P.O. Box 9718-29, Olympic Village Science Park
West Beichen Road, Chaoyang
Beijing 100101, China

This bulletin is produced by the CropWatch research team at the Digital Agriculture Division, Institute of Remote Sensing and Digital Earth (RADI), Chinese Academy of Sciences, under the overall guidance of Professor Bingfang Wu. Contributors are Sheng Chang, René Gommes, Mingyong Li, Prashant Patil , Mrinal Singha, Shen Tan, Fuyou Tian, Qiang Xing, JiamingXu, Nana Yan, Mingzhao Yu, Hongwei Zeng, Miao Zhang, Xin Zhang, Yang Zheng, and Weiwei Zhu.

Thematic contributors (Outlook of domestic price of four major crops section): Jingxin Fang (13426277825@163.com).

Thematic contributors (the Zambezi Basin section): Sue Walker (sue.walker@agro-impact.com).

English version editing was provided by Margaux Schreurs.

Corresponding author: Professor Bingfang Wu
Institute of Remote Sensing and Digital Earth, Chinese Academy of Sciences
Fax: +8610-64858721, E-mail: cropwatch@radi.ac.cn, wubf@radi.ac.cn

CropWatch Online Resources: This bulletin along with additional resources is also available on the CropWatch Website at http://www.cropwatch.com.cn.

Contents

Note: CropWatch resources, background materials and additional data are available online at www.cropwatch.com.cn.

Table of Contents

FIGURES

TABLES

Abbreviations

5YA	Five-year average, the average for the four month period from October-January, from 2010-2011 to 2014-2015; one of the standard reference periods.
14YA	Fourteen-year average, the average for the four month period from October-January, from 2001-2002 to 2014-2015; one of the standard reference periods and typically referred to as “average.”
BIOMSS	Agroclimatic indicator for biomass production potential
BOM	Australian Bureau of Meteorology
CALF	Cropped Arable Land Fraction
CAS	Chinese Academy of Sciences
CWSU	CropWatch Spatial Units
DM	Dry matter
EC/JRC	European Commission Joint Research Centre
ENSO	El Niño Southern Oscillation
FAO	Food and Agriculture Organization of the United Nations
GAUL	Global Administrative Units Layer
GMO	Genetically Modified Organism
GVG	GPS, Video, and GIS data
ha	hectare
kcal	kilocalorie
MPZ	Major Production Zone
MRU	Monitoring and Reporting Unit
NDVI	Normalized Difference Vegetation Index
OCHA	UN Office for the Coordination of Humanitarian Affairs
PAR	Photosynthetically active radiation
RADI	CAS Institute of Remote Sensing and Digital Earth
RADPAR	PAR agroclimatic indicator
RAIN	Rainfall agroclimatic indicator
SOI	Southern Oscillation Index
TEMP	Air temperature agroclimatic indicator
Ton	Thousand kilograms
VCIx	Maximum Vegetation Condition Index
VHI	Vegetation Health Index
VHIn	Minimum Vegetation Health Index
W/m^2	Watt per square meter

Bulletin overview and reporting period

This CropWatch bulletin presents a global overview of crop stage and condition between 1 October 2015 and 10 January 2016 (from hereon referred to as October-January). It is the 100th bulletin produced by the CropWatch group at the Institute of Remote Sensing and Digital Earth (RADI) at the Chinese Academy of Sciences, Beijing. CropWatch analyses are based mostly on several standard and new ground-based and remote sensing indicators, following a hierarchical approach. The analyses cover large global zones; major producing countries of maize, rice, wheat, and soybean; and detailed assessments of Chinese regions.

In parallel to the increasing spatial precision of the analyses, indicators become more focused on agriculture as the analyses zoom into smaller spatial units. CropWatch uses two sets of indicators: (i) agroclimatic indicators—RAIN, TEMP, and RADPAR, which describe weather factors; and (ii) agronomic indicators—BIOMSS, VHIn, CALF, CI, and VCIx, describing crop condition and development. The indicators RAIN, TEMP, RADPAR and BIOMSS do not directly describe the weather variables rain, temperature, radiation, or biomass, but rather they are spatial averages over agricultural areas, which are weighted according to the local crop production potential. For more details on the CropWatch indicators and spatial units used for the analysis, please see the quick reference guide in Annex C, as well as online resources and publications posted at www.cropwatch.com.cn.

Chapter	Spatial coverage	Key indicators
Chapter 1	World, using Monitoring and Reporting Units (MRU), 65 large, agro-ecologically homogeneous units covering the globe	RAIN, TEMP, RADPAR, BIOMSS
Chapter 2	Major Production Zones (MPZ), six regions that contribute most to global food production	As above, plus CALF, VCIx, and VHIn, CI
Chapter 3	30 key countries (main producers and exporters)	As above plus NDVI
Chapter 4	China	As above
Chapter 5	Special topics: Southern hemisphere production update, disaster events, an overview of agricultural and environmental issues in the Zambezi basin, and El Niño.	
Online Resources	www.cropwatch.com.cn	

Newsletter and online resources

The bulletin is released quarterly in both English and Chinese. To sign up for the mailing list, please e-mail cropwatch@radi.ac.cn or visit CropWatch online at www.cropwatch.com.cn. Visit the CropWatch Website for additional resources and background materials about methodology, country agricultural profiles, and country long-term trends.

Executive summary

The period from October 2015 to mid-January 2016 is a relatively quiet period from an agricultural point of view. In the temperate northern hemisphere summer crops have been harvested, while winter crops were planted and are mostly dormant. In some tropical and equatorial countries, including the Philippines, Thailand, Vietnam and Brazil, planting of the second maize and rice generally starts around January, while in the southern hemisphere summer crops are at advanced development stages and nearing flowering, for example maize and soybean in Argentina, Brazil and South Africa.

In the same countries, wheat harvesting was mostly completed or is about to be completed and the current CropWatch Bulletin provides a production update as well a first quantitative assessment of maize in South Africa, a region badly hit by El Niño-related drought, the most noteworthy feature of the current reporting period (sections 5.1, 5.2 on disasters and the South Africa page in section 3.2).

In Argentina, the updated CropWatch wheat output estimate stands at 10.7 million tons, 11% below the 2014-2015 production; both harvested area and yield decreased when compared to last year due to complex agroclimatic patterns. In neighboring Brazil, wheat production is up 4.5% over last year, to reach a total of 7 million tons.

For Australia, CropWatch puts the overall output at 25 million tons, 1% below last year, due to prevailing drought conditions (maximum vegetation condition index VCIx at 0.68, one of the lowest national values recorded) in spite of a CALF increase of 4%. Other countries with low VCIx values include Russia, Ukraine, Kazakhstan and India.

According to the CropWatch cropped arable land fraction indicator (CALF; see tables 2.2 and 3.1) the major food producing areas in South America, which are located in Argentina and Brazil, cultivated almost all available arable land (98%), an increase of 9% over the average of the recent five years (8% in Argentina and 14% in Brazil). In contrast, all other main producers in Asia, Europe and North America cultivated about 85% of arable land, which is about the same area (referring to the October 2015-January 2016 period) as during the previous season. In none of them does the change come close to the South American values: Russia, +4%; USA +2%; France, Germany, United Kingdom, Thailand, Vietnam, Philippines: all 0%. There are also negative values which can mostly be linked with agroclimatic conditions, including Canada, -2%; Poland, -3%; Romania -5%; Ukraine, -3%; Turkey, -3% and Pakistan, -2%.

South Africa is one of the countries most seriously hit by adverse weather conditions during the current reporting period. Due to drought, CALF of South Africa dropped 12% and VCIx reached just 0.48, the absolute record low for any country. CropWatch analyses show a considerable reduction of area cultivated under maize (-34%) in otherwise significant producer provinces (Free State, North West and Limpopo). Combined with low yields (down 16% from last year) the estimated total maize output of South Africa will be down to 7.3 million tons, a 45% reduction from last year's 13.2 million tons output. The precipitation deficit reached 44% in Lesotho, 42% in Zimbabwe and 36% in Malawi.

Abnormal weather conditions are also reported from several other, spatially coherent areas (Chapter 1 and section 3.1, Figures 1.1. to 1.4 and 3.1 to 3.4). Even if, for some of them, it is still early to evaluate impacts in terms of production, they include (1) the Horn of Africa, especially Ethiopia (See sections 3.2 and 5.2) where more than ten million people are severely food insecure due to drought; (2) many southern European and Mediterranean countries, which all grow winter crops planted at the end of the year and which recorded a drop in precipitation close to or exceeding 50% (Morocco, -74%; Portugal, -55%

and Lebanon, -54%); (3) northern South America (-56% of rainfall on average, e.g. -70% in Suriname and -62% in Guyana and several states in Brazil, such as Roraima (-78%) and Amapa (-71%); (4) south-east Asia to New-Zealand (New Zealand, -66%; Timor Leste, -57%; Tasmania, -75%); (5) the northern part of the Indian subcontinent, with an average precipitation departure of -52% affecting Bangladesh and Bhutan (-38% and -37%, respectively) as well as several Indian states (Meghalaya, -81%; Jharkhand, -80%; West Bengal, -73%).

Several of the same areas have also suffered from floods; (6) California (-37% precipitation over the reporting period), north-eastern USA and Canada with deficits ranging from -52% (Maine) to -39% (Massachusetts) and (7) Baltic states (Estonia, -41%; Latvia, -37%) as well as the adjacent Russian areas to the east: S. Petersburg (-48%), Adygeya Republic, Tverskaya and Pskovskaya Oblasts.

In China, the reporting period is the major planting time of winter crops including winter wheat and rapeseed, right after the harvest of autumn crops. Agroclimatic conditions were generally warm and wet (Figures 4.1 and 4.2) in all seven agricultural regions recorded above average rainfall, especially in the areas south of Yangtze River. VCIx (Figure 4.4) was distributed unevenly, with high values mostly in Sichuan and Central Hebei Province and low values in the North China Plain and north-west region. CALF was close to average. Assuming average agro-climatic conditions to the time of harvest, CropWatch estimates that 2015-16 winter crop output will be slightly above 2014-2015.

Based on the combination of agroclimatic and agronomic indicators, CropWatch lists the following countries as likely to under-perform in terms or production: South Africa and some neighboring countries, Ethiopia, Indonesia, Turkey and other Mediterranean countries. Output is expected to only be fair in India (due to widespread and repeated environmental shocks) and Bangladesh, Ukraine and possibly Poland and Romania, where cropped arable land decreased under water stress conditions. Both Russia and Kazakhstan recorded satisfactory precipitation but poor vegetation condition is widespread. In Brazil, the overall situation is unclear due to low rainfall in the major soybean producing state of Mato Grosso.

Chapter 1. Global agroclimatic patterns

Chapter 1 describes the CropWatch agroclimatic indicators for rainfall (RAIN), temperature (TEMP), and radiation (RADPAR), along with the agronomic indicator for potential biomass (BIOMSS) for sixty-five global Monitoring and Reporting Units (MRU). Rainfall, temperature, and radiation indicators are compared to their average value for the same period over the last fourteen years (called the "average"), while BIOMSS is compared to the indicator's average of the recent five years. Indicator values for all MRUs are included in Annex A, table A.1. For more information about the MRUs and indicators, please see Annex C and online CropWatch resources at www.cropwatch.com.cn.

As mentioned already in the November 2015 CropWatch Bulletin, the global patterns of rainfall anomalies that have been affecting the globe over the recent six months are largely conditioned by the on-going El Niño.

Large and consistent areas of anomalies are particularly clear throughout Eurasia and Africa (Figure 1.1 through 1.3). The MRU with the largest departure from average is the Western Cape in South Africa (MRU-10) where the recorded rainfall of 36 mm over the period is 68% below average, indicating a dry termination of the winter crop season in the part of South Africa that has a Mediterranean climate.

MRU-10 is part of a region that also includes MRU-09 (southern Africa), where the rainfall deficit was 23%, as well as the two Malagasy MRUs MRU-05, 'main', and MRU-06, semi-arid south-western Madagascar, where the deficit reached 10% and 29%, respectively. The area experienced slightly below average temperature (-0.1°C) but above average sunshine (+3.5%) and the deficit of biomass accumulation potential (-24%) indicates poor prospects for the on-going summer crops, especially maize, in this region (Figure 1.4 and sections 5.1 and 5.2).

North Africa-Mediterranean (MRU-07) and Mediterranean Europe and Turkey (MRU-59) are among the next most serious rainfall deficit areas with -53% and -31% departures from average, respectively. During the reporting period, both MRUs have been planting winter crops under relative water stress conditions.

Next come three areas with large rain deficits that can be described as "Punjab to Gujarat", "Southern Chinese Islands to New Zealand" and "Amazon-Patagonia". Punjab to Gujarat (MRU-48, rainfall deficit of -37%) is an isolated dry area in southern Asia, while the second spans the large area from MRU-42 (Taiwan, rainfall deficit of -34%) and MRU-33 (Hainan, rainfall deficit of -27%) via MRU-49 (maritime Southeast Asia, -24%) to MRU-53 (Northern Australia, rainfall deficit of -43%) and New Zealand (MRU-56,rainfall deficit of-65%). The area also includes East Asia (MRU-43, rainfall deficit of-29%) as well as Southern Japan and Korea (MRU-46, rainfall deficit of-13%).

The Amazon-Patagonia area is not continuous but encompasses large stretches of the Northern-central Andes (MRU-21, rainfall deficit of-21%), much of the Amazon basin (MRU-24, rainfall deficit of-32%) as well as Western Patagonia (MRU-27, rainfall deficit of-56%). This area is bordering the Pampas (rainfall surplus of +62%) and other agriculturally less important areas that, nevertheless, underwent unusually favourable conditions, such as central-North Argentina (MRU-25, rainfall surplus of +38%) and the Semi-arid Southern Cone (MRU-28, rainfall surplus of +50%).

North America was generally wet as a result of higher rainfall rates(MRU-12, Northern Great Plains, 56%; MRU-14, Cotton Belt to Mexican Nordeste, +61% and MRU-18, southwest USA and north Mexican highlands, +71%) with the exception of the west coast (MRU-16, -25%).

Conditions were close to average in Western Europe as well as northern Eurasia.

The wettest areas were part of a large portion of land that was already identified in the November 2015 CropWatch Bulletin, which encompasses many arid and semi-arid areas between West Africa and East Asia across most of Central Asia ("West Africa to East Asia wet area", WAEAWA). The largest positive rainfall departures occurred in Southern Mongolia (MRU-47, +272%) and in China (MRU-32, Gansu-Xinjiang, +139%; MRU-35, Inner Mongolia, +122% and MRU37, Lower Yangtze, +110%). They continue across Huanghuaihai (China, MRU-34), Northeast China (MRU-38), the Loess region (MRU-36), Southwest China (MRU-41), Southern China (MRU-40), the Pamir area (MRU-30, +102%), Western Asia (MRU-31, +42%), the Ural to Altai mountains (MRU-62, +41%), and eventually the Sahara to Afghan deserts (MRU-64, +50%) and the west African Sahel (MRU-08, 55%).

Figure 1.1. Global map of October 2015-January 2016 rainfall anomaly (as indicated by the RAIN indicator) by MRU, departure from 14YA (percentage)

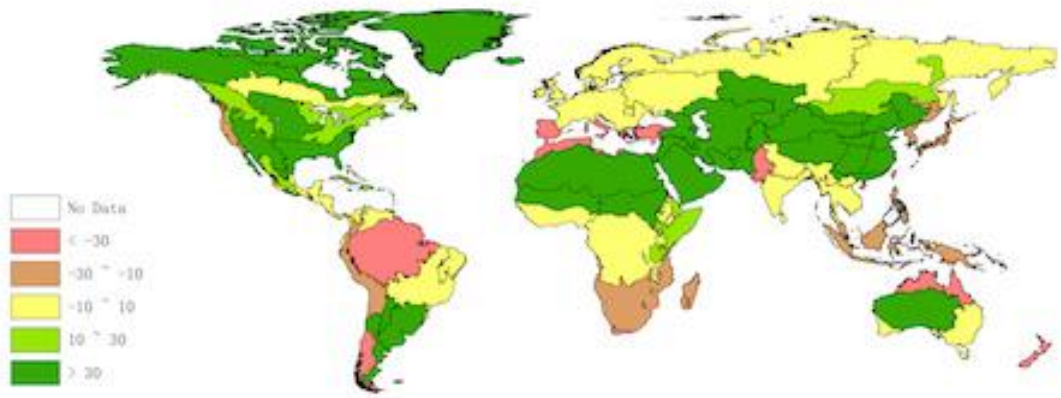

There is some consistency between the global patterns of rainfall and those of the other agroclimatic indicators, especially with regards to BIOMSS (Figure 1.4) and in particular with regard to the above-mentioned WAEAWA (Figure 1.2). The area also experienced generally low sunshine (less than 3% below average) and close to average positive temperature departures (close to +0.5°C).

Figure 1.2. Global map of October 2015-January 2016 air temperature anomaly (as indicated by the TEMP indicator) by MRU, departure from 14YA (degrees Celsius)

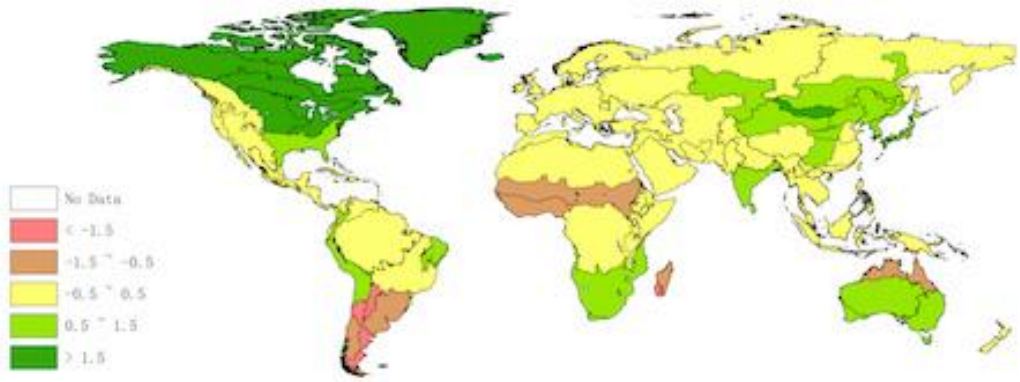

Particularly in the east, however, some areas had unusually low sunshine as shown by the RADPAR map (Figure 1.3): the Lower Yangtze (MRU-37, -22%), Southern China (MRU-40, -14%), Southwest China (MRU-41, -10%) and Huanghuaihai (MRU-34, -9%). Parallel departure patterns are recognizable in North America (Boreal America, MRU-61, -13%; Cotton Belt to Mexican Nordeste, MRU-14, -9%) and in the south of the continent (Pampas, MRU-26, -14% and Central-north Argentina, MRU-25, -11%).

Figure 1.3. Global map of October 2015-January 2016 PAR anomaly (as indicated by the RADPAR indicator) by MRU, departure from 14YA (percentage)

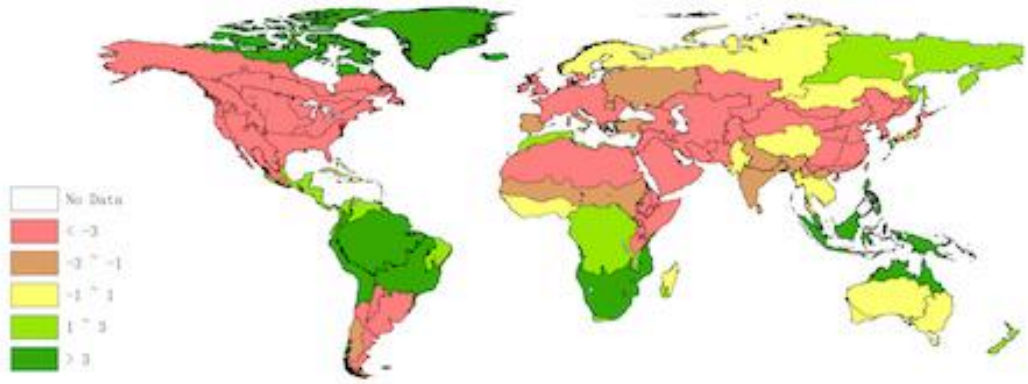

The most significant negative temperature departures occurred in precisely the same areas in South America (central-North Argentina, MRU-25, -2.0°C; Pampas, MRU-26, -1.3°C as well as the neighbouring semi-arid Southern Cone, MRU-28, -2.2°C), in Southwest Madagascar (MRU-06, -1.5°C) and in the Sahel (MRU-08, -1.0°C). Positive temperature departures were notable in areas that grow at least some winter crops (Cotton Belt to Mexican Nordeste, MRU-14, +1.5°C; Northern Great Plains, MRU-12, +2.0°C; Corn Belt, MRU-13, +2.3°C) but mostly at high latitudes with negative average temperature such as Boreal America (MRU-61, +2.9°C), Sub-boreal America (MRU-15, +2.9°C) and Sub-arctic America (MRU-65, +4.6°C). In Asia, the largest positive departure occurred in the Southern Mongolian MRU (MRU-47, +1.8°C).

Figure 1.4. Global map of October 2015-January 2016 biomass accumulation (BIOMSS) by MRU, departure from 5YA, (percentage)

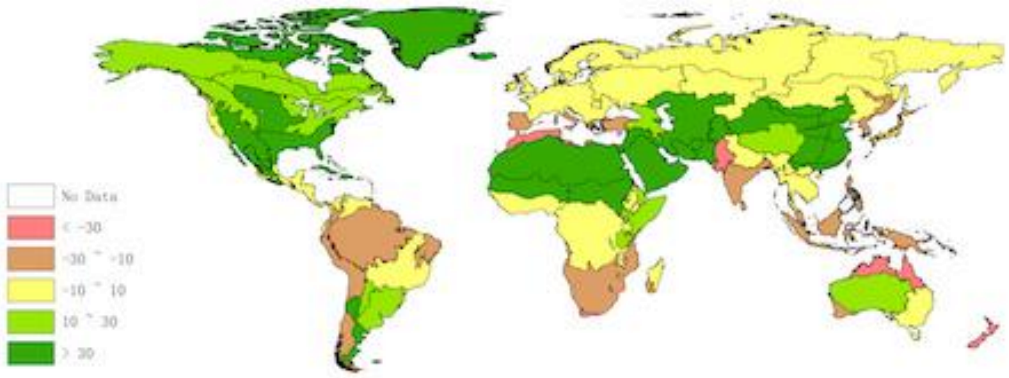

Chapter 2.Crop and environmental conditions in major production zones

Chapter 2 presents the same indicators—RAIN, TEMP, RADPAR, and BIOMSS—used in Chapter 1, and combines them with the agronomic indicators—cropped arable land fraction (CALF) and maximum vegetation condition index (VCIx)—to describe crop condition in six Major Production Zones (MPZ) across all continents. For more information about these zones and methodologies used, see the quick reference guide in Annex C as well as the CropWatch bulletin online resources at www.cropwatch.com.cn.

2.1 Overview

Tables 2.1 and 2.2 present an overview of the agroclimatic (table 2.1) and agronomic (table 2.2) indicators for each of the six MPZs, comparing the indicators to their fourteen- and five-year averages.

Table 2.1. October 2015-January 2016 agroclimatic indicators by Major Production Zone, current value and departure from 14YA

	RAIN		TEMP		RADPAR	
	Current (mm)	Departure from 14YA (%)	Current (°C)	Departure from 14YA (°C)	Current (MJ/m^2)	Departure from 14YA (%)
West Africa	227	9	26.4	-0.9	962	1
South America	782	39	23.5	-0.6	1005	-7
North America	375	56	8	1.9	432	-8
South and SE Asia	194	1	23.3	0.5	795	0
Western Europe	204	-13	8	0.2	262	-4
C. Europe and W. Russia	182	10	1.2	0.3	198	-3

Note: Departures are expressed in relative terms (percentage) for all variables, except for temperature, for which absolute departure in degrees Celsius is given. Zero means no change from the average value; relative departures are calculated as (C-R)/R*100, with C=current value and R=reference value, which is the fourteen-year average (14YA) for the same period (October-January) for 2001-14.

Table 2.2. October 2015-January 2016 agronomic indicators by Major Production Zone, current season values and departure from 5YA

	BIOMSS (gDM/m^2)		Cropped arable land fraction		Maximum VCI Intensity
	Current	Departure from 5YA (%)	Current	Departure from 5YA (%)	Current
West Africa	706	-1	83	0	0.85
South America	1944	14	98	9	0.87
North America	982	37	83	2	0.77
South and SE Asia	520	-8	85	-2	0.79
Western Europe	888	-10	91	-1	0.89
C Europe and W Russia	683	1	83	-1	0.69

Note: Departures are expressed in relative terms (percentage) for all variables. Zero means no change from the average value; relative departures are calculated as (C-R)/R*100, with C=current value and R=reference value, which is the five-year (5YA) average for the same period (October-January) for 2010-2014.

2.2 West Africa

Over the reporting period of October 2015 to January 2016, cereals and tubers were harvested throughout the West Africa MPZ, with small spatial differences in harvest times conditioned by latitude and elevation (e.g. in the case of Guinea). Conditions in the MPZ as a whole were close to average with rainfall exceeding average by 9% and fluctuating but generally below average temperature (-0.9°C); the biomass production potential is close to average (-1%). CALF, at 83%, was average as well for this MPZ.

Guinea and Guinea-Bissau are the only countries in the MPZ where agroclimatic conditions significantly departed from average, both with precipitation departures reaching +32% and +126%, respectively. This was accompanied by below average temperature (close to -1.5°C) and sunshine but nevertheless an increased biomass production potential (+23% and +76%, respectively). All other countries underwent a slight drop in biomass production potential (around -10%) when compared to the most recent five years, with the exception of Sierra Leone, where expectations are approximately average.

The spatial distribution of rainfall, maximum VCI and minimum VHI all concur in presenting a spatially coherent picture with favourable conditions in the north of the MPZ and some water stress increasing towards the south. This corresponds to a weakening of the final stages of the rainy season where this season is long (in the west and east of the region), or a delay and weakening of the short rainy season in the central areas (in Côte d'Ivoire and Ghana, for example). This is consistent with a slower than usual southward movement of the inter-tropical convergence zone away from the Sudano-Sahelian north.

Altogether, there is no reason for concern about the condition of cereals and the (dominant) roots and tubers in the West African MPZ. Indicators are shown in Figure 2.1.

Figure 2.1. West Africa MPZ: Agroclimatic and agronomic indicators, October 2015-January 2016

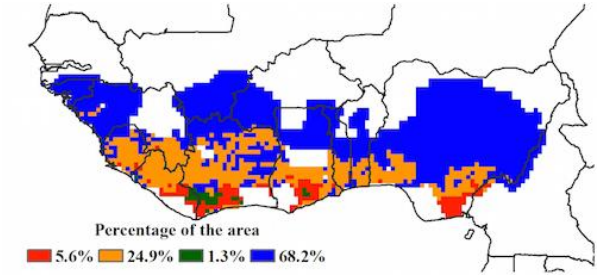

a. Spatial distribution of rainfall profiles

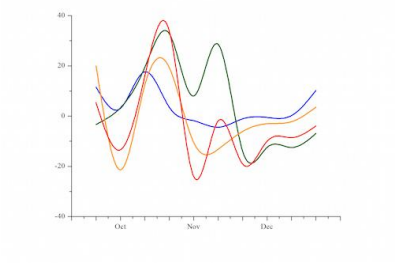

b. Profiles of rainfall departure from average (mm)

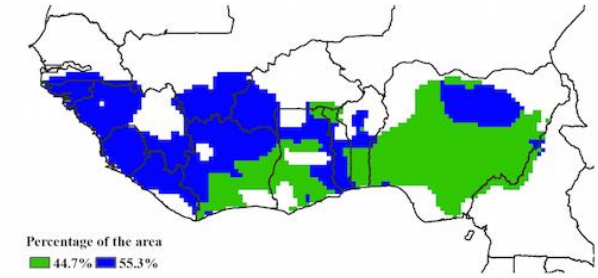

c. Spatial distribution of temperature profiles

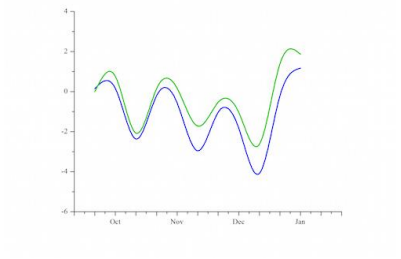

d. Profiles of temperature departure from average (°C)

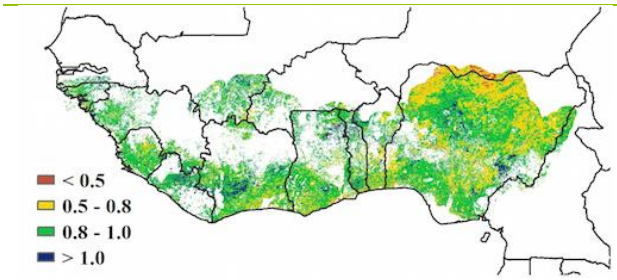

e. Maximum VCI

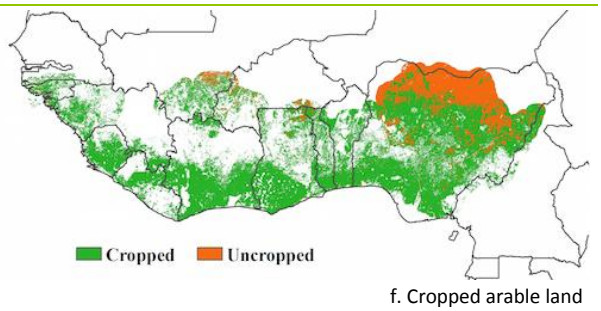

f. Cropped arable land

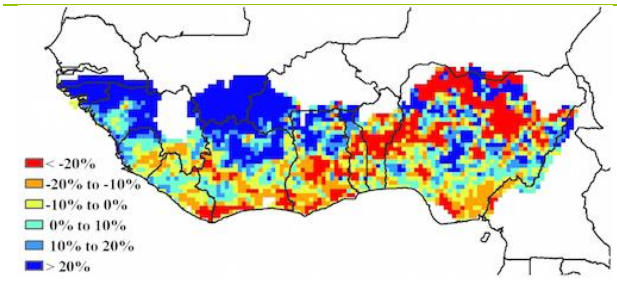

g. Biomass accumulation potential departure

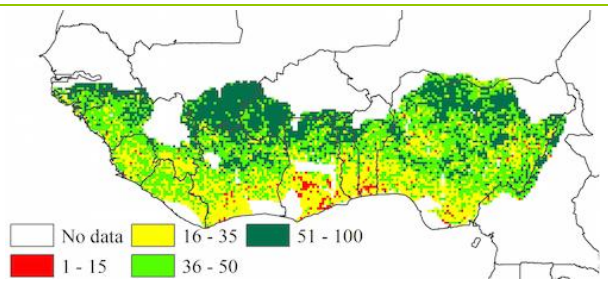

h. VHI minimum

Note: For more information about the indicators, see Annex C.

2.3 North America

In general, crop condition was average in the North American MPZ (Figure 2.2). The summer crops (maize, soybean and spring wheat) were completely harvested at this time, while winter crops have been planted and reached over-wintering stages.

Overall, CropWatch agroclimatic indicators show warmer than average and wet weather conditions: rainfall was 56% above average and the temperature departure was +1.9°C. Actually, wet and mild agroclimatic conditions (as displayed in Figure 2.2) were common only in the United States. Canada was dominated by dry agroclimatic conditions. In the United States, excess moisture has hampered the harvest of summer crops and the planting of winter wheat while it also replenished soil moisture for the growth of winter crops and pastures in spring.

Major winter wheat production zones recorded abundant rainfall in the South Plains (RAIN: +85%, TEMP: 0.9°C), Kansas (RAIN: +35%, TEMP: 1.5°C), Oklahoma (RAIN: +99%, TEMP: 0.6°C) and Texas (RAIN: +78%, TEMP: 0.5°C). Abundant rainfall also fell in the blue grass region (+62%) and in Kentucky and Tennessee (+33% and +78%, respectively). Biomass shows a 37% positive departure compared to last five years average. The fraction of cropped arable land (CALF) was 2% above average.

Figure 2.2. North America MPZ: Agroclimatic and agronomic indicators, October 2015-January 2016

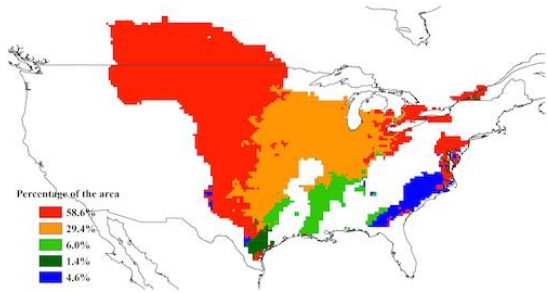

a. Spatial distribution of rainfall profiles

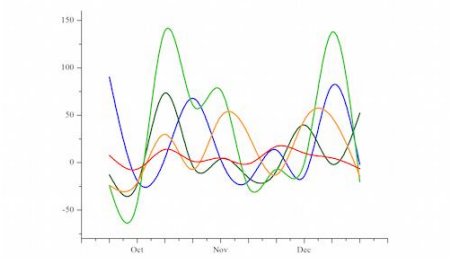

b. Profiles of rainfall departure from average (mm)

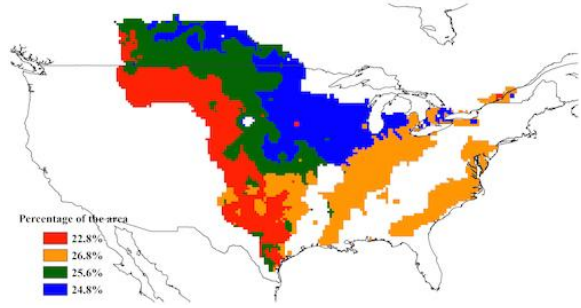

c. Spatial distribution of temperature profiles

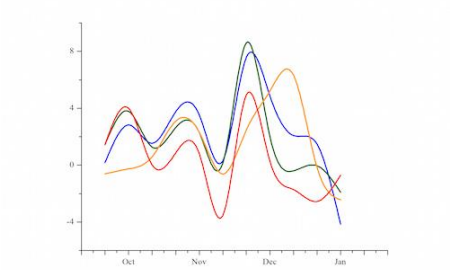

d. Profiles of temperature departure from average (°C)

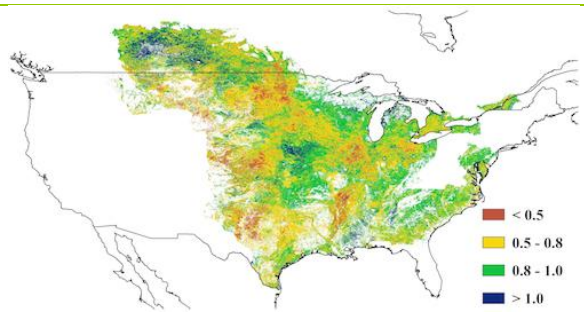

e. Maximum VCI

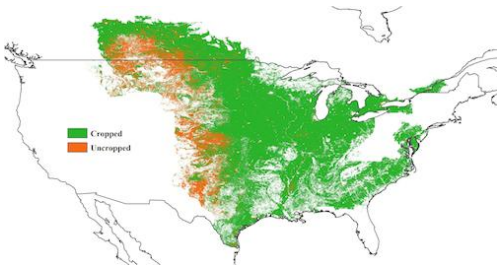

f. Cropped arable land

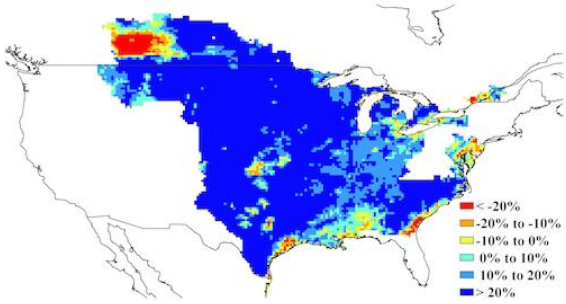

g. Biomass accumulation potential departure

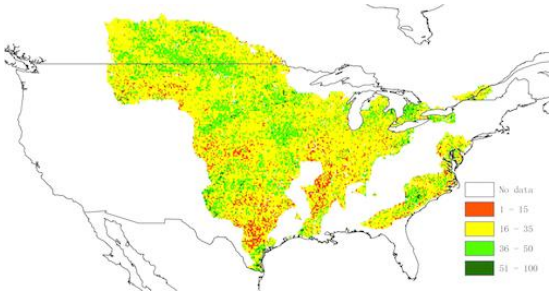

h. VHI minimum

Note: For more information about the indicators, see Annex C.

2.4 South America

Crops in the South America MPZ experienced favorable conditions from October 2015 to mid January 2016 (Figure 2.3). The winter wheat harvest was completed at the end of 2015, and currently, soybean is at its flowering stage and maize is at the silking stage. Abundant rainfall (39% above average) favoured the development of soybean and maize although temperature and RADPAR were slightly below average for this reporting period. Altogether, crops benefited from the favorable agroclimatic conditions and BIOMSS for the whole MPZ was 19% above average.

According to the spatial pattern and profiles of rainfall departure from average, rainfall was slightly above average (20mm or more) over most of Argentina as well as the northern part of MPZ. Southern Paraguay Missiones in Argentina and southern Brazil (including Rio Grande Do Sul, Parana and Santa Catarina) experienced continuously well above average rainfall. Air temperature in the MPZ was below average from October except for the most northern part covering southern Mato Grosso, Minas Gerais and Goais as shown in temperature clusters and profiles (Figure 2.3). High temperature with almost average rainfall in those areas resulted in the below average potential biomass, which is confirmed by the low value of minimum VHI: crops suffered from water stress during the monitoring period.

Although extreme weather conditions occurred in parts of the MPZ, the condition of summer crops was still comparable with five-year average as shown in the VCIx map and the high overall average VCIx value (0.87) for the MPZ. CALF for the MPZ was 98%, an increase of 9% from the previous five-year average. About 2% of the total arable land was intentionally kept fallow, mostly between Bahia Blanca and Santa Rosa, to encourage more sustainable agricultural practices. In general though, well above average rainfall provided necessary soil moisture for the development of soybean and maize.

Figure 2.3. South America MPZ: Agroclimatic and agronomic indicators, October 2015-January 2016

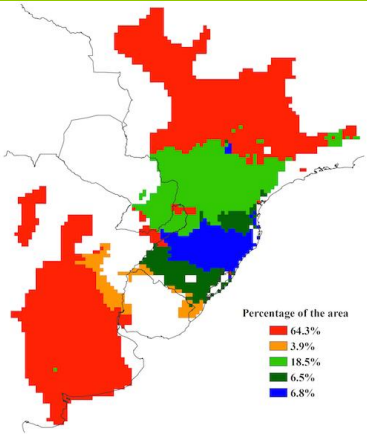

a. Spatial distribution of rainfall profiles

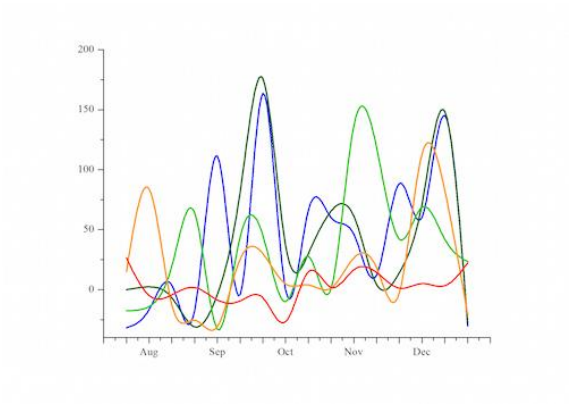

b. Profiles of rainfall departure from average (mm)

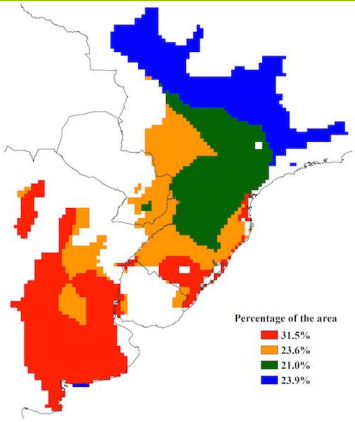

c. Spatial distribution of temperature profiles

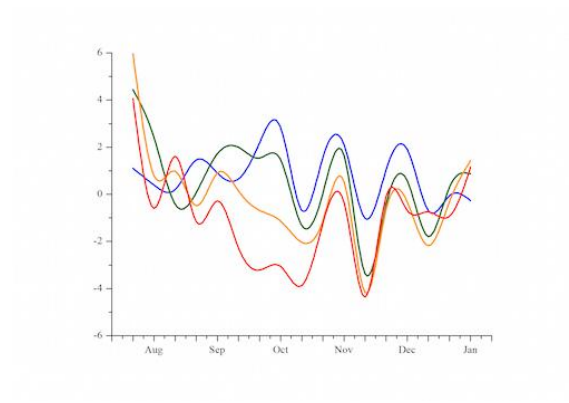

d. Profiles of temperature departure from average (°C)

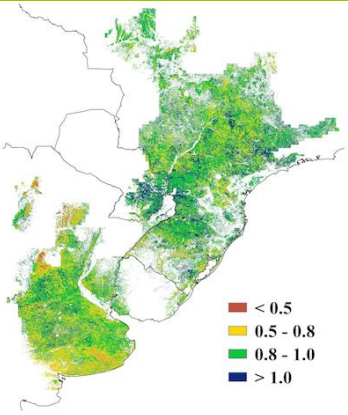

e. Maximum VCI

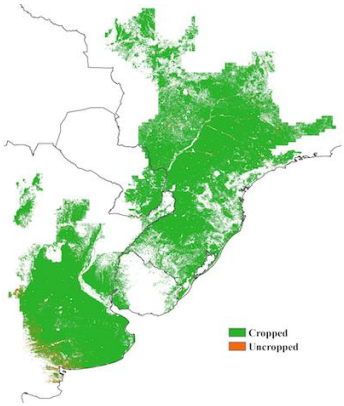

f. Cropped arable land

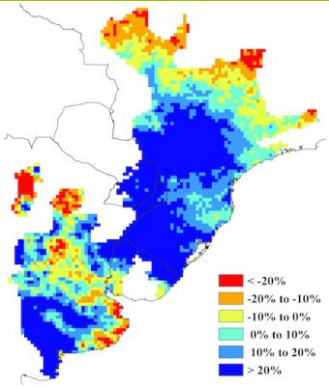

g. Biomass accumulation potential departure

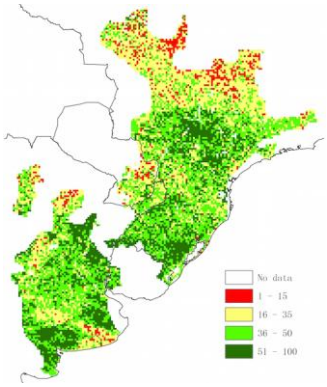

h. VHI minimum

Note: For more information about the indicators, see Annex C.

2.5 South and Southeast Asia

The reporting period mainly involves the growing and harvesting of wet season crops for this MPZ. The entire zone experienced a slight increase (+1%) of rainfall over average, but low rainfall was recorded for both Bangladesh (-38%) and India (-3%). The spatial distribution of rainfall profiles indicates that 65.6% of the area of the MPZ received average rainfall throughout the monitoring period while 26.6% received below average rainfall in early November 2015. Temperature (TEMP: +0.5°C) remained average and there was no change in the photosynthetically active radiation (RADPAR) for the MPZ. Temperature departure profile follows the same temporal pattern throughout the MPZ as shown in Figure 2.4c. Temperatures were above average during the first two dekads but fluctuated widely during the reporting period.

The maximum VCI values for the MPZ range from 0.5 to 1, indicating average to favorable crop conditions throughout. However, low VCI (< 0.5) was recorded for central India triggered by below average rainfall in Madhya Pradesh (-39%) and Rajasthan (-42%), pointing to poor crop condition in those areas.

The fraction of crop arable land (CALF) was 85%, which was 2% below the average. The uncropped areas were mainly distributed in central Myanmar and in the Indian states of Haryana, Rajasthan, Maharashtra, Karnataka and Andhra Pradesh. The biomass accumulation potential for the MPZ was below average (-8%), while the spatial distribution shows below average biomass concentration in central and eastern India, the southern part of Myanmar and some scattered areas in Thailand, Cambodia and Vietnam. Except the southern part of India, the entire country recorded low values of VHI minimum indicating water stress due to the deficit rainfall.

Overall, crop condition of the MPZ is below average primarily due to the rainfall deficit in India and Bangladesh.

Figure 2.4. South and Southeast Asia MPZ: Agroclimatic and agronomic indicators, October 2015-January 2016

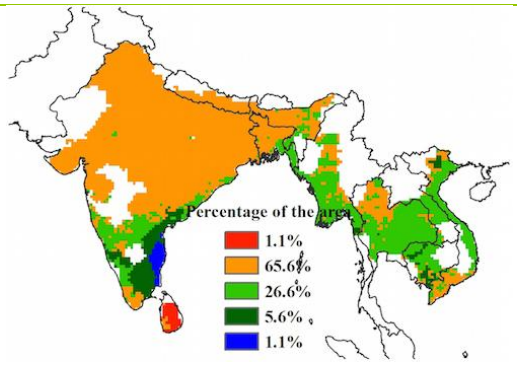

a. Spatial distribution of rainfall profiles

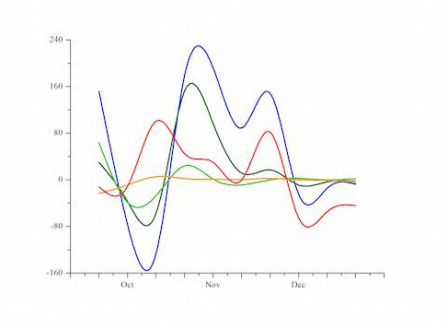

b. Profiles of rainfall departure from average (mm)

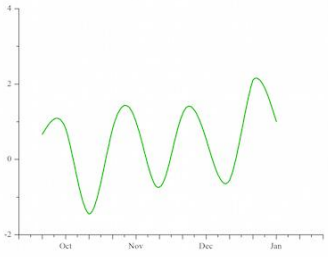

c. Profiles of temperature departure from average (°C)

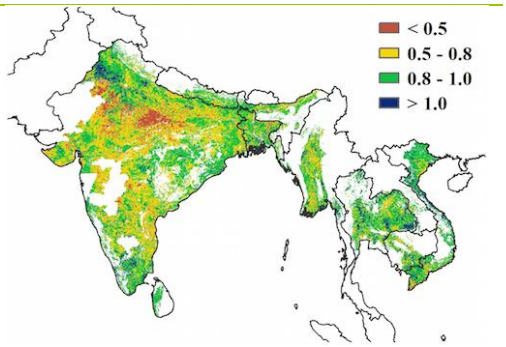

d. Maximum VCI

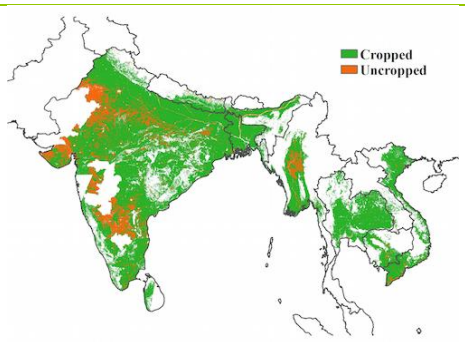

e. Cropped arable land

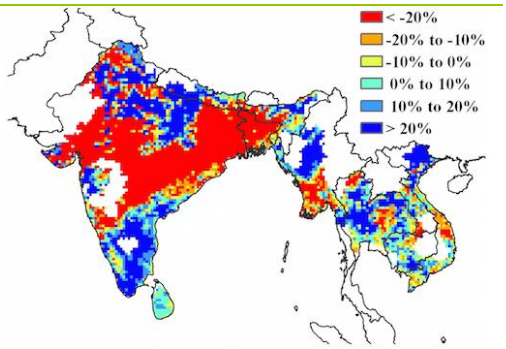

f. Biomass accumulation potential departure

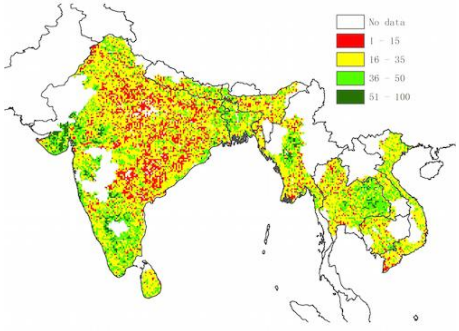

g. VHI minimum

Note: For more information about the indicators, see Annex C.

2.6 Western Europe

In general, environmental conditions were below average in most parts of the Western Europe MPZ during this reporting period. The summer crops were completely harvested, and winter crops were planted and reached over-wintering stages. Figure 2.5 represents an overview of CropWatch agroclimatic and agronomic indicators for this MPZ.

The agroclimatic indicators show that total rainfall was 13% below average, with exceptional positive departures over most of Germany, the Czech Republic, Austria, Slovakia and Hungary in early October and, from late October to early November over most of England and Denmark, the south of France, and in the east of Spain and Italy after late November. Temperatures over the whole MPZ were close to average (+0.2°C), and temperature profiles indicate that above average temperatures were observed in most of Western Europe from mid-October to late October, and from later November to mid-December in the south of France and the east and west of Spain. The radiation was 4% below average.

Due to the continuous rainfall deficit, especially after November, coupled with the impact of low temperature in mid-November, the biomass accumulation potential, BIOMSS, was 10% below the recent five-year average. The spatial distribution of BIOMSS shows that the lowest values (-20% and below) occur over most of France, Spain, the Czech Republic, northern Italy, the east of Austria, and the south of Hungary. The values for minimum VHI confirm the water deficit to a certain extent in those regions. In contrast, BIOMSS in most other regions was 10% above average.

91% of the arable land was cropped during this reporting period, 1% lower than the recent five-year average. Most uncropped arable land was concentrated in Spain and also scattered in the central part of Hungary. Accordingly, maximum VCI in Spain, south of France, north of Italy, west of the Czech Republic and the east of Hungary were lower compared to other regions in this MPZ. Average VCIx for the MPZ was 0.89. Crop condition is slightly below average in Western Europe.

Figure 2.5. Western Europe MPZ: Agroclimatic and agronomic indicators, October 2015-January 2016

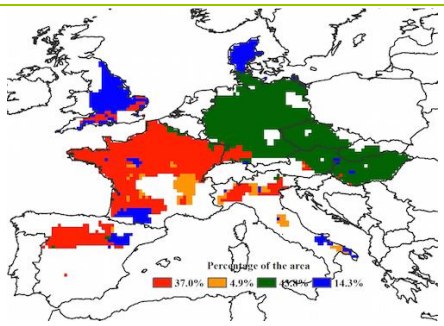

a. Spatial distribution of rainfall profiles

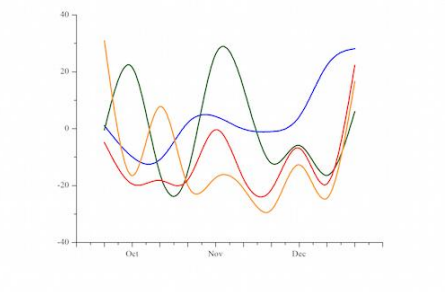

b. Profiles of rainfall departure from average (mm)

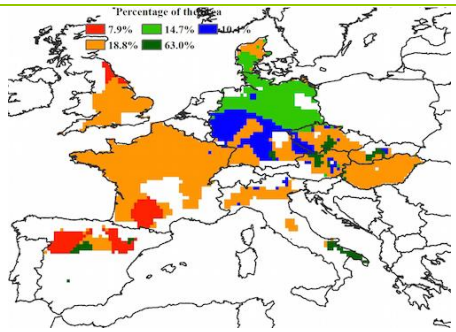

c. Spatial distribution of temperature profiles

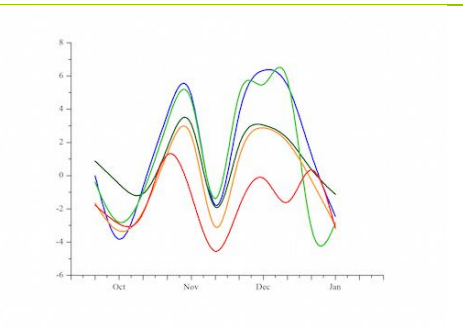

d. Profiles of temperature departure from average (°C)

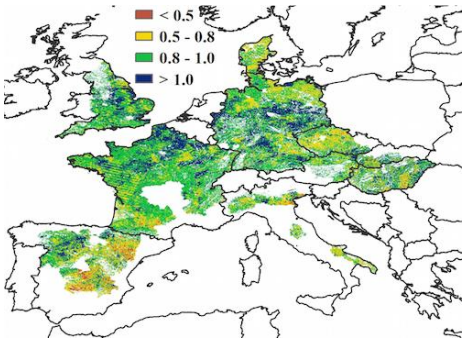

e. Maximum VCI

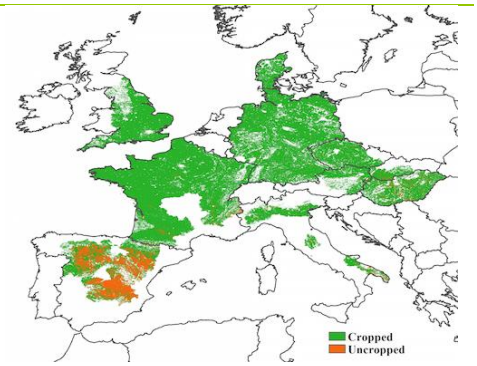

f. Cropped arable land

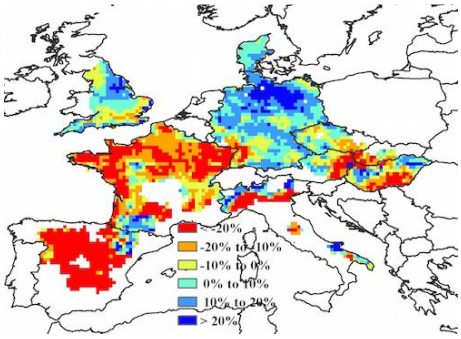

g. Biomass accumulation potential departure

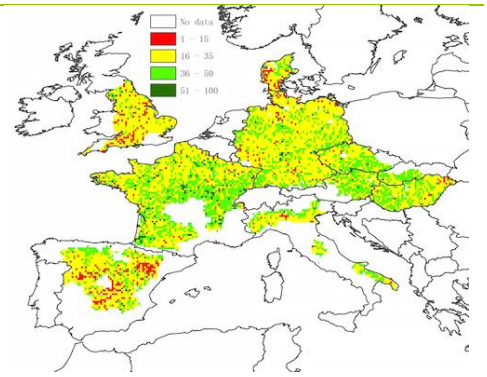

h. VHI minimum

Note: For more information about the indicators, see Annex C.

2.7 Central Europe to Western Russia

During the current monitoring period, the harvest of summer crops was completed and winter crops were in the early vegetative stages under mostly favorable weather conditions. The region experienced slightly below normal thermal conditions, while rainfall increased by 10% and RADPAR dropped by 3%.

According to the rainfall profiles, almost all areas of Central Europe to Western Russia enjoyed approximately average precipitation from October through to December, while abundant rainfall was recorded in the southwest of Russia between late December and early January, including Krasnodarskiy and Stavropolskiy Krays and the Oblasts of Rostovskaya and Volgogradskaya. From November, the MPZ enjoyed warmer-than-average temperatures, including temperature departures as high as +4°C in early December in most regions. In the second and third dekad of December, remarkably below average temperatures prevailed over Central Europe, reaching 8°C below average in southern Belarus in January. As a result of bad weather conditions during the sowing stages of winter crops (see the November 2015 Bulletin), crop conditions in eastern Ukraine and many parts of southern Russia were well below average, which is confirmed by the maximum VCI distribution map (Figure 2.6).

BIOMSS is up 1% compared to the recent five-year average. 83% of the arable lands were cropped from October 2015 to January 2016. Most uncropped arable land was scattered in the south of western Russia (including the Oblasts of Volgogradskaya, Saratovskaya and Samarskaya).The maximum VCI (0.69) of this MPZ is much lower than that of other MPZs. According to the VHI map of this monitoring period, most pixels of southern Ukraine and Russia showed bad soil moisture conditions.

In conclusion, below average production is to be expected in Central Europe and Western Russia.

Figure 2.6. Central Europe-Western Russia MPZ: Agroclimatic and agronomic indicators, October 2015-January 2016

a. Spatial distribution of rainfall profiles

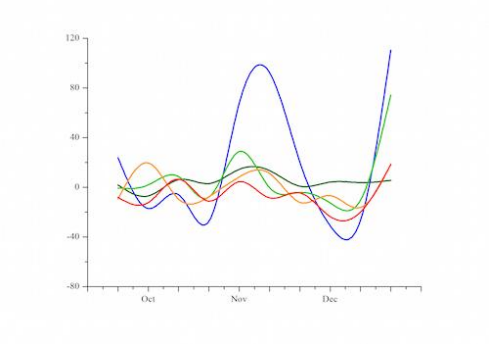

b. Profiles of rainfall departure from average (mm)

c. Spatial distribution of temperature profiles

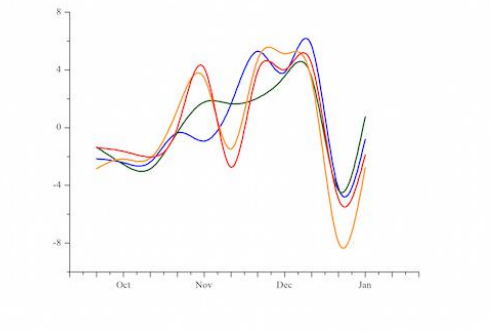

d. Profiles of temperature departure from average (°C)

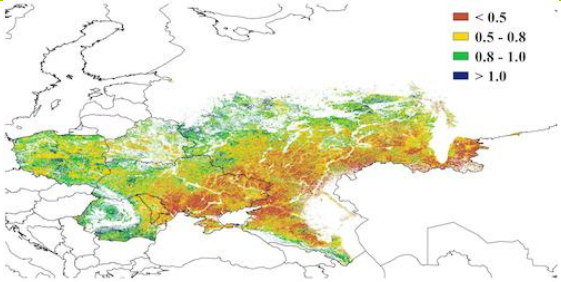

e. Maximum VCI

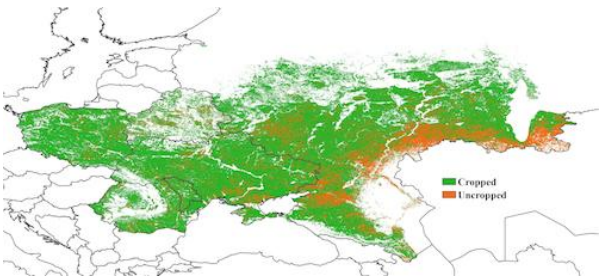

f. Cropped arable land

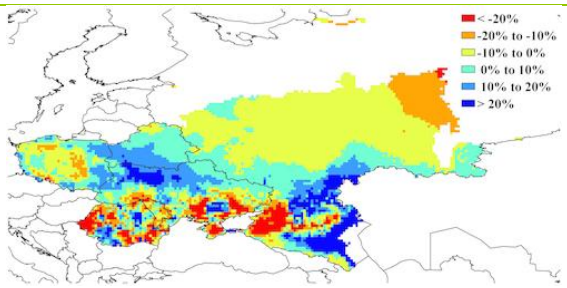

g. Biomass accumulation potential departure

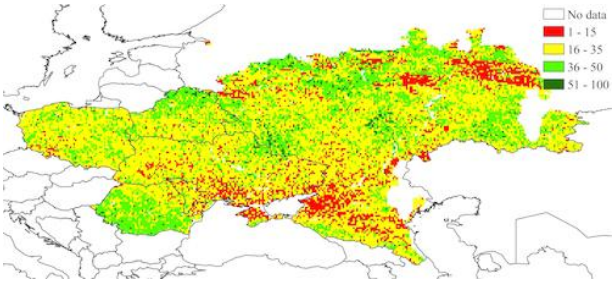

h. VHI minimum

Note: For more information about the indicators, see Annex C.

Chapter 3. Main producing and exporting countries

Building on the global patterns presented in previous chapters, this chapter assesses the situation of crops in 30 key countries that represent the global major producers and exporters or otherwise are of global or CropWatch relevance. In addition, the overview section (3.1) pays attention to other countries worldwide, to provide some spatial and thematic detail to the overall features described in section 1.1. In section 3.2, the CropWatch monitored countries are presented, and for each country maps are included illustrating NDVI-based crop condition development graphs, maximum VCI, and spatial NDVI patterns with associated NDVI profiles. Additional detail on the agroclimatic and BIOMSS indicators, in particular for some of the larger countries, is included in Annex A, tables A.2-A.11. Annex B includes 2016 production estimates for Argentina, Brazil, Australia and South Africa.

3.1 Overview

Section 1.1 of this bulletin stressed that the global patterns of the CropWatch agroclimatic indicators (CWAIs: RAIN, TEMP and RADPAR) anomalies identify well-delimited zones but that the zones mostly do not coincide with, or only imperfectly overlap for, different indicators. This is apparent in figures 3.1 to 3.4 as well.

Figure 3.1. Global map of October 2015-January 2016 rainfall (RAIN) by country and sub-national areas, departure from 14YA (percentage)

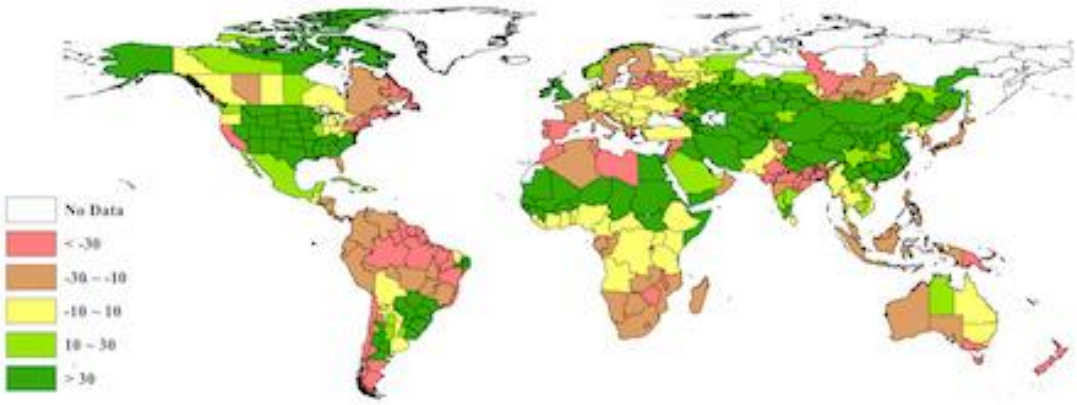

Figure 3.2. Global map of October 2015-January 2016 temperature (TEMP) by country and sub-national areas, departure from 14YA (degrees)

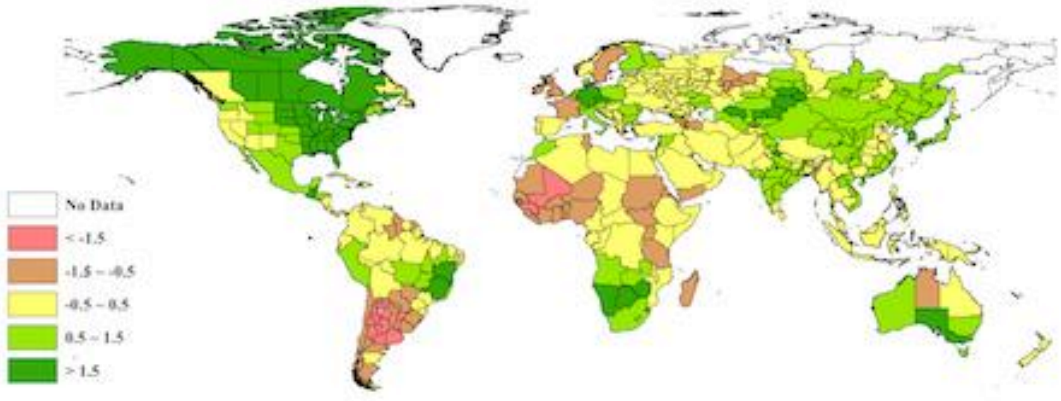

Figure 3.3. Global map of October 2015-January 2016 PAR (RADPAR) by country and sub-national areas, departure from 14YA (percentage)

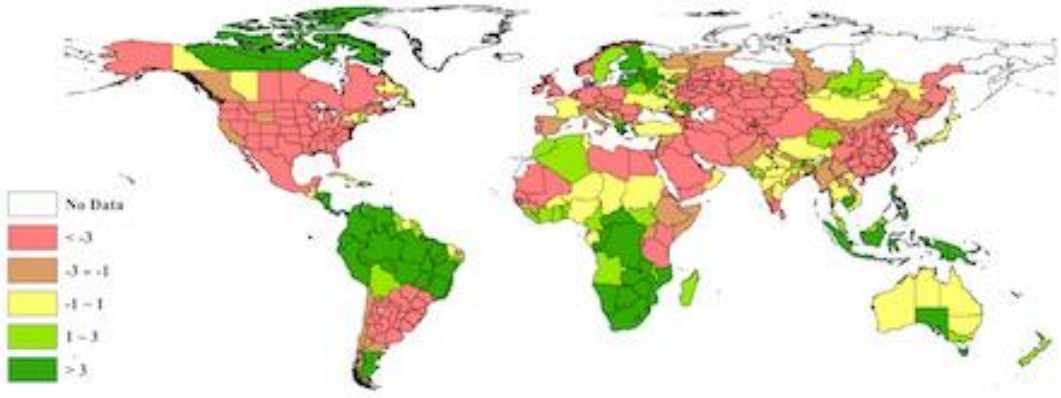

Figure 3.4. Global map of October 2015-January 2016 biomass (BIOMSS) by country and sub-national areas, departure from 14YA (percentage)

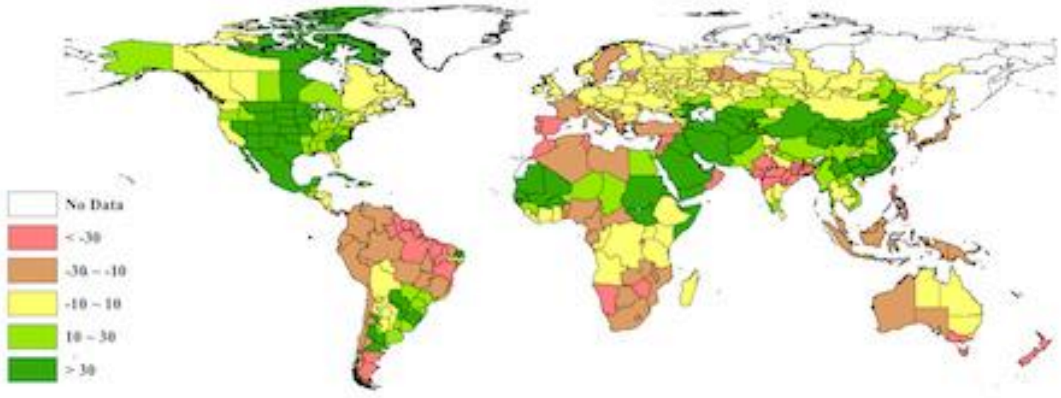

At the national and sub-national levels, the countries that underwent the most severe levels of environmental stress can be subdivided into several groups, which confirm the patterns identified in Chapter 1 but also but also provide additional detail more closely related to the likely outcome of the growing seasons. Figure 3.1 lists CropWatch agronomic and agroclimatic indicators for the monitoring period.

Table 3.1. CropWatchagroclimatic and agronomic indicators for October 2015-January 2016, departure from 5YA and 14YA

Country	Agroclimatic Indicators			Agronomic Indicators		
	Departure from 14YA (2001-2014)			Departure from 5YA (2010-2014)		Current
	RAIN (%)	TEMP (°C)	RADPAR (%)	BIOMSS (%)	CALF (%)	Maximum VCI
Argentina	24	-1.7	-10	13	8	0.82
Australia	-11	0.9	0	-11	4	0.68
Bangladesh	-38	-0.2	-1	-33	0	0.83
Brazil	-1	0.4	3	-9	14	0.84
Cambodia	23	0.5	3	-3	1	0.85
Canada	-15	2.4	-5	13	-2	0.84
China	85	0.5	-12	41	0	0.86
Egypt	32	0.3	-5	15	0	0.89
Ethiopia	2	0.3	-3	6	-2	0.79
France	-27	-0.9	0	-18	0	0.91
Germany	3	1.7	-7	4	0	0.93
India	-3	0.6	-1	-18	-4	0.75
Indonesia	-24	-0.1	6	-21	0	0.84
Iran	50	-0.3	-5	47	0	0.73
Kazakhstan	52	1.1	-9	12	-1	0.55
Mexico	21	0.5	-6	49	0	0.81
Myanmar	6	-0.4	-1	12	-1	0.84
Nigeria	-4	-0.7	1	-13	-3	0.80
Pakistan	3	-0.1	-2	18	-2	0.81
Philippines	-18	-0.1	10	-32	0	0.89
Poland	-1	0.7	-4	5	-3	0.81
Romania	-9	0.9	-7	-10	-5	0.88
Russia	16	0.3	-3	0	4	0.66
S. Africa	-26	1.4	9	-27	-12	0.48
Thailand	0	0.4	1	-3	0	0.89
Turkey	-1	0.5	0	-12	-3	0.73
United Kingdom	48	-0.7	-13	-2	0	0.92
Ukraine	1	0.2	0	4	-3	0.63
United States	47	1.6	-7	35	2	0.75
Uzbekistan	59	0.7	-9	51	11	0.83
Vietnam	-8	0.9	-1	13	0	0.90

Note: Departures are expressed in relative terms (percentage) for all variables, except for temperature, for which absolute departure in degrees Celsius is given. Zero means no change from the average value; Relative departures are calculated as (C-R)/R*100, with C=current value and R=reference value, which is the five-year (5YA) or fourteen-year average (14YA) for the same period (July-October).

The countries and sub-countries that suffered mostly from drought are located in (1) northern South America and (2) south-east Asia to New Zealand both at approximately -56% of rainfall on average: (1) The first group includes the Guyanas (Suriname, -70%; Guyana, -62%; Trinidad and Tobago, -53% as well as Dominica, -49%). This area also covers several states in Brazil, such as Roraima (-78%), Amapa (-71%), Para (-52%), Maranhao (-50%) and Amazonas (-32%). While almost all of them score low on the biomass production potential (-45% on average) and high on RADPAR (+5% on average), other agroclimatic indicators are close to average, with some exceptions such as temperature in French Guyana (-1.2°C), and sunshine in Para and Amazonas (+10% and +11%, respectively), two areas where rainfall should nevertheless have been sufficient for normal crop development.

Group (2) includes New Zealand (-66% precipitation), New Caledonia (-60%) and Timor Leste (-57%) as well as the Australian states of Tasmania (-75%) and Victoria (-45%), which deserve a mention in the area from Southeast Asia through to New Zealand. With the exception of temperature in New Caledonia (-1.3°C), all other agroclimatic variables behave as expected, in particular a biomass production potential drop of 46%.

(3) Dry conditions also prevailed in the northern part of the Indian subcontinent, with an average precipitation departure of -52% affecting Bangladesh and Bhutan (-38% and -37%, respectively) as well as the following areas in India: Meghalaya (-81%), Jharkhand (-80%), West Bengal (-73%), Bihar (-60%). Chhattisgarh, Orissa, Gujarat, Sikkim, Rajasthan, Madhya Pradesh, Delhi and Himachal Pradesh recorded rainfall deficits between -59% and -34%. Other agroclimatic variables are close to average, except for a biomass production drop expected to reach 42% on average. In Bhutan, however, the drop would reach only 5% due to more favorable temperature than adjacent areas in India.

(4) Most Mediterranean countries, which all grow winter crops, planted at the end of the year suffered a marked drop in precipitation close to 50%. This includes mostly Morocco (-74%), Portugal (-55%) and Lebanon (-54%), as well as Spain, Tunisia, Syria, Montenegro, Cyprus, Libya, Israel and Greece, with deficit values ranging from -51% to -35%. Civil unrest is an aggravating factor in several of them, but due to the fact that firstly, several months are still needed until the harvest, and secondly, low or no water consumption still prevails for the dormant crops, the outcome of the season will depend on rainfall during the coming months. For the reporting period, the biomass potential drop averages 29%. Morocco, Syria and Lebanon all recorded abnormally high temperatures (0.9°C, 1.0°C and 1.9°C, respectively). This has increased evaporation and may negatively impact future soil water availability.

(5) In addition to California (-37% precipitation over the reporting period), several areas in the north-eastern USA and Canada suffered from unusually dry conditions with deficits ranging from -52% (Maine) to -39% (Massachusetts). The vegetation and crops in the area, which also includes Newfoundland and Labrador, Nova Scotia, New Hampshire, New Brunswick, Vermont and New Jersey is unlikely to suffer due to the early winter drought.

(6) Several countries in Africa, even with a water stress that is low compared with the previous countries, are more likely to suffer due to the semi-arid conditions and inherently more fragile farming systems. They include mostly Lesotho (-44%), Zimbabwe (-42%), Malawi (-36%) and Namibia (-29%). Other countries in the area (particularly South Africa, Botswana) are at deficit levels close to 25% on average. Rwanda deserves a particular mention in the current context (-35%) in the light of the social and political tension prevailing in the region.

(7) The last area to be mentioned includes the larger Baltic, i.e. the Baltic States as well as the adjacent Russian areas to the east. Low rainfall was accompanied by large positive RADPAR values and positive temperature anomalies, which, similar to the situation in the Mediterranean countries, may negatively affect soil moisture availability in the coming months depending on the amounts of rainfall still to come

between now and the time of harvest. Rainfall in other countries also saw a decrease, for example Estonia (-41%) and Latvia (-37%) with the area of S. Petersburg in Russia (-48%) and several areas to the east including Moscow, Adygeya Republic, Tverskaya and Pskovskaya Oblasts which record deficits between 37% and 32%.

3.2 Country analysis

This section presents CropWatch results for each of thirty key countries (China is addressed in Chapter 4). The maps refer to crop growing areas only and include (a) Crop condition development graph based on NDVI average over crop areas, comparing the April-July 2015 period to the previous season and the five-year average (5YA) and maximum. (b) Maximum VCI (over arable land mask) for October 2015-January 2016 by pixel; (c) Spatial NDVI patterns up to January 2016 according to local cropping patterns and compared to the 5YA; and (d) NDVI profiles associated with the spatial pattern under (c). See also Annex A, tables A.2-A.10, and Annex B, tables B.1-B.4, for additional information about indicator values and production estimates by country. Country agricultural profiles are posted on www.cropwatch.com.cn.

Figures 3.5-3.34. Crop condition for individual countries ([ARG] Argentina- [ZAF] South Africa) for October 2015-January 2016

[ARG] Argentina

Generally, crops in Argentina experienced favorable conditions from October 2015 to mid January 2016. The harvest of winter wheat was concluded by mid January, and summer crops (maize and soybean) approached the peak of the growing season. Agroclimatic conditions were generally favorable for Argentina with 24% above average RAIN; accordingly, TEMP was 1.7 °C and RADPAR was 10% below average. Major agricultural provinces experienced similar patterns but with different departures from average RAIN, ranging from 0% to about 80% above average. Abundant rainfall accompanied by well below average radiation occurred in Corrientes, La Pampa, Misiones, and San Luis; this delayed farm operations and hampered the growth of summer crops. Sufficient rainfall (about 10% above average) in Buenos Aires, Cordoba, Entre Rios, and Santa Fe was beneficial for the development of soybean and maize crops. BIOMSS in each province was above average except for Salta and Chaco where the indicator was 6% below average and average, respectively.

According to the NDVI development profiles, crop condition was above the five-year average and at the same level as the previous year. The national average VCIx at 0.82 also confirms good crop condition. Areas in the west of Mar Chiquita Lake were the only regions with continuously below average crop condition during the monitoring period. A great diversity of crop conditions was observed as shown in the NDVI departure from the five-year average clustering and the corresponding profiles: in northern Argentina, San Luis, central Buenos Aires, and northern La Pampa crop condition was below average before November but it improved thereafter. In contrast, the condition of crops deteriorated in southern Santa Fe and the neighboring regions from November 2015. CALF for Argentina was 8% above average, indicating an increased summer crops planting area.

Based on the time series of NDVI data over the whole winter wheat growing season, winter wheat production was revised down to 10.7 million tons, 11% below that of the 2014-2015 growing season. The harvest area and yield for winter wheat was both below 2014-2015 (See Annex B Table B.1).

Figure 3.5. Argentina crop condition, October 2015-January 2016

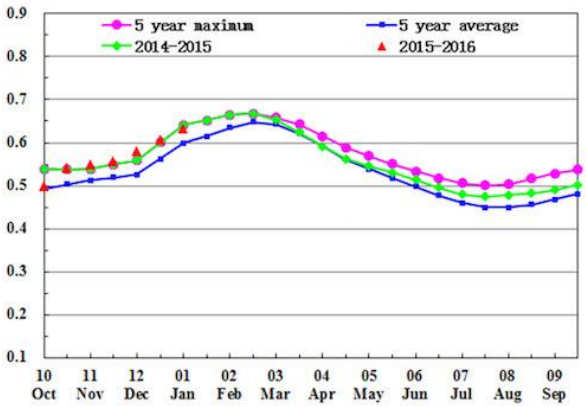

(a) Crop condition development graph based on NDVI

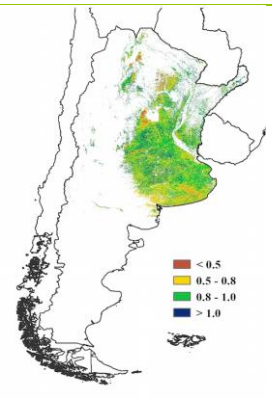

(b) Maximum VCI

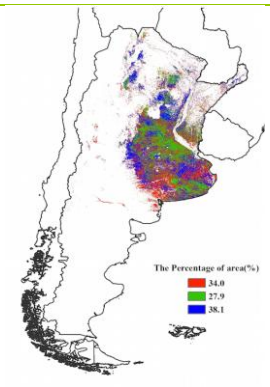

(c) Spatial NDVI patterns compared to 5YA

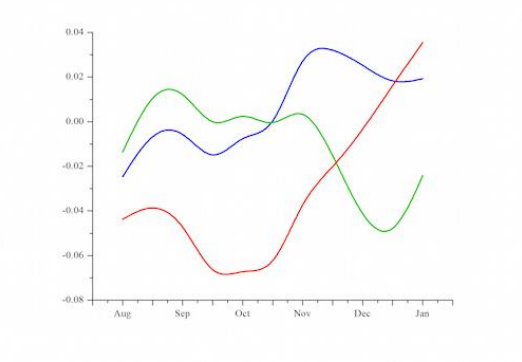

(d) NDVI profiles

[AUS] Australia

Crops in Australia showed below average conditions throughout the monitoring period from October 2015 to January 2016, which included the harvest season for winter crops (wheat and barley) from October.

The unfavorable crop condition is linked to below average precipitation (Southern Australia: -29%, Victoria: -45%, Western Australia:-12%) and high temperature (Southern Australia: +1.8°C, Victoria: +2.1°C, Western Australia: +1.1°C) which has increased plant water demand above average levels. The average maximum VCI only reaches 0.68 for Australia's cropped land (Table 3.1). The NDVI profiles also reflect below average conditions in most parts of south-western Western Australia, south-eastern Southern Australia as well as northern and middle Victoria.

Although the cropped arable land has increased by 4%, CropWatch reports a reduction of 1% in production for wheatin 2015-16. (Table B.2 in Annex B.)

Figure 3.6. Australia crop condition, October 2015-January 2016

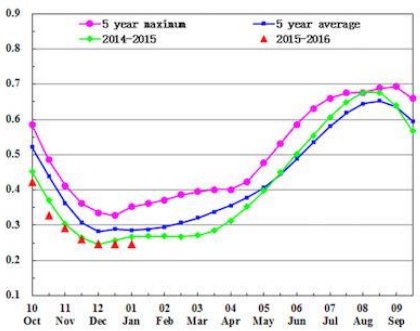

(a) Crop condition development graph based on NDVI

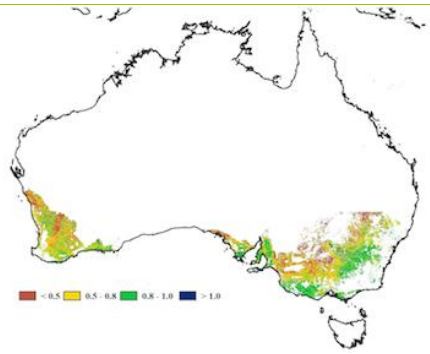

(b) Maximum VCI

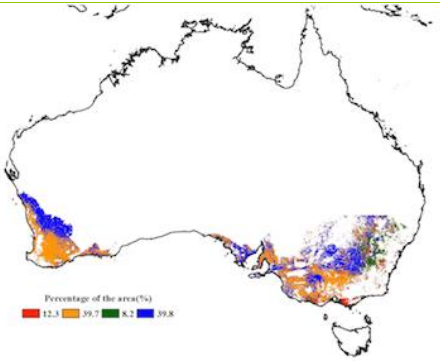

(c) Spatial NDVI patterns compared to 5YA

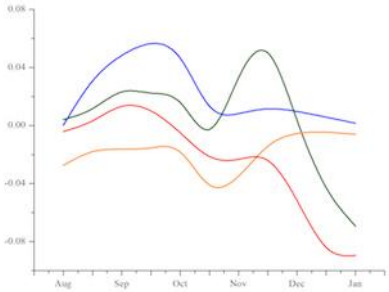

(d) NDVI profiles

[BGD] Bangladesh

According to the CropWatch indicators overall crop condition is poor for Bangladesh. The reporting period corresponds to the harvesting of Aman and planting of irrigated Boro dry season rice. The rainfall (RAIN) was 38% below average including the coastal region (-15%) and Gangetic plain (-76%). The biomass accumulation potential (BIOMASS, -33%) was below average, but both temperature (TEMP, -0.2°C) and photosynthetically active radiation (RADPAR, -1%) were average. The national NDVI profile was below the average of the previous five years pointing at poor crop condition. The maximum VCI below 0.5 was recorded in Sylhet and in some coastal parts of Khulna and Barisal indicating poor crop condition. Spatial NDVI profiles for the country improved after November and reached above average levels in January.

Figure 3.7. Bangladesh crop condition, October 2015-January 2016

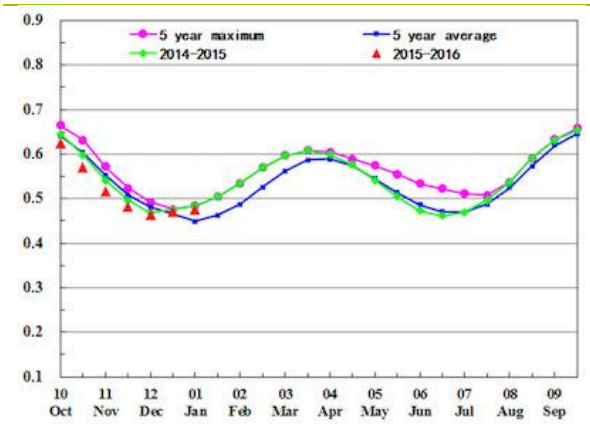

(a) Crop condition development graph based on NDVI

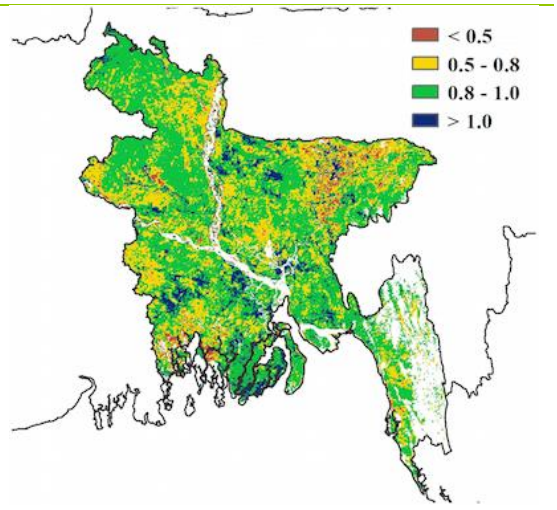

(b) Maximum VCI

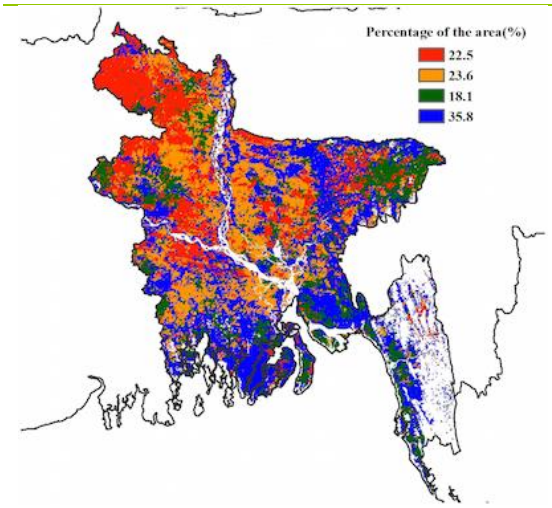

(c) Spatial NDVI patterns compared to 5YA

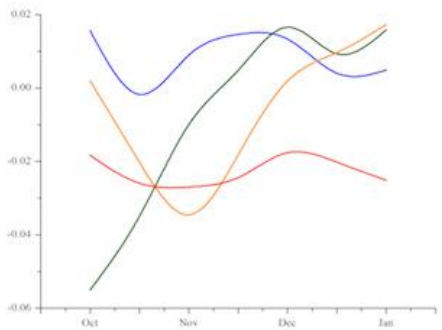

(d) NDVI profiles

[BRA] Brazil

During the monitoring period from October 2015 to mid January 2016, crops in Brazil suffered from unfavorable conditions. Currently soybean is at the flowering stage and first season maize has reached grain-filling. The harvesting of wheat was concluded by the end of 2015. Nationally, agroclimatic indicators show average conditions with 1% below average RAIN, 0.4°C above average air temperature and 3% above average radiation. However, BIOMSS still decreased 9% compared to the average. For the current season, states can be ranked into two groups: (1) excessive rainfall in southern Brazil and north-eastern Brazil which resulted in insufficient photosynthesis of summer crops, including Sao Paulo, Santa Catarina, Parana and Mato Grosso Do Sul with precipitation 40% or more above average. RAIN was even double compared with average in Paraiba, Rio Grande Do Norte and the key agricultural states of Rio Grande Do Sul; (2) shortage of rainfall was observed in most other states leading to low BIOMSS. Although they are not major agricultural states, it is noteworthy that BIOMSS in Rio Grande Do Norte and Paraiba was at least 50% above average.

The unevenly distributed rainfall in Brazil generally resulted in below average crop condition as shown by the well below average NDVI since December 2015 (Figure 3.8). Below average crops occur in north-eastern coastal regions. In contrast, crops in Mato Grosso Do Sul, Sao Paulo and Minas Gerais are above the five-year average due to favorable moisture during the monitoring period. The low VCIx values in north-eastern Brazil coincide with below average crops according to the NDVI departure cluster map. Due to rainfall in major agricultural regions, CALF was 14% above the five-year average, indicating an increased summer crops area, which promises a good summer growing season outcome.

The overall situation for Brazil is still unclear due to low rainfall in the major soybean producing state Mato Grosso. CropWatch will update the production outlook in the next Bulletin to be released in May 2016. With the updated NDVI time series up to the end of 2015, the whole growing season of wheat can now be covered and the wheat production estimate was revised to 7 million tons, 4.5% above the previous year and 67 ktons above the November 2015 forecast.

Figure 3.8. Brazil crop condition, October 2015-January 2016

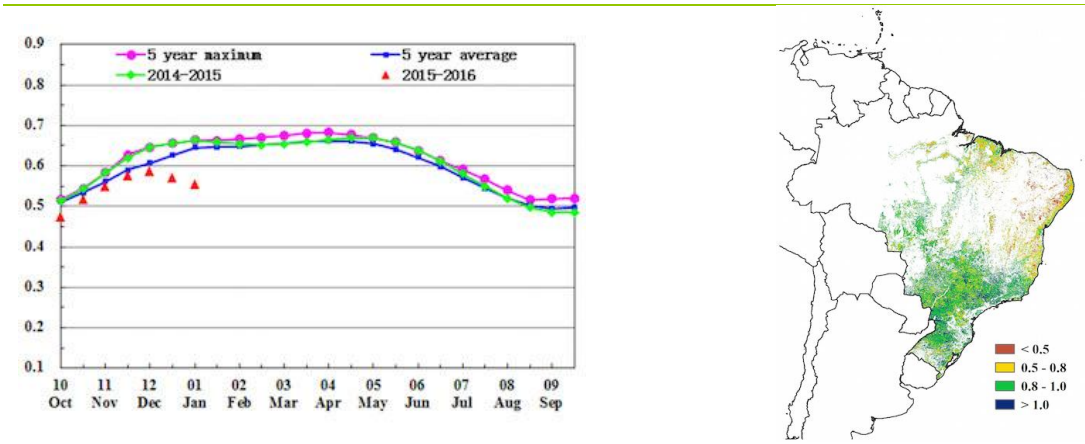

(a) Crop condition development graph based on NDVI (b) Maximum VCI

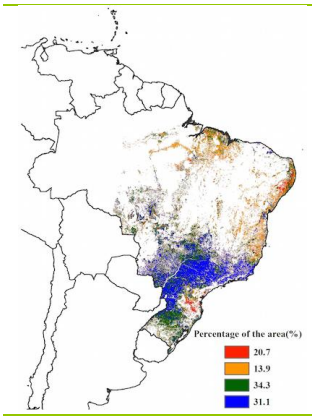

(c) Spatial NDVI patterns compared to 5YA

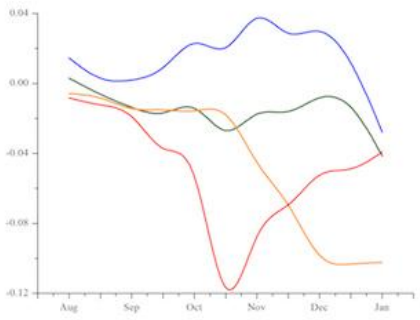

(d) NDVI profiles

[CAN] Canada

This monitoring period includes the end of the harvest of spring-summer crops, and all crops had been harvested by the end of November 2015. In general, the crop condition as assessed by the NDVI (Figure 3.9) looks average at this monitoring stage.

Warm yet dry agroclimatic conditions were common during the monitoring period. Rainfall over agricultural areas was 15% below average while temperature was significantly above (+2.4°C). As a result, soil moisture shortage may become a more serious issue due to continued drought, which may negatively affect the coming planting season in 2016. The RAIN and TEMP indicators for the three main agricultural provinces of Canada are as follows: Alberta, -17% and +2.1°C; Manitoba, +13% and +3.5°C; Saskatchewan, +3% and +3.2°C.

As mentioned in the last two CropWatch Bulletins, two of the major crop production provinces of Canada, Alberta and Manitoba suffered serious drought during the key growth stage of spring-summer crops, resulting in lower crop production in 2015; the relatively high NDVI values in this monitoring period may have resulted in the delayed harvest of summer crops in 2015.

The cropped arable land fraction (CALF) decreased by 2% compared to last five-year average.

Figure 3.9. Canada crop condition, October 2015-January 2016

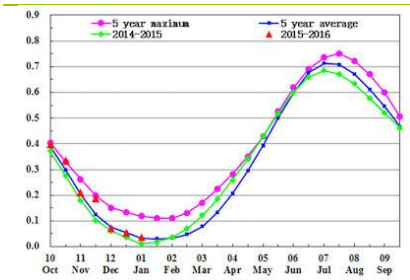

(a) Crop condition development graph based on NDVI

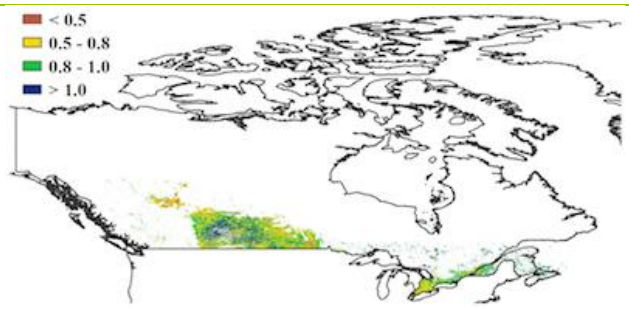

(b) Maximum VCI

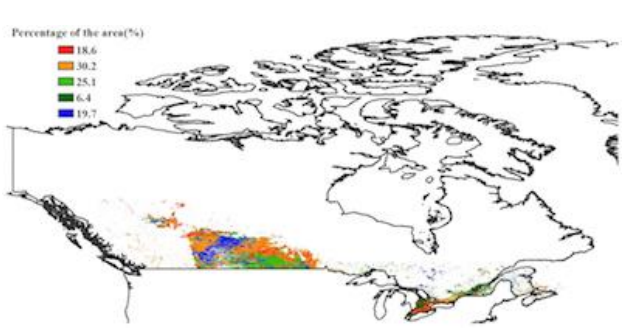

(c) Spatial NDVI patterns compared to 5YA

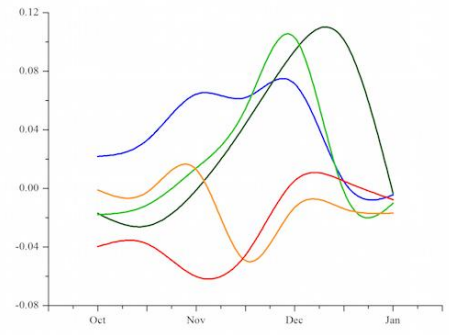

(d) NDVI profiles

[DEU] Germany

The crops in Germany showed below-average to above-average conditions (according to areas) during the reporting period from October 2015 to January 2016. This time period covers the late stages of sugar beets (October harvest) and early vegetative stages of winter wheat and winter barley (planted in October).

The Crop Watch agroclimatic indicators show above average rainfall and temperature (+3% and +1.7°C), and a 7% decrease in radiation. With positive moisture and thermal anomalies, biomass is expected to increase by 4% nationwide compared to the five-year average.

As shown by the crop condition development graph, national NDVI values were below average from October to early November due to lack of rainfall. National NDVI values started well above average and came close to the five-year maximum from mid-November to January, which is consistent with sufficient rainfall and suitable temperatures during this period. The spatial NDVI patterns also indicate that NDVI was above average from mid-November to January in 58.3% of arable land. This spatial pattern is also reflected by the maximum VCI in the different areas, with a VCIx of 0.93 for Germany overall. Generally, due to the suitable temperature and moisture conditions after mid-November, the agronomic indicators mentioned above indicate a favorable condition for most winter crop areas of Germany at the moment. Crops are nevertheless still vulnerable and the coming months may result in increased winter death due to poor hardening

Figure 3.10. Germany crop condition, October 2015-January 2016

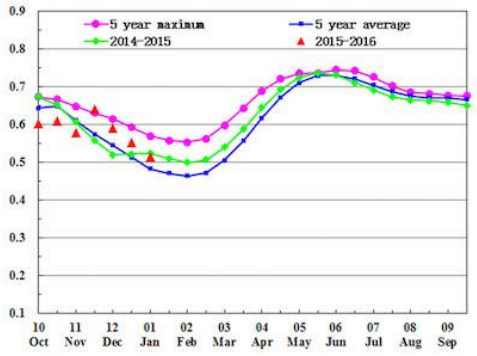

(a) Crop condition development graph based on NDVI

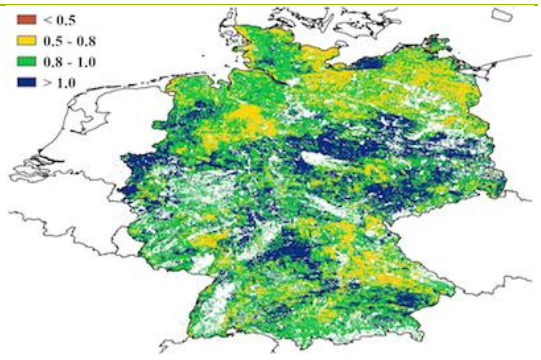

(b) Maximum VCI

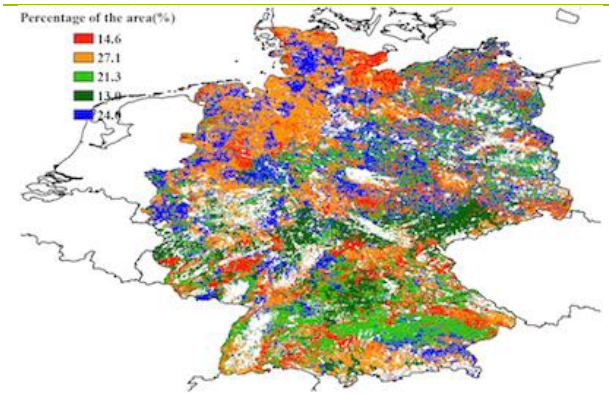

(c) Spatial NDVI patterns compared to 5YA

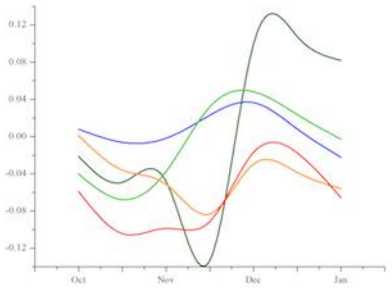

(d) NDVI profiles

[EGY] Egypt

During the monitoring period, summer crops had been harvested while winter crops were still growing. The crop condition development graph based on NDVI (Figure 3.11) indicates that crop condition was slightly below the recent five-year average at the national scale. As for the sub-national regions, poor crop condition occurred in the western Nile Delta and the Nile Valley until December 2015. Conditions improved in January at the margin of the western and south-western Nile Delta, as indicated by the spatial NDVI patterns and NDVI profiles. Altogether, 58.6% of crops were at an average level, mostly in the northern and eastern Delta.

The CropWatch agroclimatic indicators show that rainfall was above average by 32% while temperature and RADPAR were near and below average, respectively (+0.3°C and -5%). As a result BIOMSS increased 15% compared to average. Moreover, the value of the maximum VCI reached 0.89 at a national scale, with 0.8-1.0 in most regions of the Nile Delta and Valley and 0.5-0.8 in the southern Valley, as implied by the graph of maximum VCI. The cropped arable land fraction (CALF) was at the average level. Considering the fair crop condition and stable CALF, CropWatch estimates the yields of winter crops will be close to the recent five-year average level.

Figure 3.11. Egypt crop condition, October 2015-January 2016

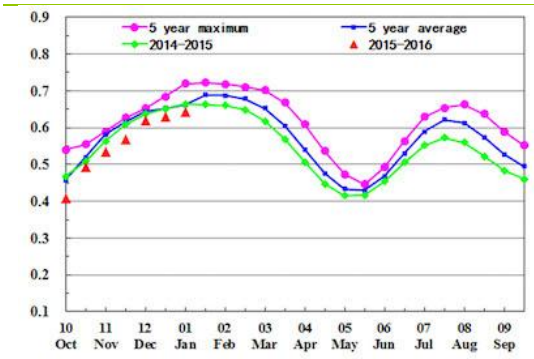

(a) Crop condition development graph based on NDVI

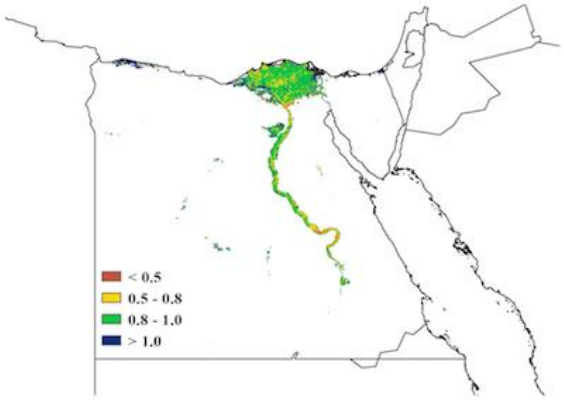

(b) Maximum VCI

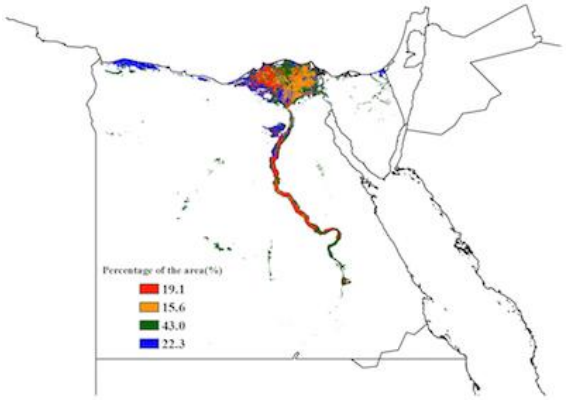

(c) Spatial NDVI patterns compared to 5YA

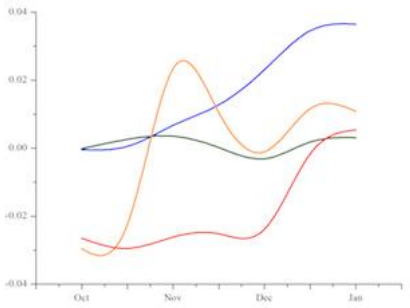

(d) NDVI profiles

[ETH] Ethiopia

The harvest of all major crops and Meher crops was completed in December 2015, leaving only some minor coarse grains to be harvested in January 2016. Over the reporting period, all agroclimatic indicators were about average, including seasonally low rainfall. Crop condition at the time of harvest was below the average of the previous five seasons, and marked regional differences can be identified based on NDVI profiles (Figure 3.12).

In general, conditions were average in western and southern areas representing about 50% of croplands. This includes the northwest lowland areas where sesame, roots and cereals are cultivated (rainfall +52%) as well as the south-western coffee-enset highlands (+16% precipitation). The other half experienced consistently below average conditions in particular in centre and east Oromia and in Tigray; the rainfall deficit was largest in the north-western sesame irrigated lowlands (-22%). In the south-eastern Mendebo Highlands (-12% to 156mm for the reporting period) rainfall was moderately below average, as well as in the mixed maize zone (-8% to 149mm). The cropped arable land fraction dropped 2% but this figure is difficult to interpret because of unusual crop condition and phenology. Overall, environmental and crop conditions were unfavorable.

Figure 3.12. Ethiopia crop condition, October 2015-January 2016

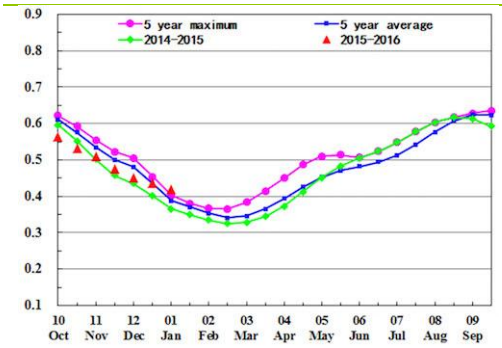

(a) Crop condition development graph based on NDVI

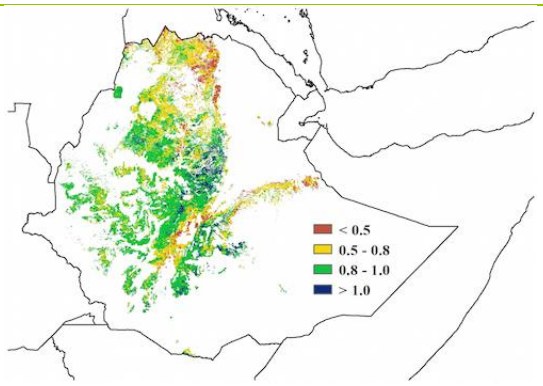

(b) Maximum VCI

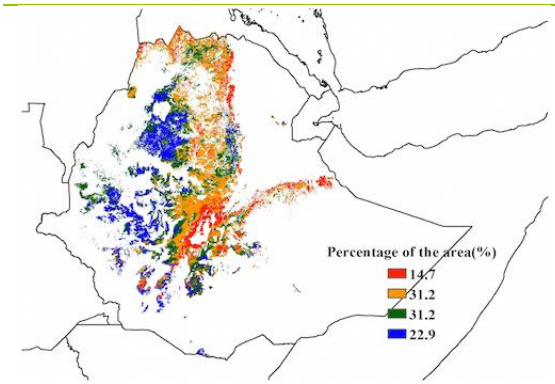

(c) Spatial NDVI patterns compared to 5YA

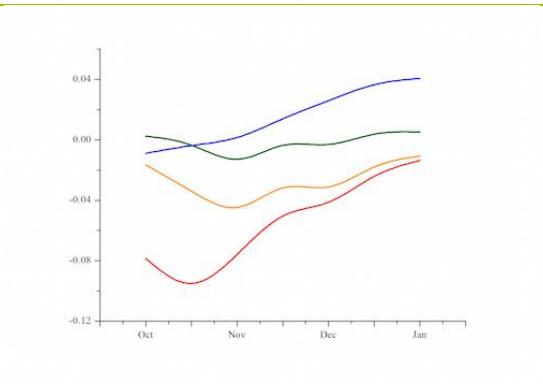

(d) NDVI profiles

[FRA] France

This report's monitoring period covers the late stages of sugar beets (October harvest) and the early vegetative stages of soft wheat and winter barley (planted in October). At the national scale, the CropWatch RADPAR indicator was average but TEMP and rainfall decreased by 0.9°C and 27% below average, resulting in a BIOMSS drop of 18% below the recent five-year average (Figure 3.13).

As shown by the NDVI profiles, however, national NDVI values were well above average and even above the five-year maximum from early November to January, consistent with a maximum VCI of 0.91 for France overall. The country's spatial NDVI patterns indicate a situation that on the whole is better than the five-year average, except in 27.4% of agricultural areas (3.6% + 23.8%) regions, including most of Limousin, Poitou-Charentes and north of Midi-Pyrenees, most of Lorraine and Alsace and east of Rhone-Alpes, which were influenced by water stress. Generally, the agronomic indicators mentioned above indicate favorable condition for most winter crop areas of France.

Figure 3.13. France crop condition, October 2015-January 2016

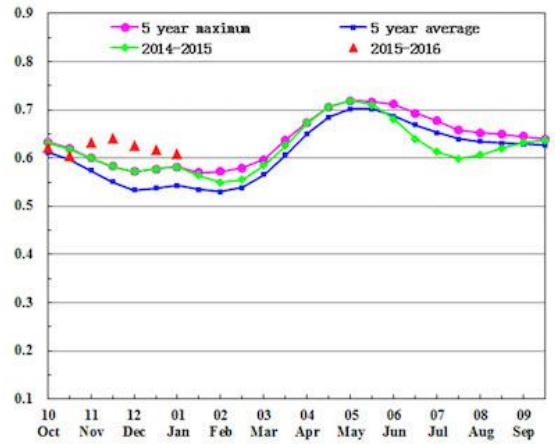

(a) Crop condition development graph based on NDVI

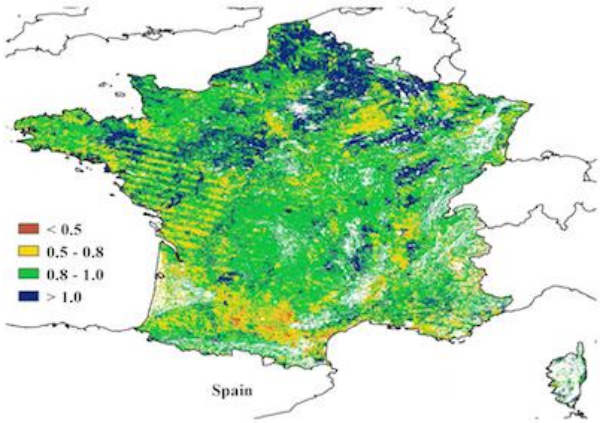

(b) Maximum VCI

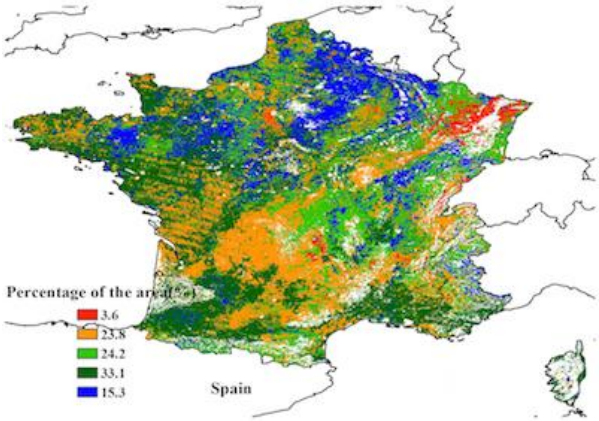

(c) Spatial NDVI patterns compared to 5YA

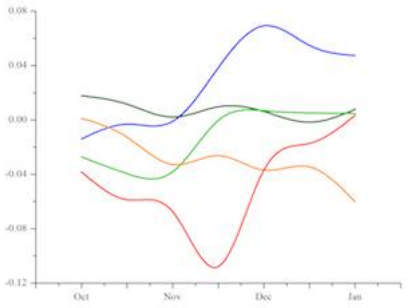

(d) NDVI profiles

[GBR]United Kingdom

Crops in the United Kingdom showed below average conditions during this reporting period. Summer crops (including sugar beets) have been harvested, and winter crops (winter wheat, winter barley and rapeseed) have been planted. The country experienced unusually favourable, and sometimes catastrophic, rainfall conditions with an increase of the RAIN CropWatch agroclimatic indicators (Figure 3.14) of 48% compared to average.

As shown by the NDVI profiles, national NDVI values were lower than average from November to January, but close to average by mid-October. According to the crop condition map based on NDVI, close to 65.9% of the country recorded lower than average NDVI from October to January. Only 34.1% of the region was higher than the average (Somerset, Wiltshire, Gloucestershire, Warwickshire, Northamptonshire, Leicestershire, West Midlands and Cheshire). This spatial pattern is also reflected by the maximum VCI in the different areas, with a VCIx of 0.92 for the country overall.

Temperature (TEMP, -0.7°C) and radiation (RADPAR, -13%) were below average. Due to excessive rain and low temperatures, BIOMSS decreased by 2% compared to the five-year average at the national scale, reflecting the above-mentioned crop conditions. Overall, the agronomic indicators currently show rather unfavorable conditions for the winter crop areas of the United Kingdom. The situation is likely to improve in spring.

Figure 3.14. United Kingdom crop condition, October 2015-January 2016

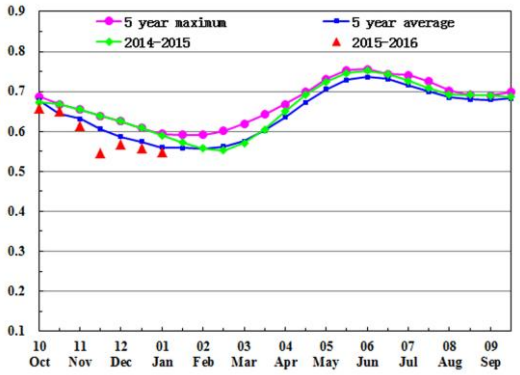

(a) Crop condition development graph based on NDVI

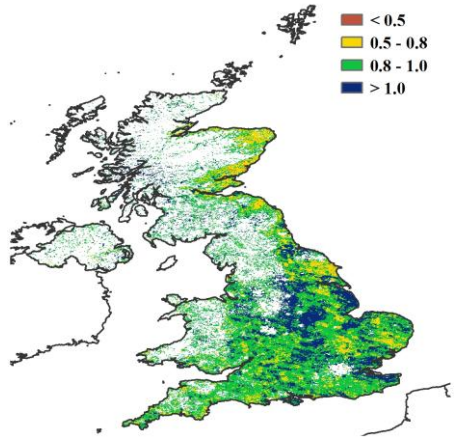

(b) Maximum VCI

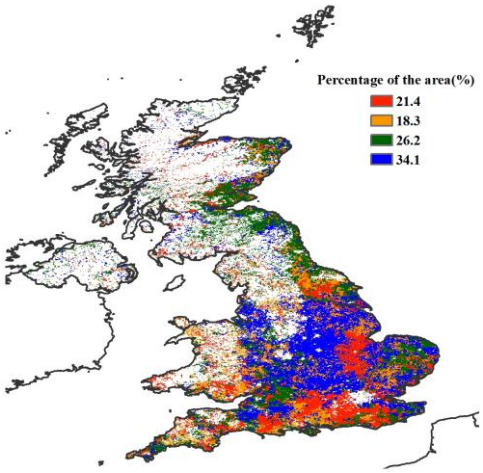

(c) Spatial NDVI patterns compared to 5YA

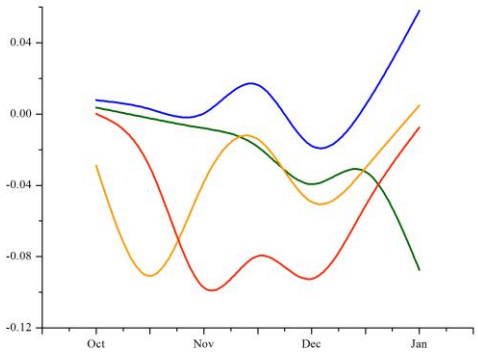

(d) NDVI profiles

[IDN] Indonesia

The crops in Indonesia generally showed poor condition between October and January. The monitoring period covers the harvesting stage of the dry season maize and rice, while wet season crops are currently in the field.

Compared with the recent average, precipitation was significantly below average (-24%) while the country enjoyed favorable PAR with values about 6% higher than average. As a result of the ongoing El Niño, the rainy season started late in Indonesia: dry and warm conditions had negative effects on rice planting, resulting in a drop of 21% in BIOMASS compared with the recent five-year average, which is confirmed by the national NDVI profiles showing poor crop condition in October and November (Figure 3.15).

According to the spatial patterns of NDVI profiles, NDVI behavior was very poor in most parts of Sumatra and central Kalimantan island during the whole monitoring period, and crop condition in Java and eastern islands of Indonesia recovered to average or above average in December and January. Altogether, CropWatch estimates that dry conditions have caused yield reduction to this season's crops.

Figure 3.15. Indonesia crop condition, October 2015-January 2016

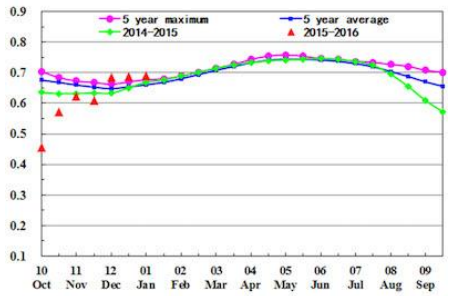

(a) Crop condition development graph based on NDVI

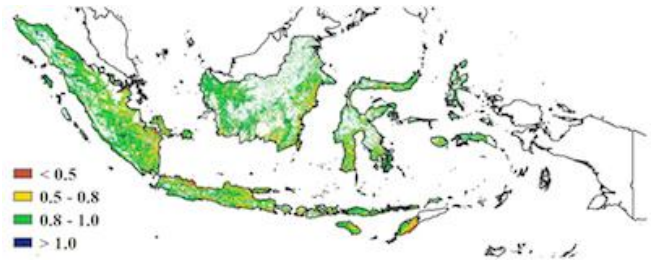

(b) Maximum VCI

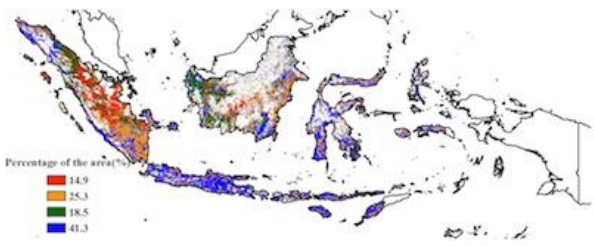

(c) Spatial NDVI patterns compared to 5YA

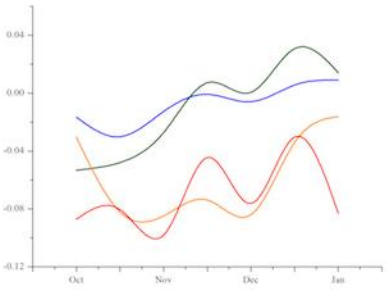

(d) NDVI profiles

[IND]India

The monitoring period covers mainly the harvesting season of Kharif crops. Crop condition development was below both the previous year and the five-year average. Rainfall (RAIN) was below average for the country including Assam (-16%), Bihar (-60%), Chhattisgarh (-59%), Gujarat (-56%), Goa (-11%), Himachal Pradesh (-34%), Jharkhand (-80%), Maharashtra (-21%), Madhya Pradesh(-39%), Odisha (-57%), Rajasthan(-42%), West Bengal(-73%) and Sikkim (-50%). Several states experienced above average rainfall including Tamil Nadu (+57%), Uttarakhand (+37%), Karnataka (+14%), Kerala (+7%), Haryana (+25%), Nagaland (+18%) and Mizoram (+70%).

Low rainfall triggered the negative (-18%) biomass accumulation (BIOMASS) for the country mainly in Bihar (-54%), Chhattisgarh (-57%), Gujarat (-64%), Himachal Pradesh (-27%), Jharkhand (-72), Maharashtra (-41%), Madhya Pradesh (-42%), West Bengal (-58%), Rajasthan (-58%) and Odisha (-48%). Temperature (TEMP, +0.6°C) and photosynthetically active radiation (RADPAR,-1%) were close to average.

In central and western India, both maximum VCI values below 0.5 and NDVI profiles indicate poor crop condition (Figure 3.16). Overall, deficit rainfall resulted in the poor crop condition for the country as a whole and reduced output is expected.

Figure 3.16. India crop condition, October 2015-January 2016

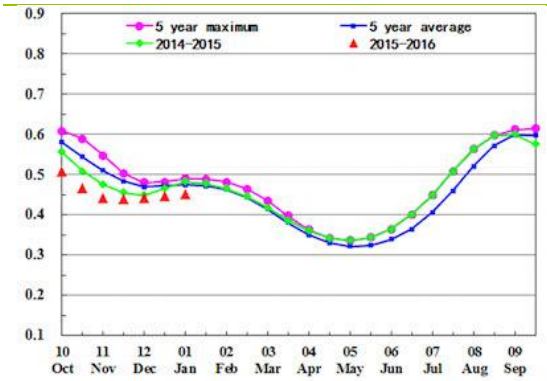

(a) Crop condition development graph based on NDVI

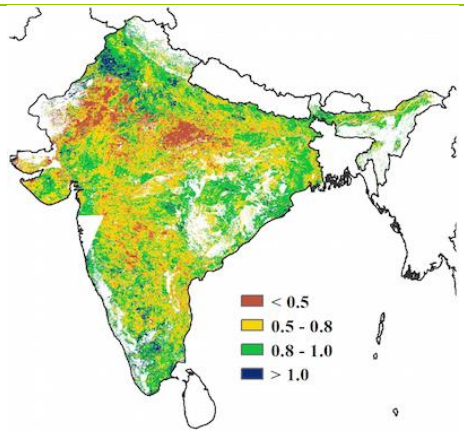

(b) Maximum VCI

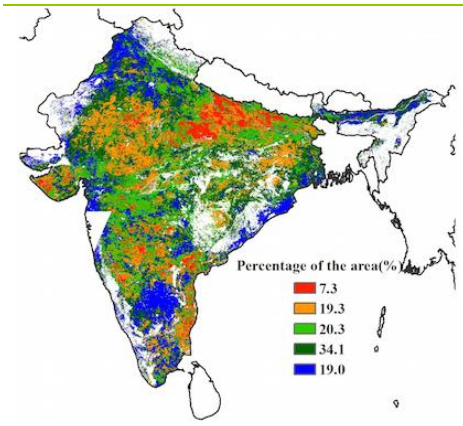

(c) Spatial NDVI patterns compared to 5YA

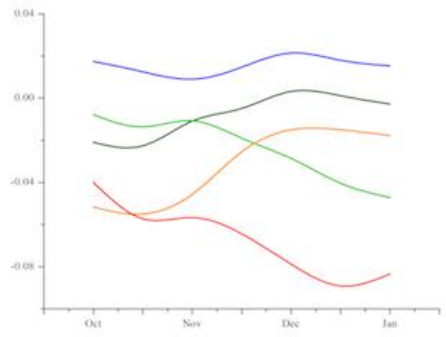

(d) NDVI profiles

[IRN] Iran

The crop condition was below average from November 2015 but recovered by January 2016. The planting of winter wheat has been completed while it was still underway for barley (to be completed at the end of January). Accumulated rainfall (+50%) was above average, but temperature (-0.3°C) and RADPAR (-5%) were below average.

The agroclimatic conditions (Figure 3.17) for the current season resulted in an increase of the BIOMSS index by 47%. The national average of VCIx (0.73) was above average conditions, and the CALF was close to the five-year average. Crop conditions were close to, or above, the five-year average in the Razavi Khorasan and North Khorasan provinces of the northeast region, and the Khuzestan and Fars province in the southwest region. The northwest region experienced crop conditions below the five-year average. In the central-northern region, particularly Mazandaran and Golestan provinces, the condition of crops was below the five-year average from October to the mid of November. Overall, the crop condition is mixed in the current season, however, the growth of winter crops will benefit from favorable soil moisture conditions in the coming months.

Figure 3.17. Iran crop condition, October 2015-January 2016

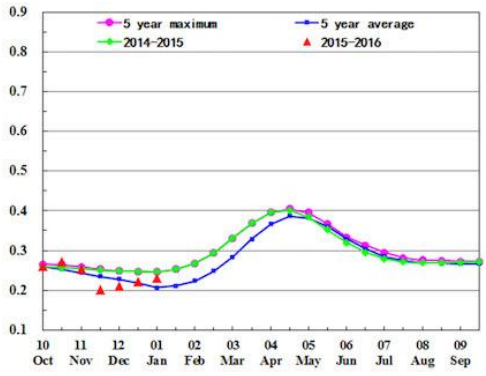

(a) Crop condition development graph based on NDVI

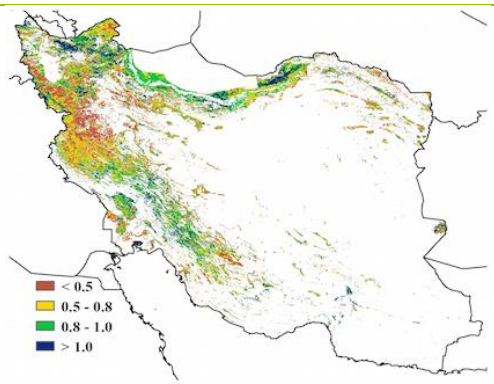

(b) Maximum VCI

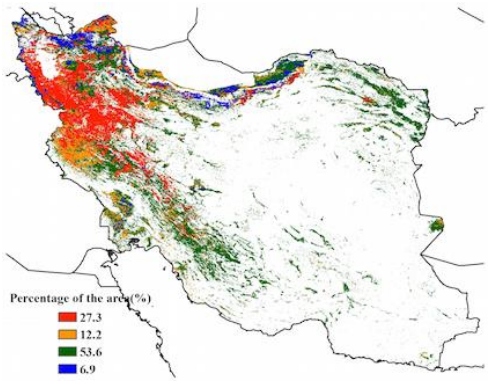

(c) Spatial NDVI patterns compared to 5YA

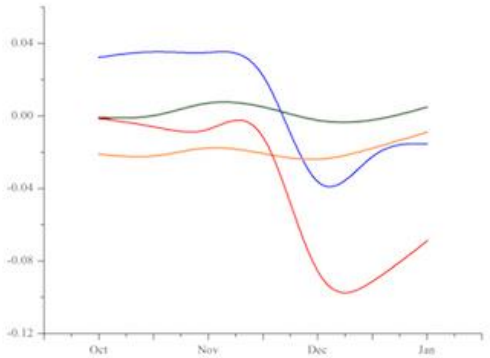

(d) NDVI profiles

[KAZ] Kazakhstan

This monitoring period covers the harvesting of last year's summer crops (cereals, spring barley and wheat) from October 2015 to mid January of this year. Among the CropWatch agroclimatic indicators (Figure 3.18), compared with average, rainfall showed a sharp increase (+52%) except for Almaty City area (where there was an 8% decrease), an increase in temperature (+1.1%) and a sharp decrease of RADPAR (-9%), which combined to yield above average BIOMASS (+12%).

The maximum VCI indicates that crop condition of most arable land in north Kazakhstan was below average (pixel values below 0.5). The NDVI clusters indicate that crops were in poor condition from October to middle December in the areas of Aktyubinskaya, Kustanayskaya, Severokazachstanskaya, Akmolinskaya, Pavlodarskaya, VostochnoKazachstanskaya and Almatinskaya Oblasts. No crop was planted since November and from December the NDVI index has been close to zero. The crop condition development graph also showed that crops were obviously worse off than last year and the average of the past five years, but favorable rainfall has provided the appropriate soil moisture for the initial stages of the forthcoming crops.

Figure 3.18. Kazakhstan crop condition, October 2015-January 2016

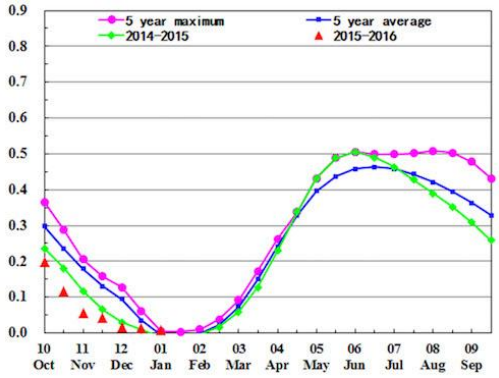

(a) Crop condition development graph based on NDVI

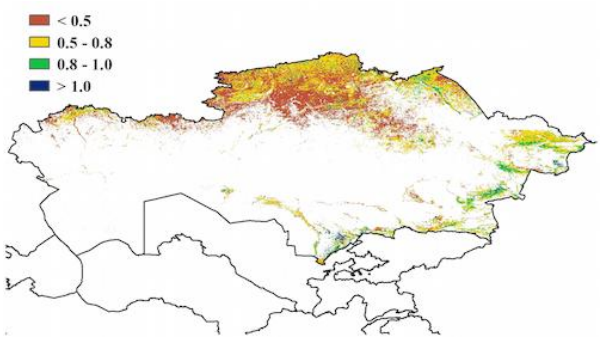

(b) Maximum VCI

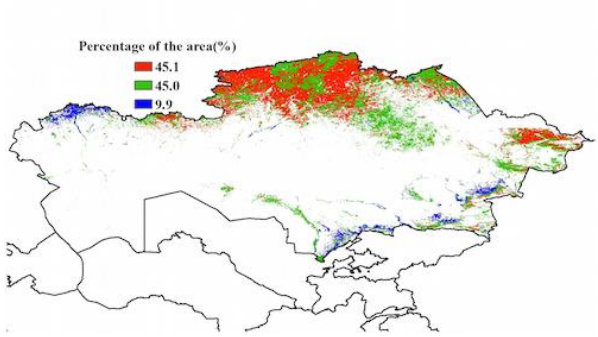

(c) Spatial NDVI patterns compared to 5YA

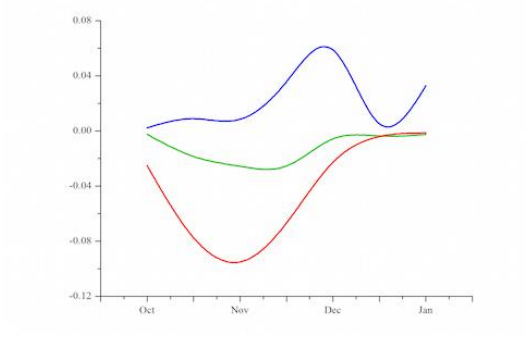

(d) NDVI profiles

[KHM] Cambodia

October to January covers the growing period of the main (wet season) rice crop, and the early stage of the second (dry season) rice in Cambodia. The fraction of cropped arable land was consistent with the average of the previous five years. Compared to average, the CropWatch agroclimatic indicators show markedly above average rainfall (+23%), a slight increase in RADPAR (+3%) and a temperature increase (+0.5°C).

Favorable conditions meant that the NDVI was near the last five-year average, with a small biomass decrease (-3%). Sufficient rainfall was beneficial for the sowing and emergence of the second rice. Vegetation condition indices (VCIx) are high (>0.8) in most parts of the country.

The condition of the crops in the country is average.

Figure 3.19. Cambodia crop condition, October 2015-January 2016

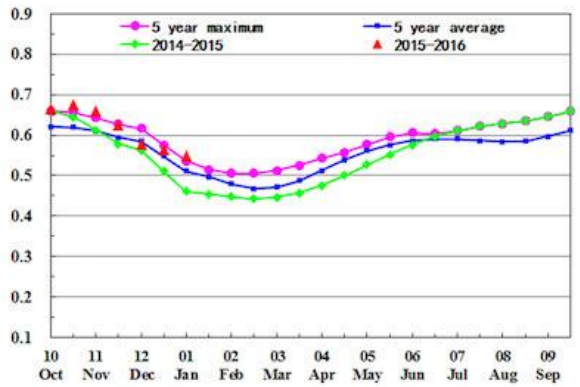

(a) Crop condition development graph based on NDVI

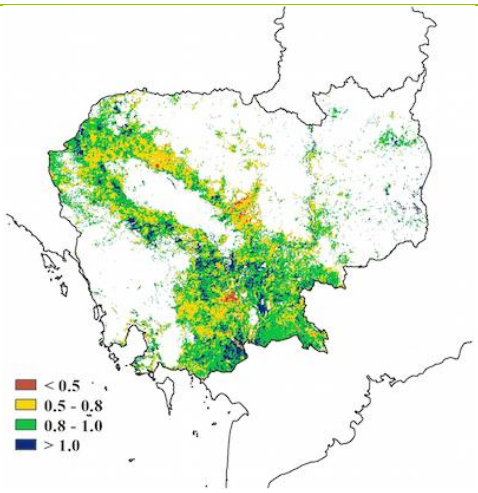

(b) Maximum VCI

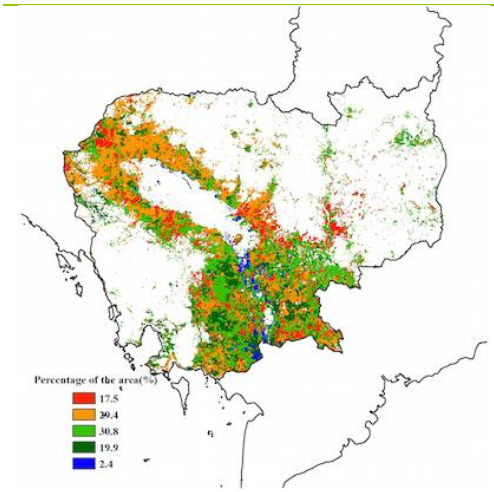

(c) Spatial NDVI patterns compared to 5YA

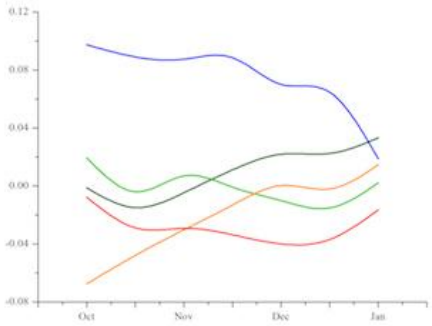

(d) NDVI profiles

[MEX] Mexico

The harvest of the 2015 main maize crop and the planting of the secondary maize as well as winter wheat were underway in Mexico during the reporting period. According to the crop condition development graph based on NDVI (Figure 3.20), crop condition was average from October to early December 2015 and close to the five-year maximum between late December 2015 and early January 2016, .

The CropWatch agroclimatic indicators show that rainfall and temperature increased respectively by 21% and 0.5°C when compared to the average while RADPAR decreased by 6%. The BIOMSS was far above average, with an increase of 49%. The value of maximum VCI was 0.81 at the national scale, with the highest values (0.8-1.0) occurring in southern, south-eastern and western Mexico, as indicated by the maximum VCI graph (Figure 3.20b). This pattern is consistent with that of NDVI profiles: 64.3% of crops were above or near average.

Considering the high values for NDVI and BIOMSS, above average crop output is expected.

Figure 3.20. Mexico crop condition, October 2015-January 2016

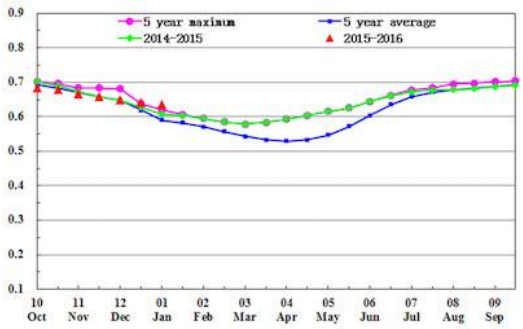

(a) Crop condition development graph based on NDVI

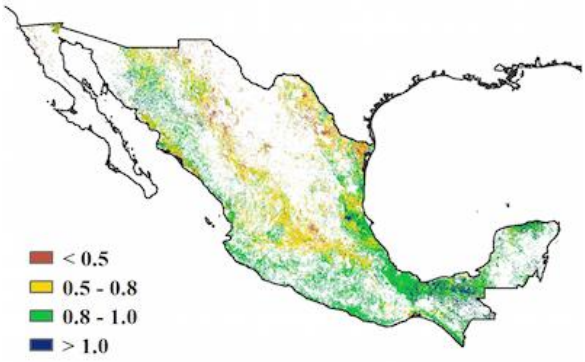

(b) Maximum VCI

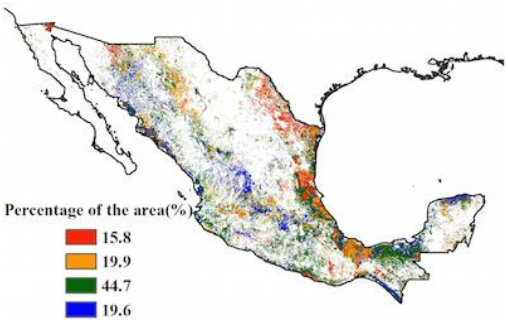

(c) Spatial NDVI patterns compared to 5YA

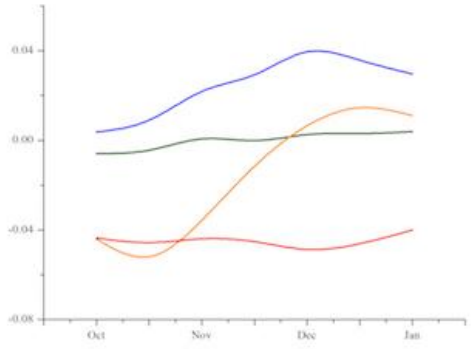

(d) NDVI profiles

[MMR] Myanmar

In Myanmar, the reporting period of October 2015 to January 2016 corresponds with the harvesting season of rice and planting season of maize and wheat.

Rainfall (RAIN) was 6% above average, temperature was only slightly below average (TEMP, -0.4°C) and radiation (RADPAR, -1%) was close to average. The biomass accumulation potential (BIOMASS) increased by 12% for the country (Figure 3.21).

National crop condition development profiles were mostly above average and exceeded the previous five-year average in early November. The maximum VCI below 0.5 was observed in scattered areas of central Myanmar; however, overall maximum VCI ranged 0.5 to 1, indicating favorable crop condition. The condition of crops is assessed as above average for the country.

Figure 3.21. Myanmar crop condition, October 2015-January 2016

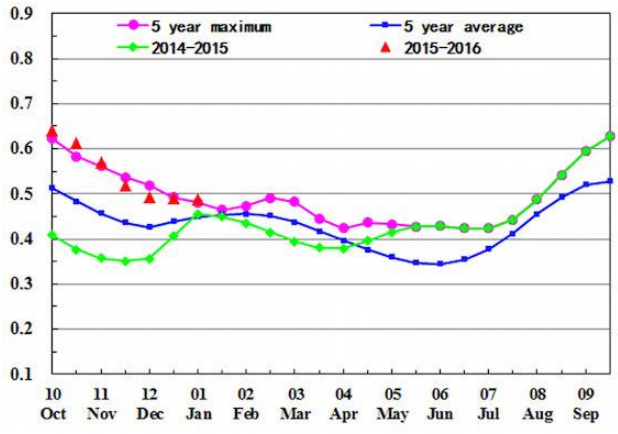

(a) Crop condition development graph based on NDVI

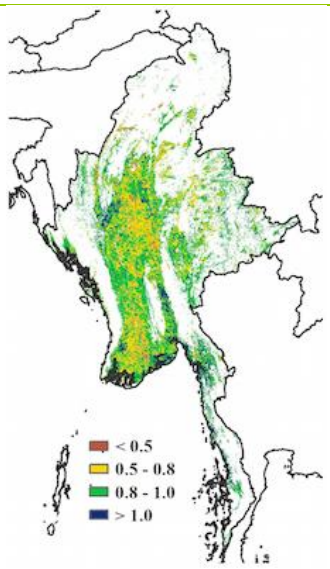

(b) Maximum VCI

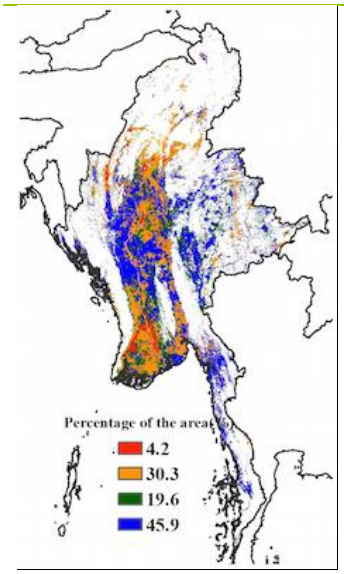

(c) Spatial NDVI patterns compared to 5YA

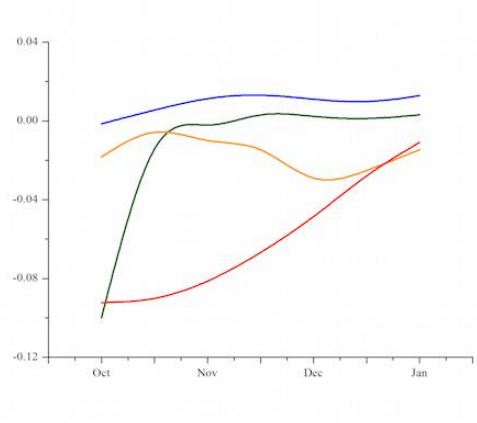

(d) NDVI profiles

[NGA] Nigeria

The reporting period coincides with the harvesting of all crops in Nigeria, as indicated by the decreasing national NDVI profiles, which reach their minimum around February 2016.

In general, NDVI was close to values observed during the previous season for the country as a whole as well as lower than the recent five-year average. RAIN and the cropped arable land fraction were slightly below average (-4% and -3%, respectively) although vegetation condition indices were fair.

Rainfall was slightly above average in the Sudano-Sahelian zone (+9%) and slightly below average elsewhere (-3 to -4%). Due to lower than average temperature, the expected biomass production potential is below average (-7% in the northern half of the country to -20% in the southern half). Below average crop condition affect 7.9% of the areas and concentrate in the southern half of the country, especially in the southwest (Moyo and east Ogun). Pockets of unfavourable conditions also occur in a scattered way in other areas throughout the country.

Altogether, crop condition was close to average (Figure 3.22).

Figure 3.22. Nigeria crop condition, October 2015-January 2016

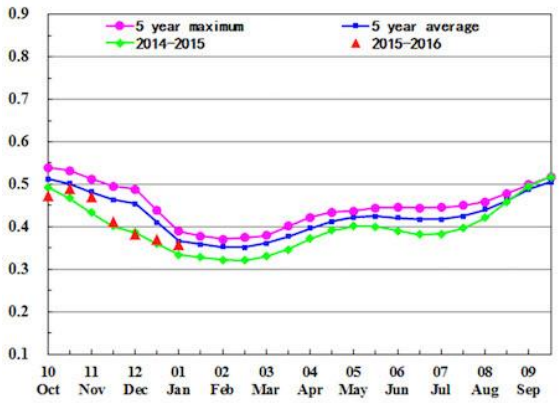

(a) Crop condition development graph based on NDVI

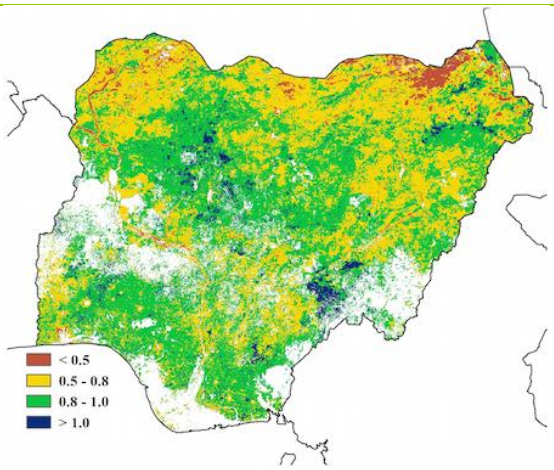

(b) Maximum VCI

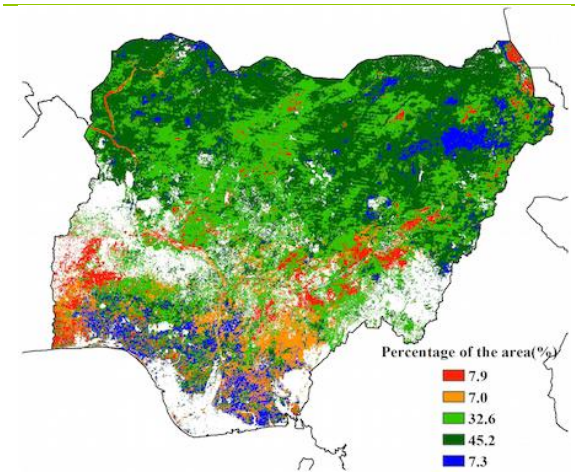

(c) Spatial NDVI patterns compared to 5YA

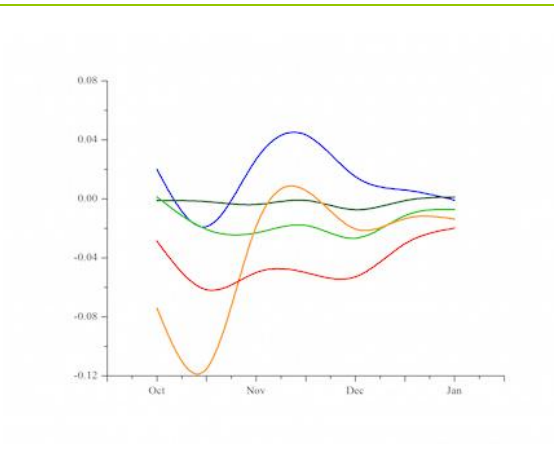

(d) NDVI profiles

[PAK] Pakistan

In Pakistan, the reporting time coincides with the sowing of winter crops (wheat, barley, oats, lentils and sugar beet) between October and December, and the harvesting time of maize, rice, cotton and soybean (autumn).

The agroclimatic indicators show an average value for rainfall (RAIN, +3%) and a slight decrease of radiation (RADPAR, -2%) compared to the average. Temperature was below average (TEMP, -0.8 C), while biomass production potential was above (BIOMSS, +18%). CALF decreased (-2%) below the five-year average.

The national NDVI development graph (Figure 3.23) indicates that crop condition was unfavorable in the month of November, but that it started gradually improving in December and that it later became comparable to the five-year maximum. The lowest maximum VCI values (<0.5) occur in North Baluchistan and Southeast Sindh. According to the NDVI profile, 63% of the cropped areas display above average conditions from December, much of it is in Khyber Pakhtunkhwa, FATA, Punjab and Sindh. Remaining areas (37% of land) show average conditions.

Altogether, crop condition is estimated to be above average.

Figure 3.23. Pakistan crop condition, October 2015-January 2016

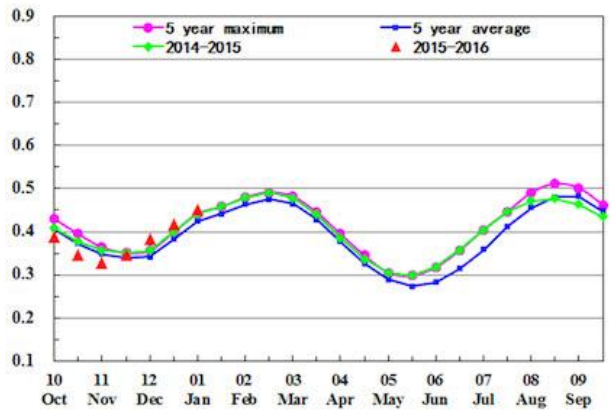

(a) Crop condition development graph based on NDVI

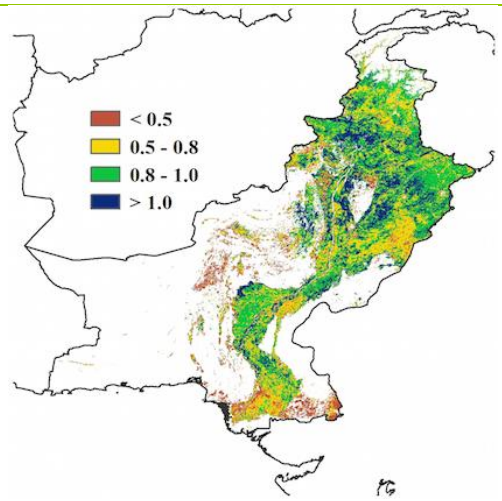

(b) Maximum VCI

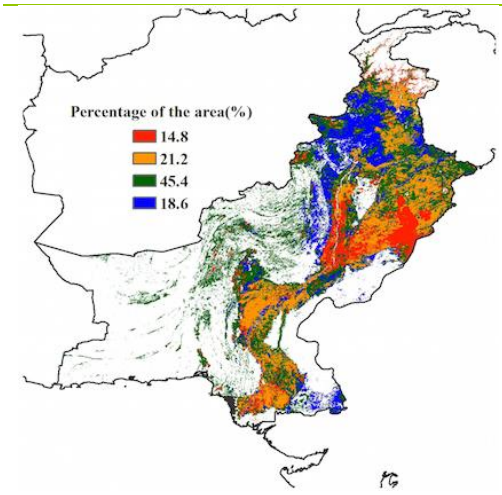

(c) Spatial NDVI patterns compared to 5YA

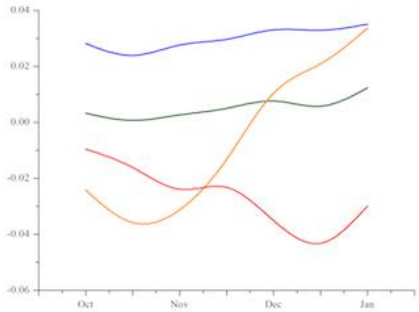

(d) NDVI profiles

[PHL] The Philippines

Crop condition in the Philippines was generally average for the monitoring period between October 2015 and January 2016. This period covers the harvesting stage of last year's main rice, as well as the sowing and growing stage of secondary rice and maize. Nationwide, PAR was above average by 10%, while rainfall decreased by 18%, mainly resulting from El Niño conditions. As a result of rainfall deficit, the biomass accumulation shows a significant 32% decrease compared to the most recent five years.

Considering the spatial patterns of NDVI profiles (Figure 3.24), crop condition in the Ilocos region and Cagayan Valley was below average in the second and third dekad of December. In addition, tropical cyclone Melor landed in Philippines in mid-December, bringing short-term heavy rainfall for the central islands and secondary rice suffered in some areas.

Altogether, the output of rice is expected to be below average.

Figure 3.24. Philippines crop condition, October 2015-January 2016

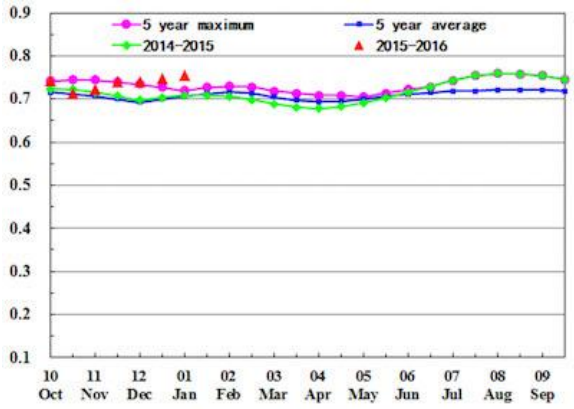

(a) Crop condition development graph based on NDVI

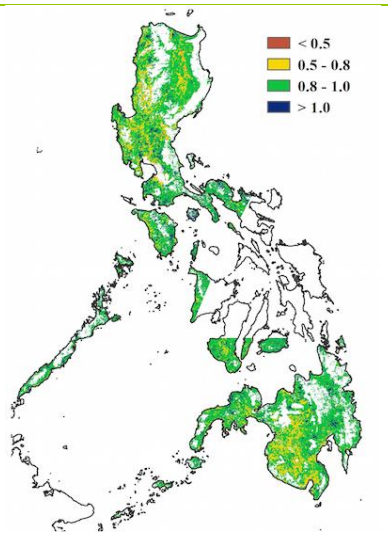

(b) Maximum VCI

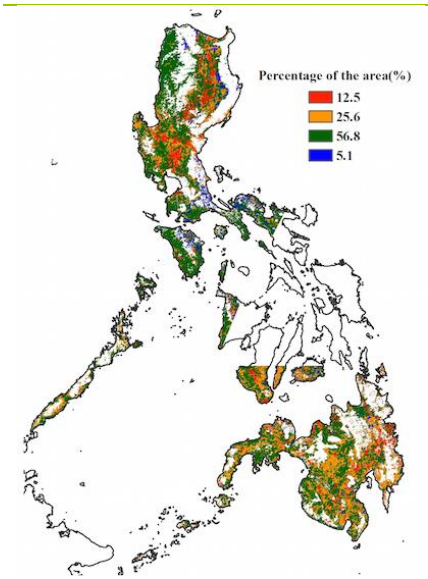

(c) Spatial NDVI patterns compared to 5YA

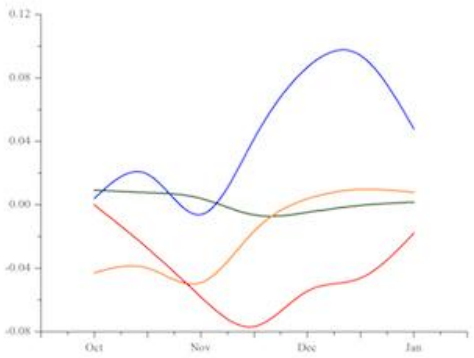

(d) NDVI profiles

[POL] Poland

In Poland this monitoring period witnessed the harvest of maize (before October) and the sowing of winter wheat. The cropped arable land fraction (CALF) was 3% below average. From October to January, the weather conditions improved from dry and cold conditions during the previous monitoring period. The rainfall departure was 1% and the temperature increased 0.2°C above average. RADPAR was average and the potential biomass was above average due to favourable weather conditions (Figure 3.25).

As shown in the NDVI condition development graph, due to the delayed sowing of winter wheat, the NDVI in October was lower than the five-year average and then significantly above average from November. This phenomenon is most apparent in the east of Poland, including Lubeiskie, Mazowieckie and Podlaskie.

In most other parts of Poland, NDVI was lower than average, especially in Dolnoslaskie and Opolskie.The VCIx in Poland during this monitoring period is 0.81.

Due to the unusual weather condition in Poland last summer, the outlook for the winter crop is cautiously optimistic.

Figure 3.25. Poland crop condition, October 2015-January 2016

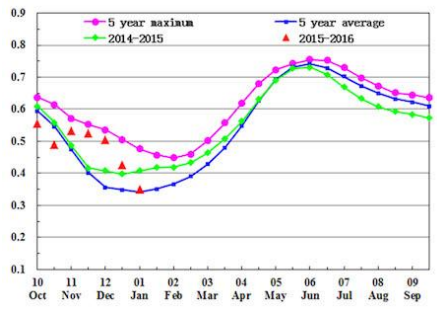

(a) Crop condition development graph based on NDVI

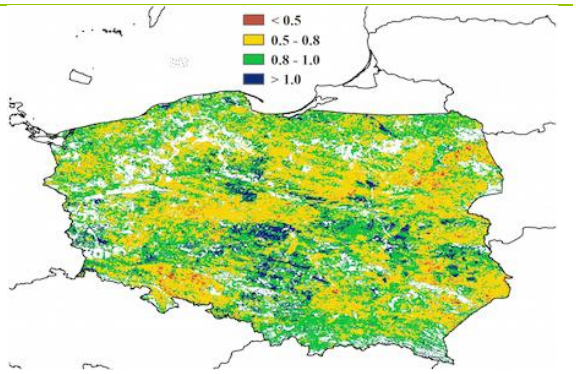

(b) Maximum VCI

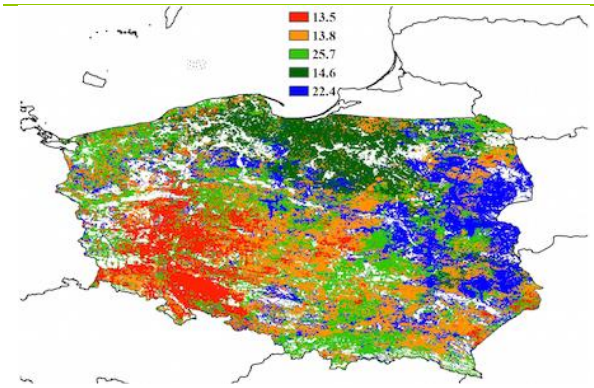

(c) Spatial NDVI patterns compared to 5YA

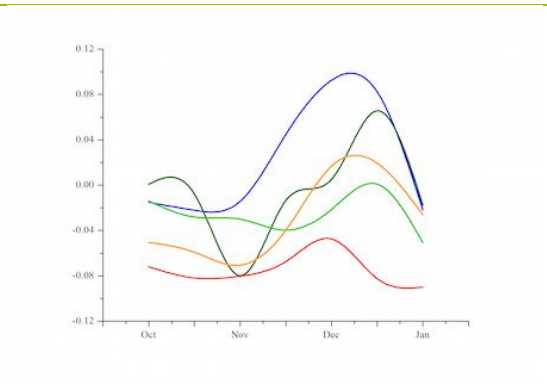

(d) NDVI profiles

[ROU] Romania

During this monitoring period, the maize harvest and sowing of winter wheat was completed before the end of October; the next three months are the early wintering period of crop. Cropped arable land dropped 5% compared with the last five-year average. Overall, the temperature increased when compared to the average (+0.9°C) while rainfall dropped (-9%). The potential biomass accumulation decreased 10% compared with the average of the last five years.

During this monitoring period, as shown in the NDVI development graph (Figure 3.26), due to the continued warm weather, the NDVI is significantly above last year's and close to the last five-year maximum. Most parts of Romania enjoyed favourable conditions from last summer except Satu Mare, Bihor, Timis and Hunedoara in the west of Romania. As the VCIx in Romania during this monitoring period is 0.88, the final assessment for Romania's output is just fair.

Figure 3.26. Romania crop condition, October 2015-January 2016

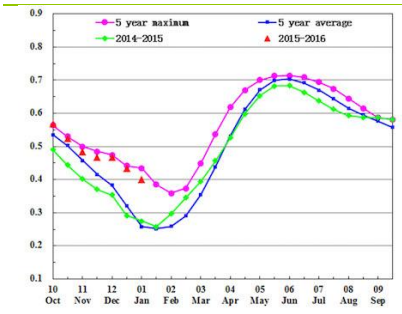

(a) Crop condition development graph based on NDVI

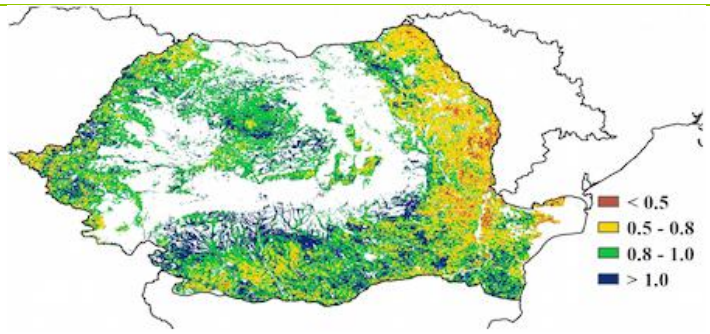

(b) Maximum VCI

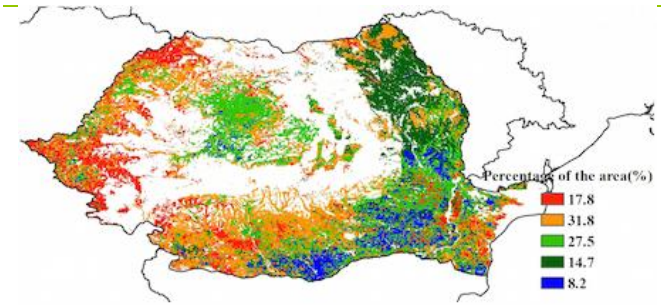

(c) Spatial NDVI patterns compared to 5YA

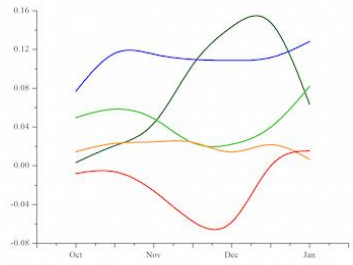

(d) NDVI profiles

[RUS] Russia

During the monitoring period, the sowing of winter wheat was delayed but nevertheless completed before November, while maize and spring wheat were harvested before October. Cropped arable land increased 4% compared to the last five-year average. Like the whole Central Europe to Western Russia region, the weather in Russia improved during this monitoring period from dry and cold. The rainfall departure was +16% and the temperature increased 0.3°C above average. The BIOMASS was average.

As shown in the NDVI development graph (Figure 3.27), due to the delayed sowing of winter wheat, the NDVI was first recorded as low but later began to recover from the end of November onwards. In the South Urals and Volga areas, due to the abundant rainfall (above 30% RAIN departure), the NDVI is above average for October and December. NDVI of cropland in the Caucasus, Central area, Kaliningrad, North Subarctic area, Northwest area and South Siberian area was significantly lower than average. The VCIx in Russia during this monitoring period was 0.66 and the outlook for Russian winter crops is below average.

Figure 3.27. Russia crop condition, October 2015-January 2016

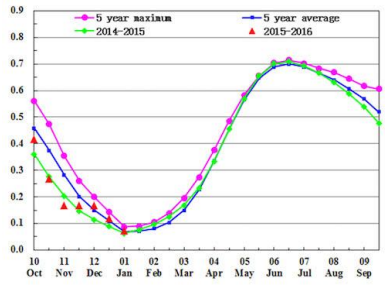

(a) Crop condition development graph based on NDVI

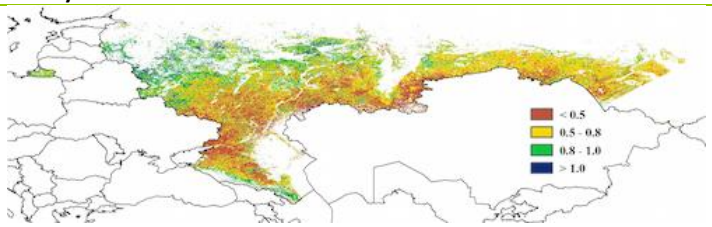

(b) Maximum VCI

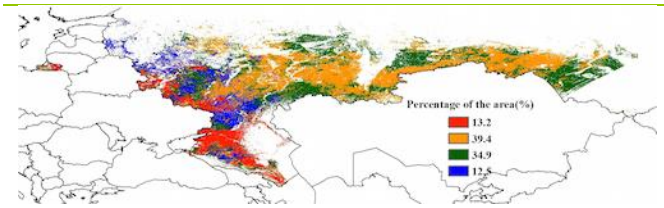

(c) Spatial NDVI patterns compared to 5YA

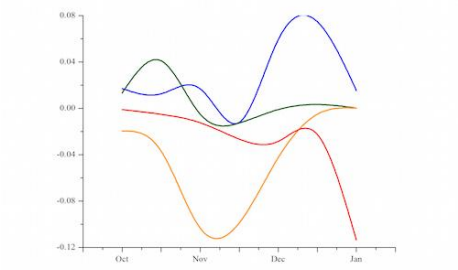

(d) NDVI profiles

[THA] Thailand

During the monitoring period in Thailand, the harvest of the first (main) rice crop started in October and was completed in January. Sowing of the second rice crop began in early January. According to agroclimatic and agronomic indicators (Figure 3.28), there was a slight increase in temperature (+0.4°C) and radiation (+1%) compared to the average, while rainfall was average. Based on the indices, the situation of crops during the reporting period was comparable to the previous five years, which is consistent with the decrease of the biomass index (-3%).

The NDVI profiles in the areas around the Chao Phraya river basin and southern region show decreased values below the average, while favorable crop conditions are found in the north-eastern and eastern regions, as well as in the south of the central region. The maximum VCI index displays a spatial pattern consistent with the NDVI cluster map in the central and northeast region; they present high values (>0.8) in the southern region. Generally, the crop production prospects are favorable.

Figure 3.28. Thailand crop condition, October 2015-January 2016

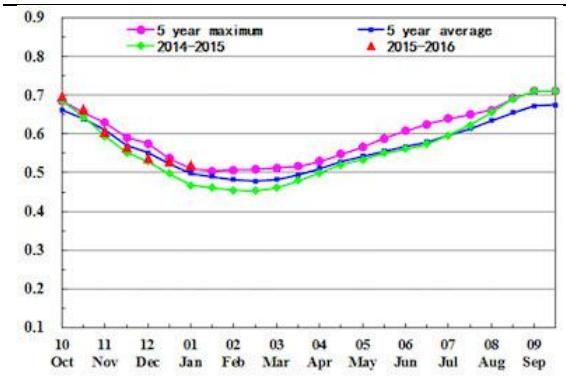

(a) Crop condition development graph based on NDVI

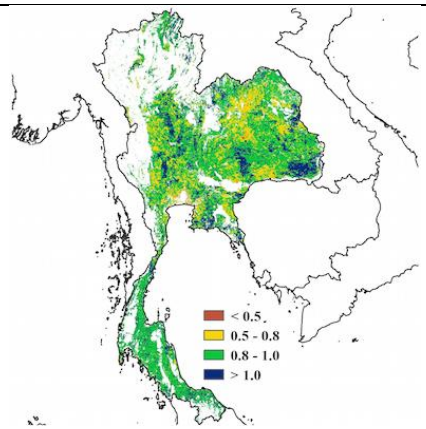

(b) Maximum VCI

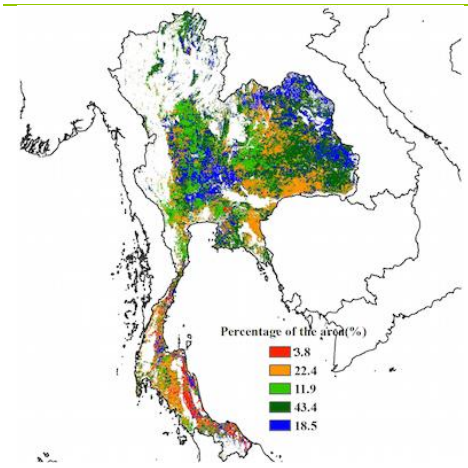

(c) Spatial NDVI patterns compared to 5YA

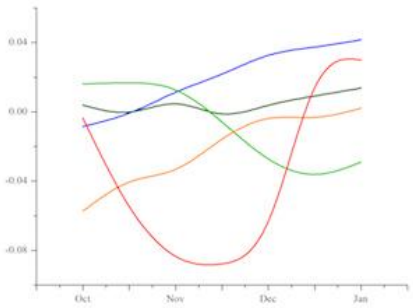

(d) NDVI profiles

[TUR] Turkey

From October 2015 to January 2016 the condition of crops was generally below average in Turkey. The planting of winter grains was completed, accumulated rainfall (-1%) and RADPAR were slightly below or close to average, while the temperature (+0.5°C) was above average.

The agroclimatic indices for the current season indicate unfavorable conditions for crop growth, which are confirmed by the decrease of the BIOMSS index by 12%. The map of maximum VCI (0.73 on average) presents a consistent pattern with the NDVI cluster map in the Central Anatolia Region. CALF decreased by 3% compared to the recent five-year average.

Crop condition in most areas across Turkey was below average from November during the whole monitoring period. Compared to the most recent five-year average, most areas in the Marmara Region, Aegean Region, Eastern and south-eastern Anatolia Region experienced favorable crop conditions from October to the mid of November, while unfavorable crop conditions prevailed in the Black Sea Region and Central Anatolia.

Overall, Turkey's current winter crop has been subject to unfavorable conditions so far. The final outcome of the season will be largely determined by soil moisture in March when vegetative grows will resume.

Figure 3.29. Turkey crop condition, October 2015-January 2016

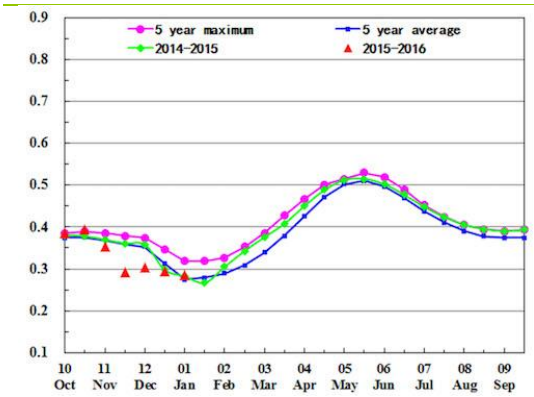

(a) Crop condition development graph based on NDVI

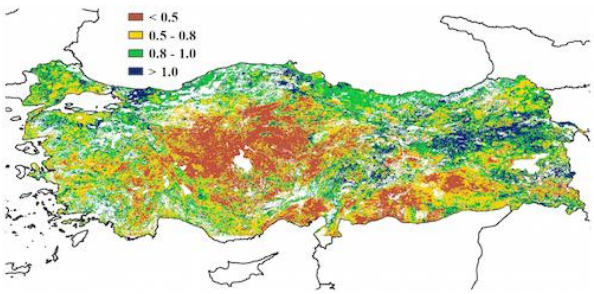

(b) Maximum VCI

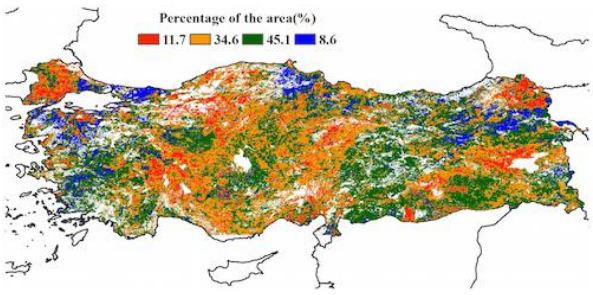

(c) Spatial NDVI patterns compared to 5YA

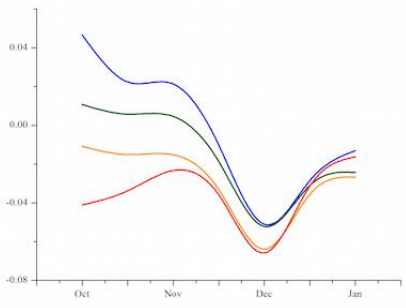

(d) NDVI profiles

[UKR] Ukraine

The planting of winter wheat in Ukraine concluded by mid-October and is currently in its dormancy period. Rainfall and radiation were slightly above average.

As illustrated in the section on the Central Europe to Western Russia MPZ, the decrease in potential biomass potential (as described by BIOMSS) is large in the southeast part of the country (-20%), while part of northwest and some patches in the southeast had favorable conditions with good average BIOMSS (>20%).

At the national level, a BIOMSS increase of 4% is expected. According to the NDVI profiles, crop condition in Ukraine is close to the reference five-year average with a maximum VCI index of 0.66. According to the spatial NDVI patterns and compared to the five-year average, southern and eastern areas of the country underwent unfavorable conditions (except for limited favorable patches) while northern, western and some central areas of the country showed favorable conditions in December through January, which is confirmed in the maximum VCI map (Figure 3.30). The pixels with values >1.0 in the VCI map indicate good crops in those areas.

Altogether, the situation of both autumn and winter crops has recovered from the poor conditions in the northwest but the situation is still poor in the south-eastern part of the country. The current expectation is that crop production will be close to or below average.

Figure 3.30. Ukraine crop condition, October 2015-January 2016

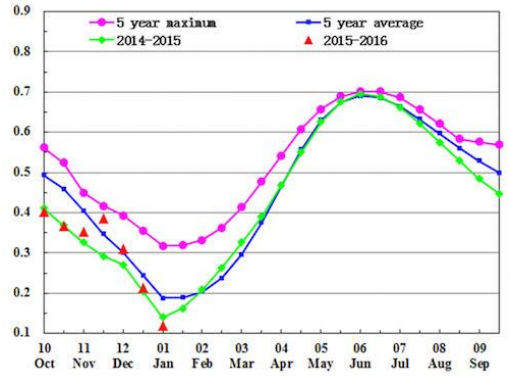

(a) Crop condition development graph based on NDVI

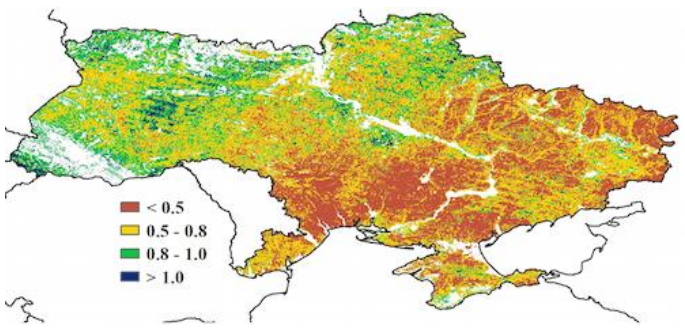

(b) Maximum VCI

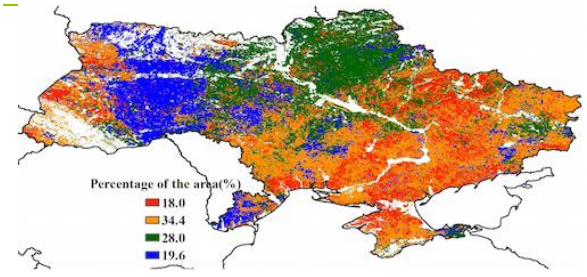

(c) Spatial NDVI patterns compared to 5YA

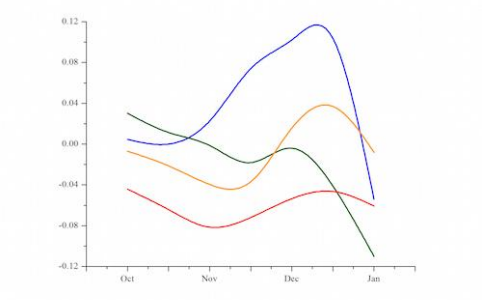

(d) NDVI profiles

[USA] United States

In general, crop condition was average in the United States over the CropWatch monitoring period, which covers the harvesting season of 2015 summer crops as well as the planting of 2016 winter crops.

Warm and wet agroclimatic conditions were common (Figure 3.31) with agroclimatic indicators showing significant positive departures of rainfall (+47%) and temperature (1.6°C). The main production zones for winter crops, the south of the Great Plains, enjoyed overly wet conditions (RAIN: +85%; TEMP: +0.9°C), including in Kansas (+35%), Oklahoma (+99%), northern Texas (+78%) and Nebraska (+75%). Although excess precipitation hampered farm operations, it improved soil moisture conditions to ensure growth of winter crops.

Serious flooding was recorded in the Mississippi River Basin and resulted from continued heavy rainfall in Tennessee (+78%), Arkansas (+88%), Iowa (+62%), Minnesota (+76%), Missouri (+86%), Nebraska (+75%), Oklahoma (+99%), Wisconsin (+59%) and the lower Mississippi region (+55%). Summer crops were harvested before the onset of the heavy rainfall and production losses are minimal, and abundant rainfall will benefit the planting of maize, soybeans and paddy in 2016. The cropped arable land fraction shows a positive departure of 2%.

Figure 3.31. United States crop condition, October 2015-January 2016

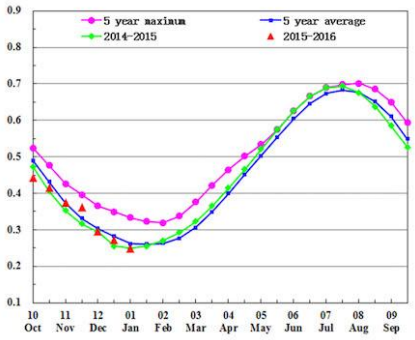

(a) Crop condition development graph based on NDVI

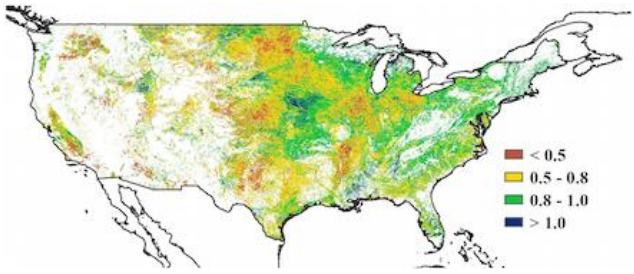

(b) Maximum VCI

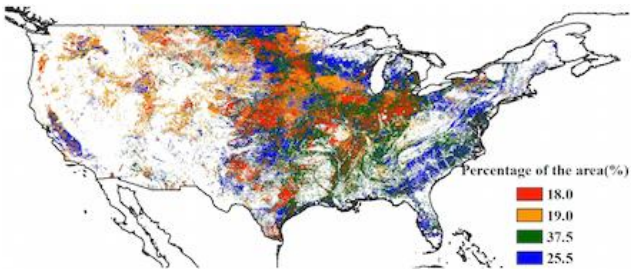

(c) Spatial NDVI patterns compared to 5YA

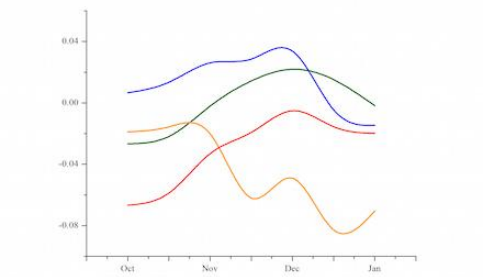

(d) NDVI profiles

[UZB] Uzbekistan

This monitoring period covers the sowing and early growing stage of winter cereals in Uzbekistan, mostly winter wheat and barley. The country as a whole enjoyed a sharp increase in rainfall (+59%) and biomass (+51%) with temperature being close to average while RADPAR (-9%) was below average (Figure 3.32).

Crop condition was favorable in many areas (such as Ferghana, Andijan, Tashkent, Samarkhand, Nawoiy, Denow, Sherabad and Termez) where the maximum VCI was mostly above 0.8.

Crop condition in 29% of arable land was below the five-year average from early December to early January. More precise spatial information is provided by the NDVI clusters, which show a sharp drop in late November, and a recovery thereafter in western and central areas of the country (Karakalpakistan, Shakhrisabz, Gulistan, Jazzakh and Tashkent). From December to January, crops benefited from abundant rainfall, leaving crop condition above average according to both crop condition development graphs and the NDVI cluster profiles (See Figure 3.32).

Figure 3.32. Uzbekistan crop condition, October 2015-January 2016

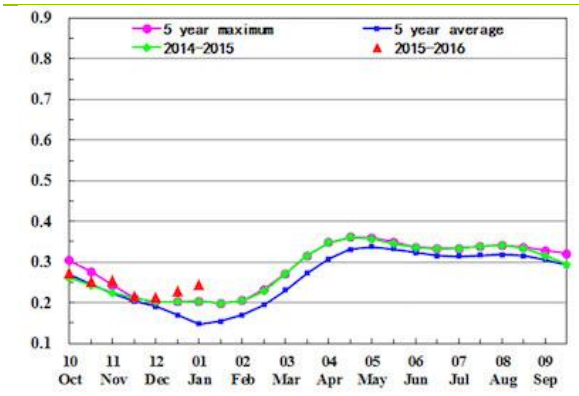

(a) Crop condition development graph based on NDVI

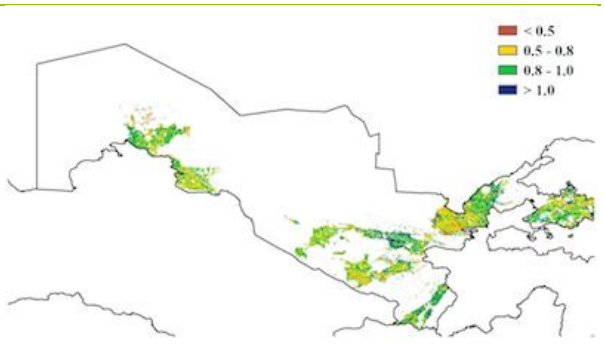

(b) Maximum VCI

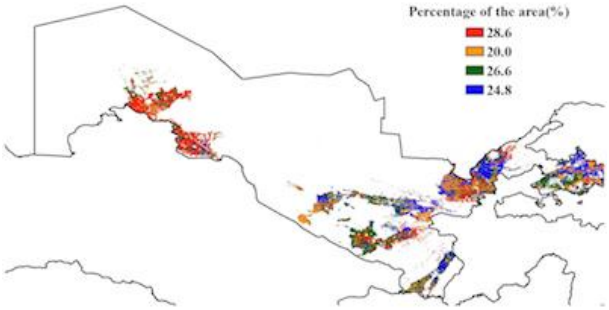

(c) Spatial NDVI patterns compared to 5YA

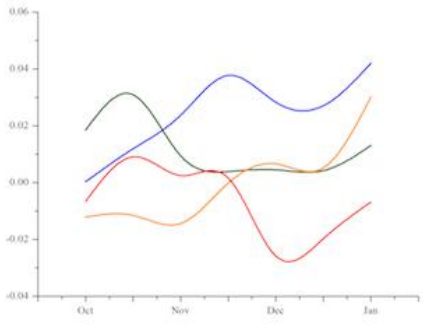

(d) NDVI profiles

[VNM] Vietnam

This monitoring period from October 2015 to January 2016 covers the growing stages of the 10th month rice, and the sowing of the winter and spring rice in Vietnam. Most of the rice cultivation regions are distributed in the northern Red River delta in the Mekong River delta in the south.

The fraction of cropped arable land was similar to the average of the previous five years. Vegetation condition indices (maximum VCI) were favorable (>0.8). For the period under consideration, the CropWatch agroclimatic indicators show below average rainfall (-8%) and a slight decrease in radiation (-1%) with increased temperature (+0.9°C), leading to the increase of biomass (+13%). Crop condition was at the five-year average, and slightly lower than five-year maximum.

Correspondingly, the profiles of NDVI clusters (Figure 3.33) also show most of the country (mainly at the Mekong River delta) are experiencing favorable crop condition.

Figure 3.33. Vietnam crop condition, October 2015-January 2016

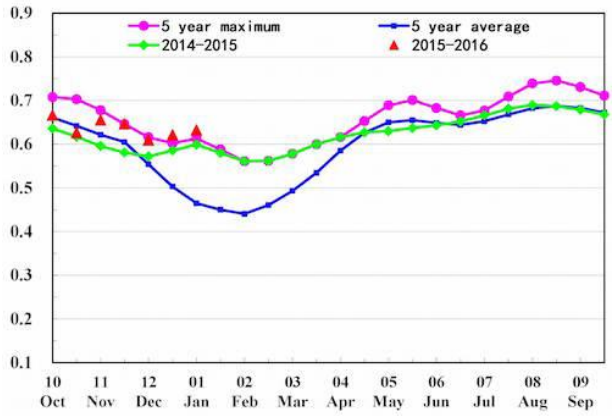

(a) Crop condition development graph based on NDVI

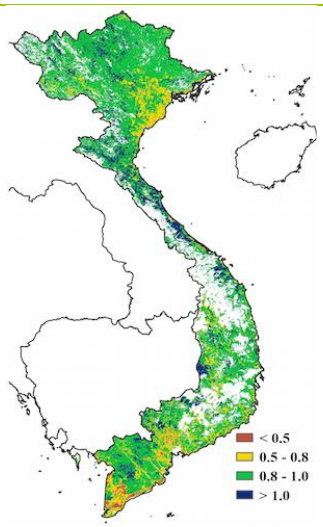

(b) Maximum VCI

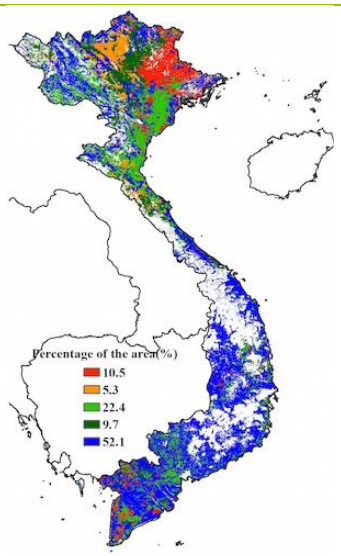

(c) Spatial NDVI patterns compared to 5YA

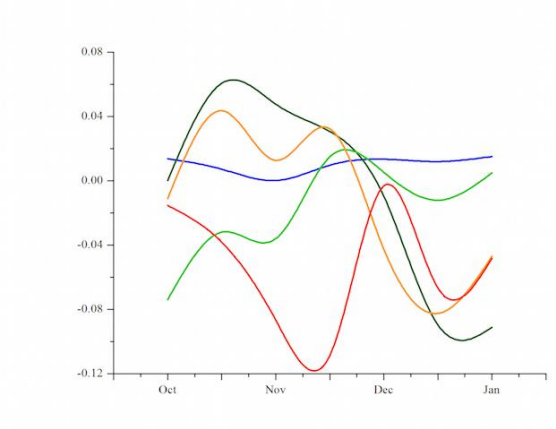

(d) NDVI profiles

[ZAF] South Africa

Winter crops, essentially barley and wheat, were harvested in November and December, and the summer crops have reached mid-season stages by the end of this reporting period. Nationwide, rainfall from October was well below average (-26%), with slightly above-average temperature (+1.4°C) and increased radiation (+1%). For the period under consideration, and compared with the previous five cropping seasons, the biomass production potential fell 27% and cropped arable land fraction value was 12% below the reference values.

VCIx did not exceed 0.48. Conditions are close to average (but deteriorating) in about one third of agricultural areas only which, at the time of reporting, include Eastvaal district in Mpumalanga and Westcoast district and the southern Western Cape. The least favourable conditions are recorded in about 21% of cropped areas, especially in the northern Free State. They extend into the north-western province. The driest areas suffered most in relative terms, with biomass production potential drops between 25% and 75% according to zone. Given the overall rather gloomy prospects for the current summer season, especially maize, in South Africa, it is worth nothing that a relative improvement has affected about 10% of the national cropland, mostly in Kwazulu-Natal in December and January, where NDVI however remains below average. With national NDVI values 0.2 units below average, prospects for the current summer crop can only be poor to very poor. Refer to section 5.2 for additional detail.

Figure 3.34. South Africa crop condition, October 2015-January 2016

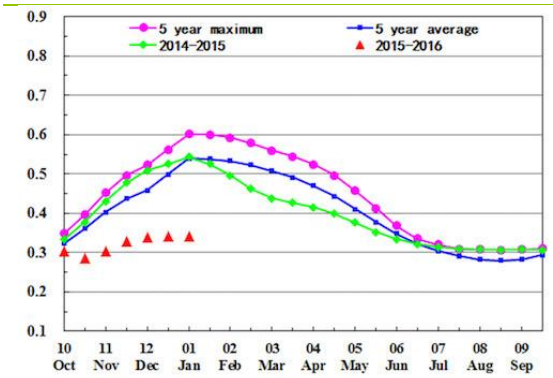

(a) Crop condition development graph based on NDVI

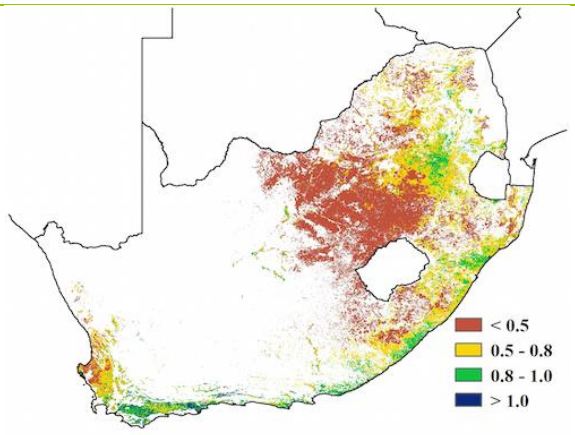

(b) Maximum VCI

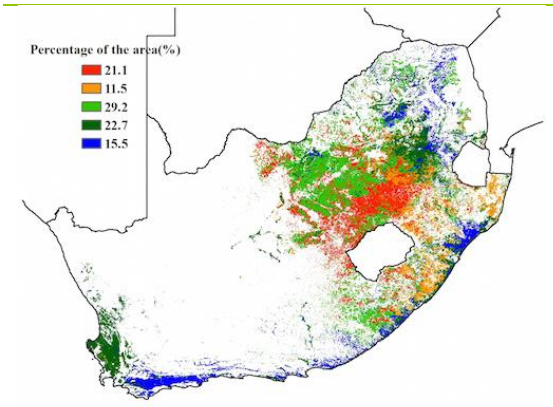

(c) Spatial NDVI patterns compared to 5YA

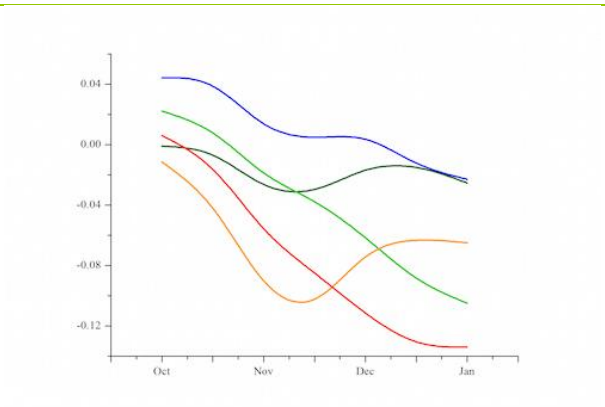

(d) NDVI profiles

Chapter 4.China

Chapter 4 presents a detailed analysis for China, focusing on the seven most productive agro-ecological regions of the east and south. After a brief overview of the agroclimatic and agronomic conditions over the monitoring period (section 4.1), section 4.2 looks at the outlook of prices for domestic crops, while section 4.4 presents analyses by region. Additional information on the agroclimatic indicators for agriculturally important Chinese provinces are listed in table A.11 in Annex A.

4.1 Overview

In China, the beginning of the reporting period for this bulletin, October, is the major planting period of winter crops including winter wheat and rapeseed, following on from the harvesting of the autumn crops.

From October 2015 to January 2016, agroclimatic conditions were generally favourable (Figures 4.1 and 4.2). Specifically, above average temperature was beneficial for winter crops' survival during winter. It is noteworthy that 85% above average rainfall was observed, accompanied by 12% below average RADPAR. Altogether, favorable agroclimatic conditions resulted in a 41% above average potential biomass in China.

As indicated in Table 4.1, the 2015-2016 winter was generally warm and wet with temperature above average in all seven regions and rainfall 60% or more above average. Spatially, rainfall patterns in China can be assigned to two categories: (1) slightly above average rainfall from October to January in most areas north of Yangtze River and (2) significantly above average rainfall in early October, mid-November, early December and early January in the areas south of Yangtze River. Temperature departure from average followed similar temporal patterns throughout the whole of China. Extreme low temperatures hit the whole country in late November as well as mid-January, but since it was wintering period for crops, the impact of the cold waves in terms of agricultural loss was limited.

Table 4.1. CropWatch agroclimatic and agronomic indicators for China, October 2015-January 2016, departure from 5YA and 14YA

Region	Agroclimatic indicators			Agronomic indicators		
	Departure from 14YA (2001-14)			Departure from 5YA (2010-14)		Current
	RAIN (%)	TEMP (°C)	RADPAR (%)	BIOMSS (%)	CALF (%)	Maximum VCI
Huanghuaihai	63	0	-9	43	0	0.78
Inner Mongolia	122	0.7	-4	41	1	0.60
Loess region	88	0.8	-6	58	-1	0.69
Lower Yangtze	110	0.4	-22	58	0	0.87
Northeast China	59	0.8	-3	9	2	0.76
Southern China	93	0.2	-14	51	0	0.90
Southwest China	69	0.6	-10	33	0	0.91

Note: Departures are expressed in relative terms (percentage) for all variables, except for temperature, for which absolute departure in degrees Celsius is given. Zero means no change from the average value; relative departures are calculated as (C-R)/R*100, with C=current value and R=reference value, which is the five (5YA) or fourteen-year average (14YA) for the same period (October-January).

Maximum VCI (VCIx, Figure 4.4) was distributed unevenly, resulting from complex agroclimatic situations. Crops in northeast China, Inner Mongolia, and southern China are off growing season and vegetation condition monitoring is irrelevant in those regions. High VCIx values occurred mostly in Sichuan and Central Hebei province. Low VCIx values are mainly located in the North China Plain and north-western region. The low VCIx in those regions results from below average crop development before wintering period due to the low temperature in late October and late November 2015. Thanks to abundant rainfall

during the wintering period, warm temperatures will activate winter crops to catch up with normal crop phenology.

Cropped arable land fraction (CALF) was at the recent five-year average level. The Loess region is the only one out of the seven regions with 1% lower CALF when compared to the five-year average. Cropped and uncropped land (Figure 4.3), was determined based on China Environmental Satellite images (HJ-1 CCD) and China high-resolution satellite images (GF-1).

Total winter crops' planting was the same as during 2014-2015. Areas planted with winter crops in Gansu, Shandong and Sichuan were 1.4%, 3.3% and 1% lower than last year's season, respectively. Increased planting was observed in other major producing provinces, for example in Shaanxi and Shanxi the area increased by more than 2%. Assuming average agroclimatic conditions and normal farm management, winter crops production will be slightly above levels observed in the 2014-2015 season. Due to the significant drop of planted area, winter crop production in Shandong province is foreseen to decrease. CropWatch will provide a first production forecast for winter crops in the May Bulletin.

Figure 4.1. China spatial distribution of rainfall profiles

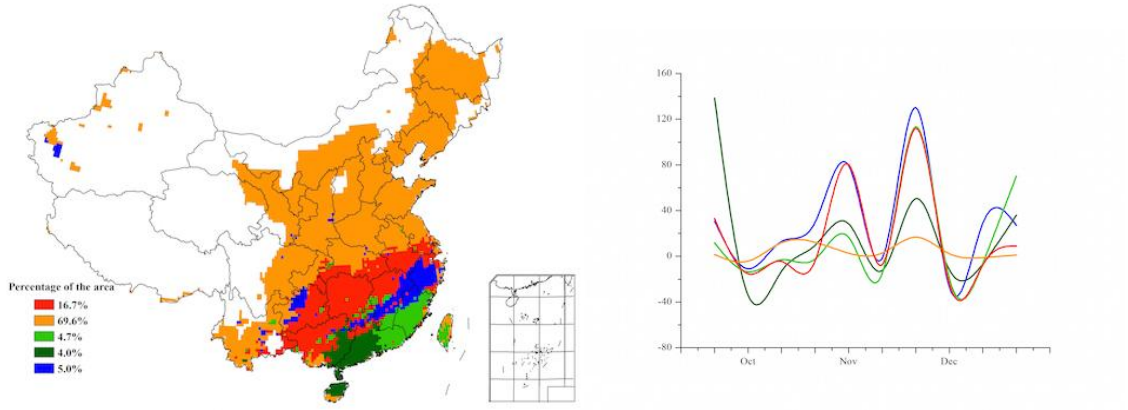

Figure 4.2. China spatial distribution of temperature profiles

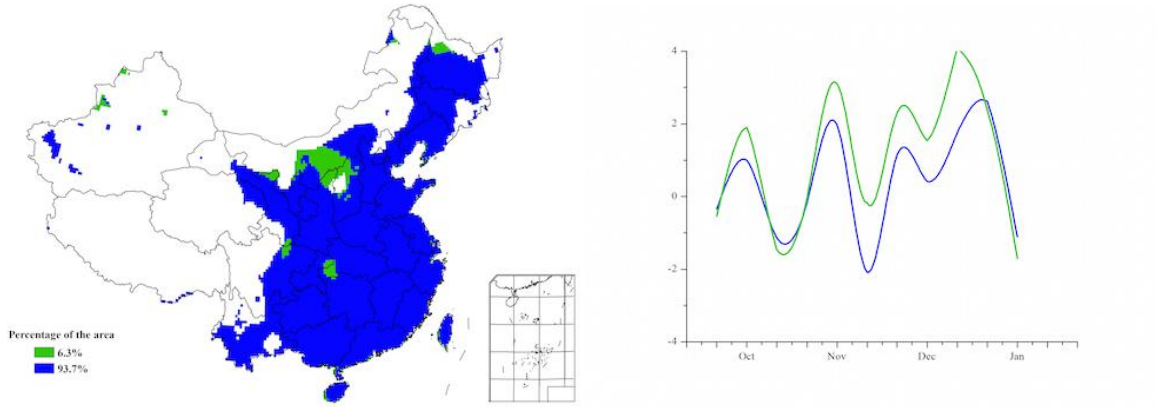

Figure 4.3. China cropped and uncropped arable land, by pixel

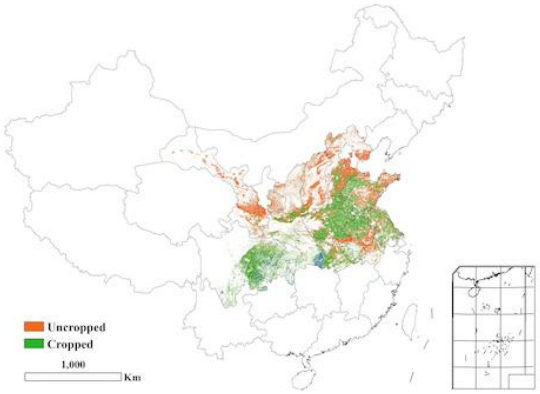

Figure 4.4. China maximum Vegetation Condition Index (VCIx), by pixel

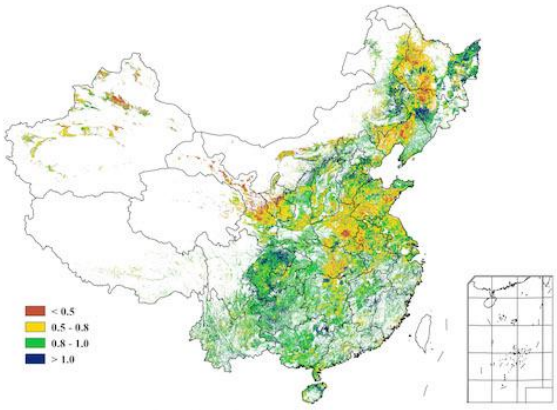

4.2 Outlook of domestic price of four major crops

Historical domestic prices of soybean from January 2004 to December 2015 were analysed based on the theory of price spiral model (PSM) (Fang, 2011) and the historic ratio of world soybean consumption to the global soybean production (consumption ratio). According to the data for the last six months (Figure 4.5), the soybean international consumption ratio is at equilibrium. Domestic soybean prices are also at equilibrium but with a downward trend. They are anticipated to continue fluctuating within an equilibrium interval while also maintaining the negative trend.

Figure 4.5. Historical soybean data from January 2004 until December 2015

Note: Top, domestic price (Yuan/50Kg). White curve: monthly average price; yellow curve: 20-weeks moving average. Bottom: Consumption ratio. The upper and lower horizontal threshold lines are the outcomes from the PSM.

According to the data for the last six months (Figure 4.6), the paddy rice and wheat consumption ratio are both out of equilibrium with signs that they have reached a minimum. Domestic rice and wheat prices are at equilibrium but their trend is decreasing. Although it is weakening, it is expected to continue for some time.

Figure 4.6. Historical rice paddy data from January 2005 to December 2015

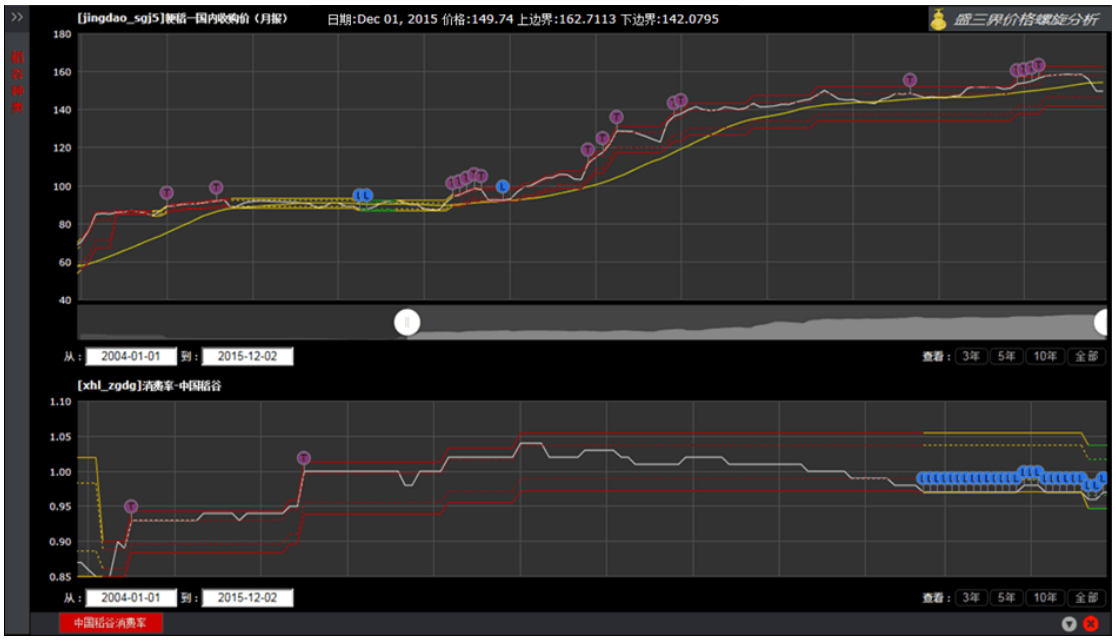

Note; Top, domestic price (Yuan/50Kg). White curve: monthly average price; yellow curve: 20-weeks moving average. Bottom: Consumption ratio. The upper and lower horizontal threshold lines are the outcomes from the PSM.

According to the long-term (2005-2015) data and data for the last six months, the maize consumption ratio and domestic price are both below the lower threshold of equilibrium intervals with signs of “bottoming”. The domestic maize price is expected to increase in the near future.

Figure 4.7 Historical maize data from January 2004 to December 2015

Note: Top, domestic price (Yuan/50Kg). White curve: monthly average price; yellow curve: 20-weeks moving average. Bottom: Consumption ratio. The upper and lower horizontal threshold lines are the outcomes from the PSM.

Figure 4.8 Historical wheat data from January 2004 to December 2015

Note: Top, domestic price (Yuan/50Kg). White curve: monthly average price; yellow curve: 20-weeks moving average. Bottom: Consumption ratio. The upper and lower horizontal threshold lines are the outcomes from the PSM.

4.3 Regional analysis

Figures 4.9 through 4.15 present crop condition information for each of China's seven agricultural regions. The provided information is as follows: (a) Crop condition development graph based on NDVI, comparing the current season up to July 2015 to the previous season, to the five-year average (5YA), the five-year maximum; (b) Spatial NDVI patterns from October 2015 to January 2016 (compared to the (5YA); (c) NDVI profiles associated with the spatial patterns under (b); (d) maximum VCI (over arable land mask); and (e) biomass for October 2015 to January 2016. Additional information about agroclimatic indicators and BIOMSS for China is provided in Annex A, table A.11.

Northeast region

No crops are grown between late October and January in Northeast China due to the low temperatures. For the period under consideration, however, agro-climatic conditions were favorable for crops to be planted in April.

The CropWatch agro-climatic indicators show markedly above average rainfall (+59%) and a slight decrease in PAR (-3%). Temperature (+0.8°C) was generally about average. These favorable agro-climatic conditions resulted in 9% above average potential biomass in the region, the only exception being the Liaohe Plain, which shows below average BIOMSS due to the severe drought during the previous monitoring period. In general, abundant snow will ensure good soil moisture, which will benefit spring crops in 2016.

Figure 4.9. Crop condition China Northeast region, October 2015-January 2016

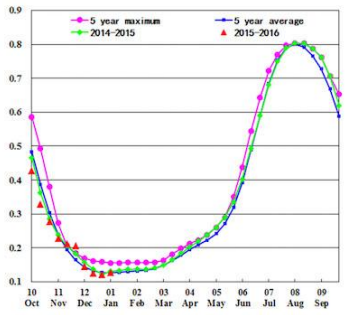

(a) Crop condition development graph based on NDVI

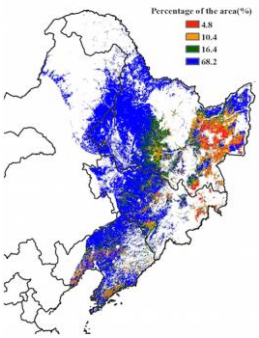

(b) Spatial NDVI patterns compared to 5YA

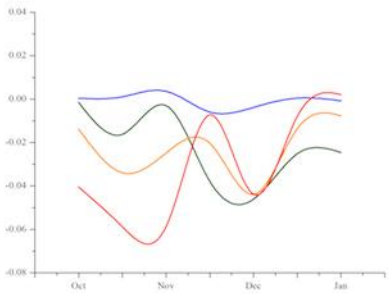

(c) NDVI profiles

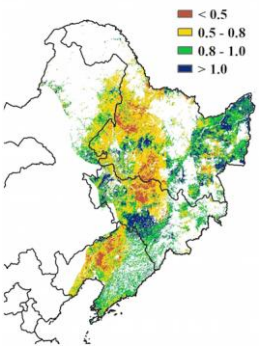

(d) Maximum VCI

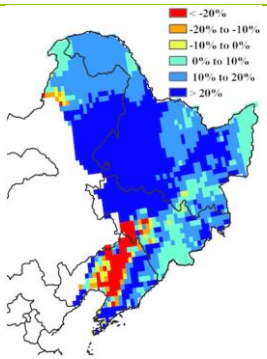

(e) Biomass

Inner Mongolia

Winter crops cannot survive in Inner Mongolia due to low temperatures from October to March. Compared with average conditions, the environmental indices show a significant increase of RAIN (+69%) and a large decrease of RADPAR (-10%), while temperature was slightly above average. BIOMSS, however, was significantly above the five-year average for the same period (+33%).

As a result, abundant snow since December will provide favorable soil moisture for the sowing of upcoming spring crops. Potential biomass during the monitoring period in most areas of Inner Mongolia was at least 20% above average (Figure 4.6). However, temperature was higher than average in most areas in Inner Mongolia, which may have some influence on spring crops by prematurely depleting soil moisture reserves.

Figure 4.10. Crop condition China Inner Mongolia, October 2015-January 2016

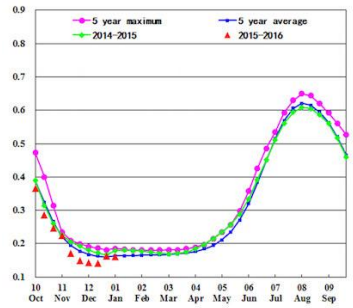

(a) Crop condition development graph based on NDVI

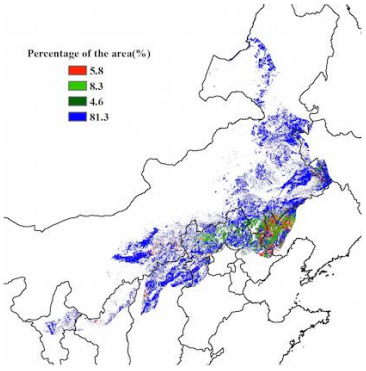

(b) Spatial NDVI patterns compared to 5YA

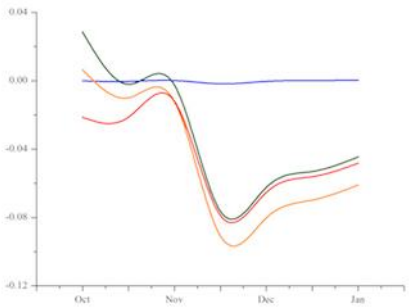

(c) NDVI profiles

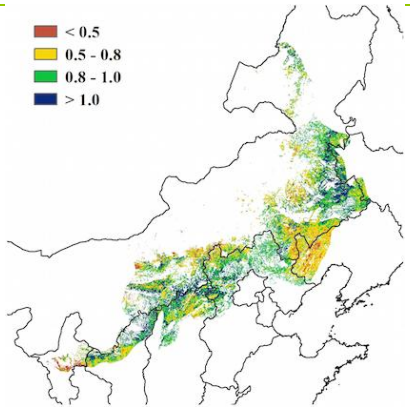

(d) Maximum VCI

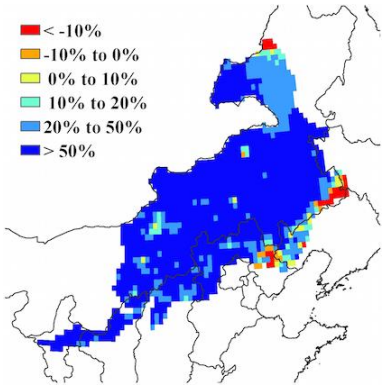

(e) Biomass

Huanghuaihai

In Huanghuahai, crop condition was generally below the five-year average, although it approached that level in January. Unfavorable meteorological conditions during the last monitoring period may have impacted the sowing and crop development at early growing stage. In addition, dry weather from July to October hindered the germination of winter wheat, which is confirmed by the well below average NDVI value before December in the NDVI development graph (Figure 4.7). Significantly above average rainfall (63%) from October 2015 to January 2016 provides sufficient soil moisture for winter wheat to develop after the wintering period.

As shown in the spatial pattern of the NDVI departure map, crop condition was below average before December in almost the whole region, especially in the east of Shandong province, and the southern fringe of the region. Since December, crops in the region, except for the most southern part, recovered to average, mainly due to abundant rainfall. The maximum VCI presents high values in Tianjin and southern Hebei provinces, while low values occur in central Henan and southern and eastern Shandong. Overall, climatic conditions so far will benefit the development of the winter wheat after dormancy.

Figure 4.11. Crop condition China Huanghuaihai, October 2015-January 2016

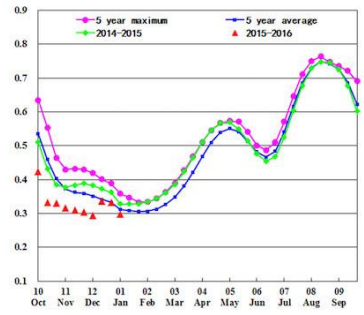

(a) Crop condition development graph based on NDVI

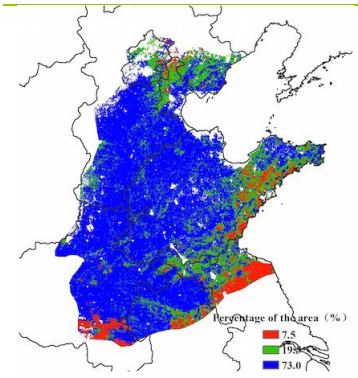

(b) Spatial NDVI patterns compared to 5YA

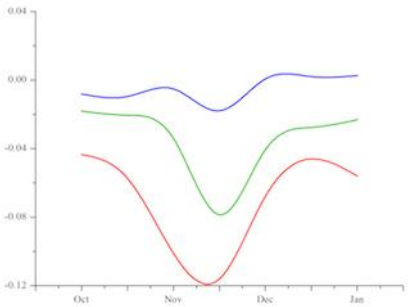

(c) NDVI profiles

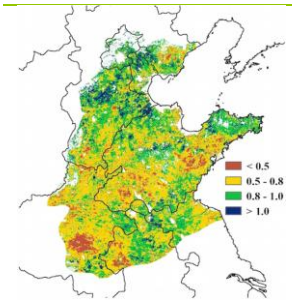

(d) Maximum VCI

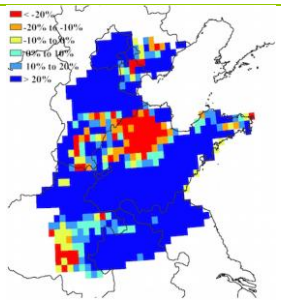

(e) Biomass

Loess region

Crop condition in the Loess region was slightly below the five-year average for the monitoring period of October 2015 to January 2016. The precipitation significantly exceeded average (+88%) and temperature was just slightly higher (+0.8°C) than average, while radiation decreased (-6%).

Suitable rainfall and temperature lead to higher biomass when compared to the average (+58%). Winter wheat was sown in October and is currently in its dormant stage, and winter crops will start growing again in late February or early March.

The NDVI clusters and profiles (Figure 4.8) show crop condition at average levels in 62% of the region, especially in the centre of Gansu, southern Ningxia and neighboring areas in Shaanxi provinces. Above average NDVI values can be observed in the northwest of Henan province from the beginning of November. However, in the centre of Shaanxi and Shanxi province, crop condition was below average due to reduced sunshine. The cropped arable land fraction was slightly below average (-1%).

Figure 4.12. Crop condition China Loess region, October 2015-January 2016

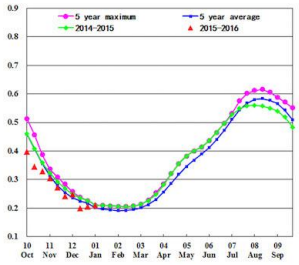

(a) Crop condition development graph based on NDVI

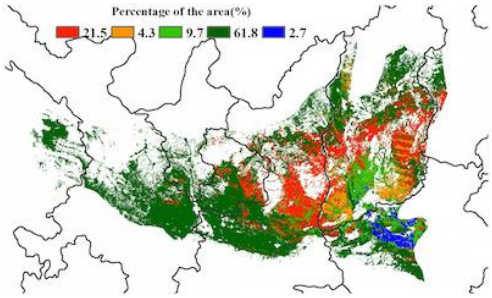

(b) Spatial NDVI patterns compared to 5YA

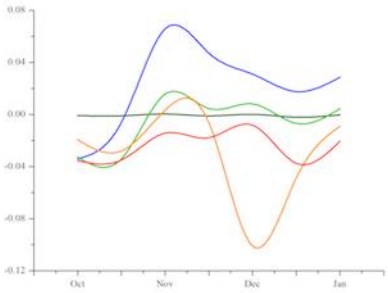

(c) NDVI profiles

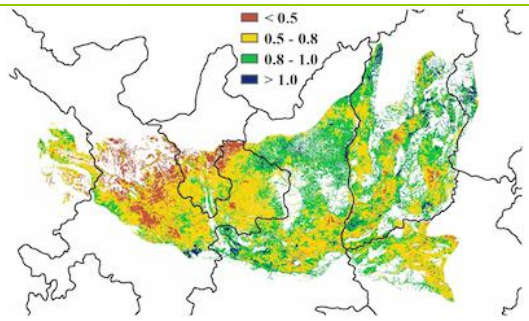

(d) Maximum VCI

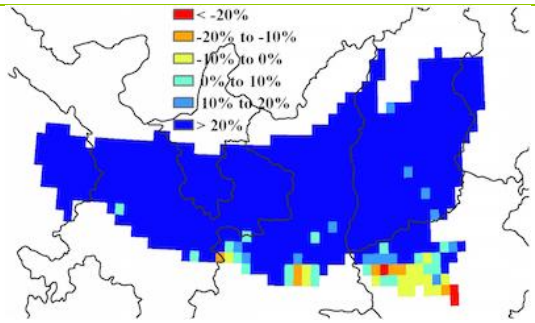

(e) Biomass

Lower Yangtze region

During the monitoring period, few crops were in the field except for winter wheat growing in the northeast and northern parts of the Lower Yangtze region. In general, crop condition was slightly below average over the reporting period.

The CropWatch agro-climatic indicators (Figure 4.9) show that rainfall was far above average (+110%) and temperature was slightly above (+0.4°C). Although RADPAR decreased by 22% compared to average, favorable rainfall and temperature conditions brought about a marked increase of BIOMSS in the region (>20%). The BIOMSS departure map also shows values at least 20% above average in most parts of the Lower Yangtze region.

The average value of maximum VCI in the whole region was 0.87, with VCIx values larger than 0.8 appearing in the central and southern parts of the region. According to the graph of spatial NDVI patterns compared to the five-year average and corresponding NDVI profiles, about 59% of crops were continuously close to the recent five-year average level over the reporting period. Other areas show variable conditions. CropWatch estimates that the yield of winter wheat in the region will be average.

Figure 4.13. Crop condition Lower Yangtze region, October 2015-January 2016

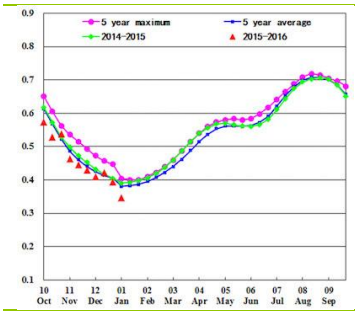

(a) Crop condition development graph based on NDVI

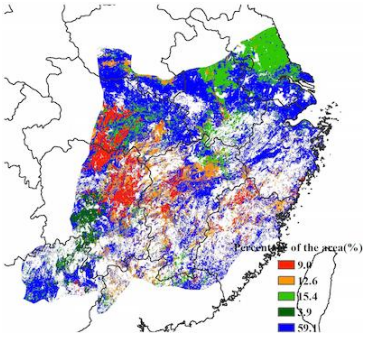

(b) Spatial NDVI patterns compared to 5YA

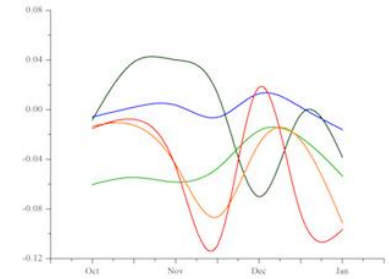

(c) NDVI profiles

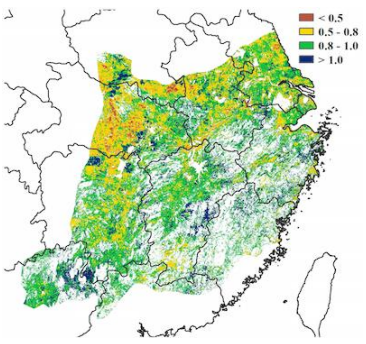

(d) Maximum VCI

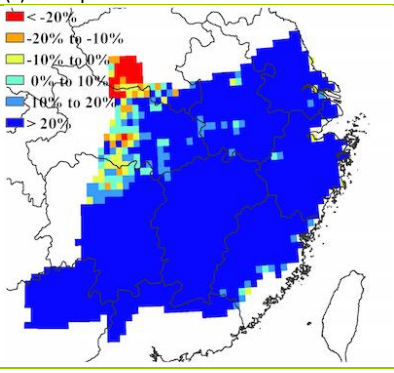

(e) Biomass

Southwest China

Winter wheat was planted during this monitoring period; the overall crop condition is average compared to the last 5YA. The CropWatch RAIN indicator reported a 13% decrease of precipitation accompanied by a positive temperature anomaly of 1.2°C.

NDVI was generally average in October, dropped below average in November and recovered in both December and January. The spatial NDVI patterns and profiles also show that crops are fair in about 88.5% of the area.

The low average NDVI in November is possibly due to the below average condition of the eastern part of Sichuan, resulting from decreased precipitation, of which the low potential biomass is another indicator (Figure 4.10). The cropped arable land fraction stayed at the same level as the last five-year average. Altogether, the expected output of winter crops is fair in Southwest China.

Figure 4.14. Crop condition Southwest China region, October 2015-January 2016

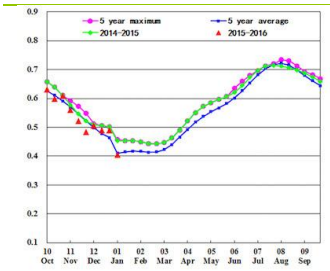

(a) Crop condition development graph based on NDVI

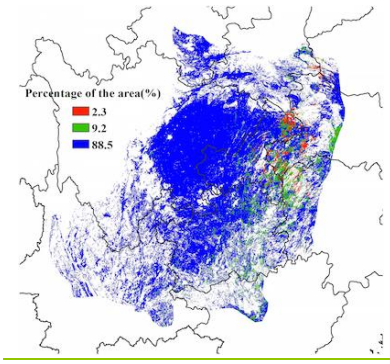

(b) Spatial NDVI patterns compared to 5YA

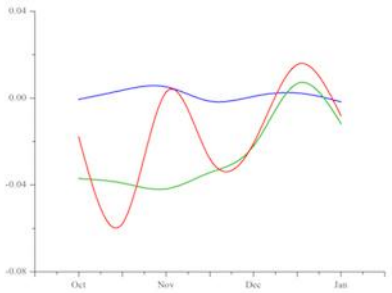

(c) NDVI profiles

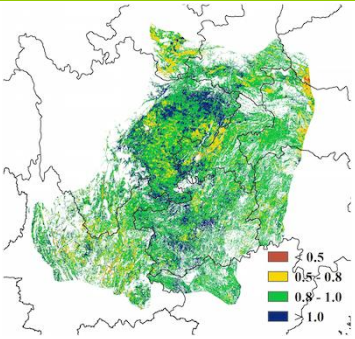

(d) Maximum VCI

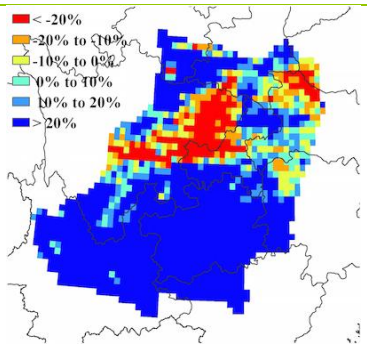

(e) Biomass

Southern China

In southern China, the monitoring period covers the harvest season of late rice. Overall crop condition is average, compared to the last five-year average, as clearly shown by the NDVI-based crop condition development graph (Figure 4.11). NDVI was generally average in October, dropped slightly below average at the beginning of November, then recovered and reached above average levels in December and January. The overall precipitation over cropped land of Southern China has decreased by 24% (reaching 725mm). The average maximum VCI was at 0.9 and the cropped arable land fraction kept at the same level as the last five-year average.

Crops in the middle of Guangdong province should be paid attention to especially, due to their below average condition throughout, as reflected by the NDVI spatial patterns and profiles. It is possibly due to the heavy increase of precipitation (+155%) and the reduction of RADPAR (-19%) in Guangdong province.

Figure 4.15. Crop condition Southern China region, October 2015-January 2016

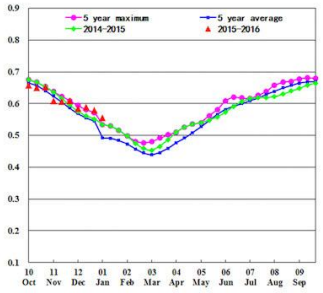

(a) Crop condition development graph based on NDVI

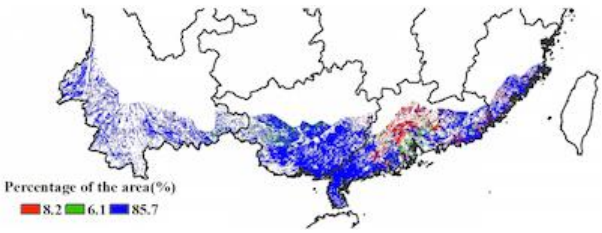

(b) Spatial NDVI patterns compared to 5YA

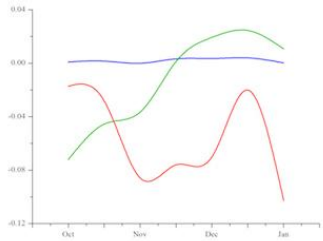

(c) NDVI profiles

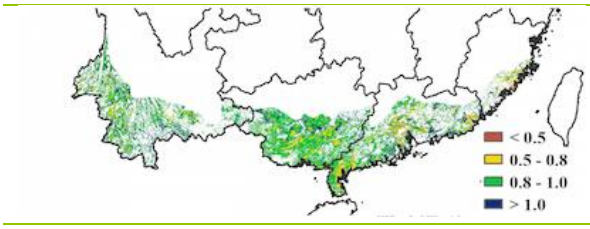

(d) Maximum VCI

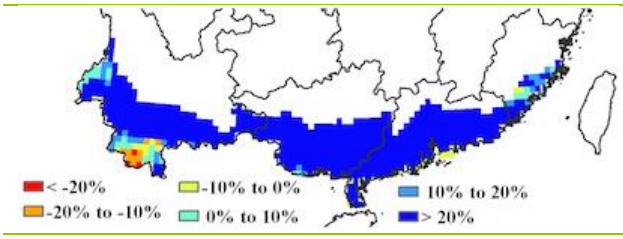

(e) Biomass

Chapter 5.Focus and perspectives

This focus section complements CropWatch analyses presented in chapters 1 through 4 by presenting additional information about topics of interest to global agriculture. Chapter 5 presents a focus on disaster events (5.1), updates on the Southern hemisphere (5.2), an overview of the agricultural and environmental settings in the Zambezi Basin (section 5.3), and an update on El Niño (5.4).

5.1 Disaster events

The three major disasters that affected 2015 can probably be listed as the 7.6 magnitude earthquake that rattled Gorkha in Nepal on April 25, the heat wave in India and Pakistan in May, and the October-November floods in India. All these disasters have in common that they occurred in developing countries, and that the vast majority of lost lives and property were uninsured.

A January 2016 press release by Munich Re states that 2015 experienced the lowest insured losses of any year since 2009. Overall losses totalled US$90 billion, of which roughly US$27 billion were insured. The largest disaster in terms of human suffering was no doubt the Gorkha earthquake in Nepal in April 2015, but the costliest for the insurance sector were the North American storms of February 2015.

In contrast, a recent report by UNISDR prepared for the latest UNFCCC COP21 in Paris estimates the **human** costs of disasters that occurred between 1995 and 2015 and provides an alternative view to assessments by the insurance industry, where costs are mostly loss of assets and property and where losses tend to be insured losses, i.e. they are highest in wealthy countries, as illustrated above.

According to UNISDR, between the 1985-94 and 2005-2014 decades, the frequency of natural disasters increased by 14%. What has not changed, however, is the nature of the most damaging factors: floods account for nearly half of all natural disasters. Over the last 20 years they affected more that 2 billion people, mostly in Asia.

Storms are less frequent than floods, but they are more deadly: they killed about a quarter of a million people; about 90% of these were in lower-income countries, even though they experienced only half as many storms as developed countries. The economic cost of weather related disasters (close to US$ 2,000 billion according to CRED's documentation) is a clear underestimation as few impact assessments include quantitative data (less than 20% in Africa).

Overall, annual economic losses from disasters are estimated by UNISDR at between US$250 billion and US$300 billion annually. This compares with the “insured loss” of US$ 2.1 billion and the overall loss of US$2.8 billion for the “costliest natural catastrophe for the insurance industry in 2015”, the above-mentioned winter storms.

Figure 5.1: Percentage of disasters due to main geophysical factors between 1995 and 2015

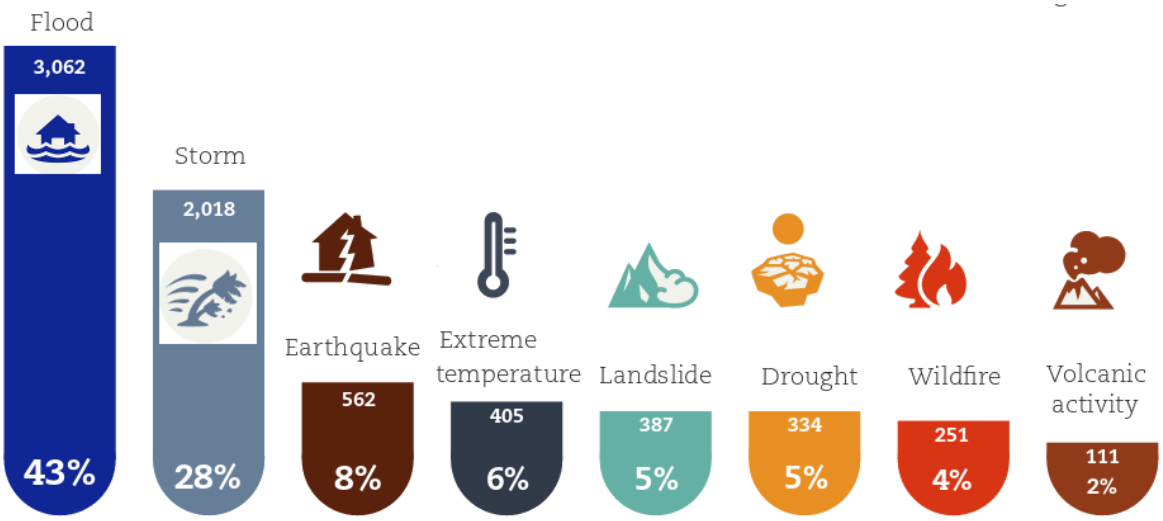

Source: modified from http://www.unisdr.org/2015/docs/climatechange/COP21_WeatherDisastersReport_2015_FINAL.pdf

Earthquakes affect crops mostly indirectly, through the disruption of the social fabric and infrastructure (roads and irrigation systems). The Nepal earthquake has been remarkable in the sense that aftershocks have continued to this day, with more than 400 (with magnitudes between 4 and 5) recorded.

Other significant earthquakes can be listed for Tajikistan (7.2 magnitude on 7 December in Murghob district), Afghanistan (26 December, 6.2 magnitude), India (3 January, 6.7 magnitude in Manipur), Peru (7 January, 5.0 magnitude) and Chile (7 January, 5.6 magnitude).

A good overview of security related crises, many of them with a climatic component and almost all of them with severe short-term and long-term impacts on food insecurity, are described in a report published by the ACAPS Global Emergency Overview (GEO).

Burundi experiences a combination of civil unrest and floods that led to internally and internationally displaced people, and left many of its people food insecure in spite of favorable growing conditions in the country. The impact of flood on the food situation will take time to resorb, as illustrated by Côte d'Ivoire where by mid-December more than 200,000 people were facing a crisis (IPC Phase3)[1] as a result of drought. Similar situations exist in Nigeria and Cameroon where internally displaced people were driven from their homes by floods.

Drought

The return of large-scale drought to parts of eastern and southern Africa is one of the most serious features of the current reporting period. Affected areas include South Sudan and Ethiopia, as well as several southern African countries where the drought is the worst since 1982. In South Africa, five out of nine provinces have been designated disaster areas for agriculture (including Free State and North West, Mpumalanga and Limpopo) and more than 2.7 million households are facing water shortages across the country. In Zimbabwe, 1.5 million people will face food insecurity until March 2016 and over 850,000 people urgently require assistance. In Malawi, one of the smallest countries in the region, close to 3 million people is estimated to be food insecure. Recent estimates put the number of persons without reliable access to food in southern Africa at approximately 29 million.

[1]For the definition of the IPC classification system, refer to http://www.fao.org/elearning/course/FI/EN/trainerresources/learnernotes0764.pdf

According to a recent ACAPS Briefing Note about south Sudan, 3.9 million people are currently classified as undergoing a food crisis (IPC Phase 3), emergency (IPC Phase 4) or catastrophe (IPC Phase 5), mainly in Jonglei, Upper Nile, and Unity States. In neighboring Ethiopia, recent estimates put the number of people in need of food assistance at more than 10 million. Most of the regions of Amhara, Oromia, and SNNPR are reported to be in crisis (IPC Phase 3) while poor households in East and West Hararghe as well as Oromia region are in emergency food insecurity (IPC Phase 4). The situation is likely to temporarily improve in areas where the main season harvest (Meher) has started, but pastoralist areas in the east are suffering most and cattle deaths have been reported. Although the Ethiopian government has taken measures to import a million tons of wheat, the number of cases of severe malnutrition cases is currently foreseen to reach 435,000 in the coming months.

Tropical cyclones

Several tropical cyclones that occurred in October were reported on in more detail in the previous CropWatch Bulletin[2]. They included Hurricane Joaquin over the Caribbean, Mujigae in the Philippines, Vietnam and China, Koppu on Luzon in the northern Philippines and, to some extent on Taiwan and Ryukyu Islands in southern Japan as well as the most powerful cyclone on record, Patricia which affected Pacific areas in Mexico but created relatively limited damage.

No additional severe cyclones occurred, except two rare events in Yemen where tropical cyclone Chapala (first days of November) has affected about 1 million people, followed on 9 January by cyclonic storm Megh which made a direct hit on Socotra Island. Both brought rain to Yemen and Saudi Arabia.

Floods

A long list of floods, including flash floods, were reported for the reporting period from all continents, including the USA (Texas on 30 October and 1 November), Spain (3 November), the Delta region of Egypt (4 November), the Red Sea coast of Saudi Arabia (19 November), Kenya (28 November), Kinshasa in the DRC (10 December), a large area over south America (Paraguay, Argentina, Brazil and Uruguay flooding in December) as well as Australia (6 January).

The most significant floods are probably those that affected Somalia, Iraq, India (Chennai) and Malaysia. South-central Somalia suffered floods in several events affecting close to 130,000 people (about half had to be relocated) from 23 October and in November. In early November 40 refugee settlements received heavy rains predominantly in Baghdad and Anbar province resulting in the death of 58 people. In Chennai and other parts of Tamil Nadu (Cuddalore), 250 people have died in due to excess water in October and November. In Malaysia a similar situation occurred, with a combined flood and landslide killed 315 people in Perak, involving Kampung Changkat Lobak, Matang Tengah and Kampung Air Hitam, on 21 November.

5.2 Southern hemisphere updates

The present section provides a concise summary of recent winter wheat harvests in the southern hemisphere, as well a first quantitative assessment of maize in South Africa, the main summer crop in the region, where prevailing drought conditions (See section 5.1 and the South Africa page in section 3.2) seriously threaten food security in several countries.

[2]http://www.cropwatch.com.cn/htm/en/files/20151123213525951.pdf

In Argentina, the updated CropWatch wheat output estimate currently stands at 10.7 million tons, 11% below the 2014-2015 production, as both harvested area and yield decreased compared with last year. Annex B lists production according to provinces: Buenos Aires and Mesopotamia (Entre Rios) both did well (+11% and +24%, respectively) while a production drop occurred in Santa Fe (-14%), Cordoba (-34%) and the rest of the country.

In neigboring Brazil wheat production is up 4.5% over last year, reaching 7 million tons. The largest increase, by state, was achieved in Santa Caterina (+20%), a relatively minor producer, and in Rio Grande do Sul (+13%). In Parana, production fell 12%.

For Australia CropWatch puts the overall output at 25 million tonnes, 1% below last year. The regional breakdown is as follows: New South Wales, +5%; South Australia, -7%; Victoria, +7% and Western Australia, -3%.

Figures 5.2 and 5.3 illustrate a detailed analysis of the current situation of maize in South Africa

Figure 5.2: Development of NDVI profiles over maize growing areas in 2014-15 and 2015-16

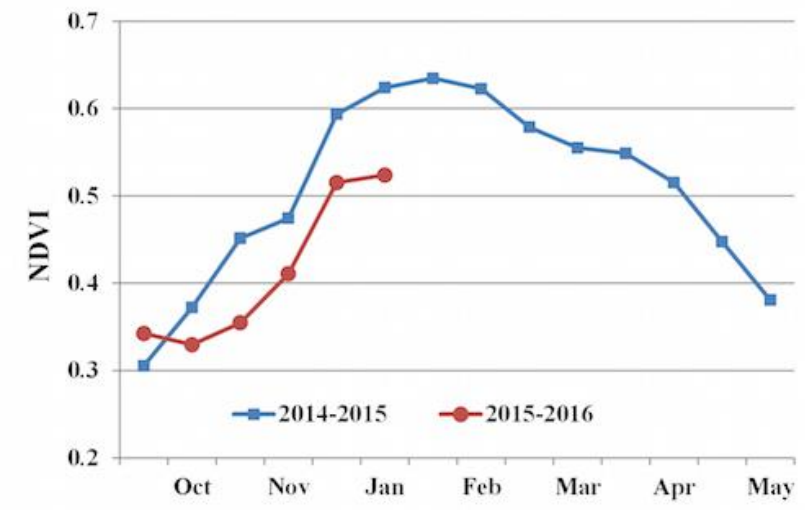

The average NDVI (Figure 5.2) is currently more that 0.1 units below the corresponding value in 2015. Figure 5.3 indicates a considerable reduction of the cultivated area in otherwise significant producer provinces (Free State, North West and Limpopo). Based on low yields (down 16% from last year) and reduced cultivated area (-34%), CropWatch estimates that the total maize output of South Africa will drop from 13.2 million tons to 7.3 million tons, a 45% reduction.

Figure 5.3: Relative distribution of maize in 2014-15 and 2015-16

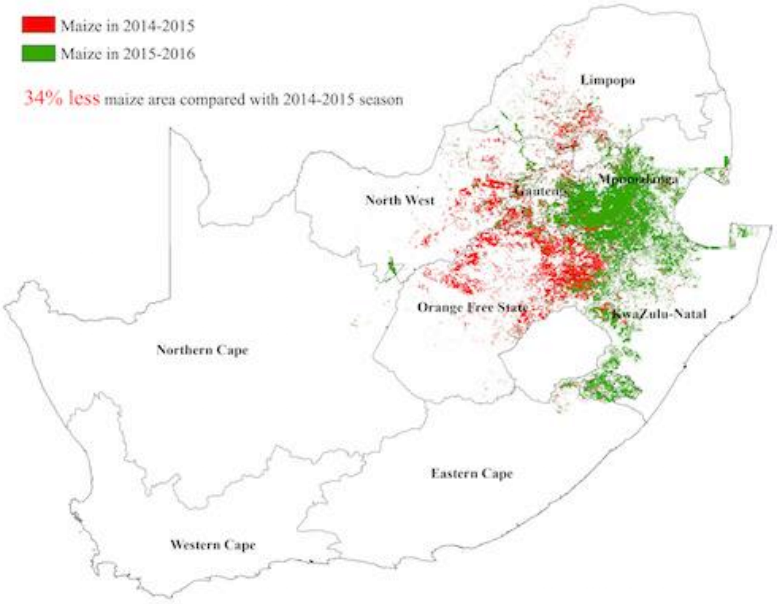

Figure 5.3 shows both red and green areas that grew maize in January 2015. In January 2016, only the green area had living maize crops.

5.3 The Zambezi basin[3]

The Zambezi River is the largest river system in southern Africa and the fourth longest on the continent. Together with its tributaries, it flows through eight countries, namely Angola, Botswana, Namibia, Malawi, Mozambique, Zambia and Zimbabwe (Figure 5.4) and has two major man-made dams, Lake Kariba and Cahora Bassa dam as well as the famous Victoria Falls (Figure 5.5).

The river is vital to the livelihoods of many citizens of these countries as it provides hydropower and water for urban, industrial and agricultural sectors. However, due to the steep terrain and poor soils along much of the river, few irrigation schemes have been developed except for those in the lowland flood-plain in Mozambique.

The dams (built in 1958 and 1969) have also changed the pattern of water flow, and thus the agricultural practices, which were traditionally dependent on the seasonal flooding bringing both water and silt to the fertile flood plains. The natural vegetation is described as a basis for the livelihoods of the people, followed by the importance of agriculture to food security and the conservation areas to tourism. An estimation of the vulnerability of these systems to climate change gives a view of the pressures affecting the people and the need for consideration of climate variability during agricultural development.

[3] Contributed by Professor Sue Walker, Emeritus Professor of Agrometerology, Dept Soil, Crop & Climate Sciences, Univ. Free State, Bloemfontein, South Africa and Honorary Professor, School of Biosciences, University of Nottingham Malaysia Campus, Semenyih, Malaysia

Figure 5.4: The Zambezi basin in southern Africa

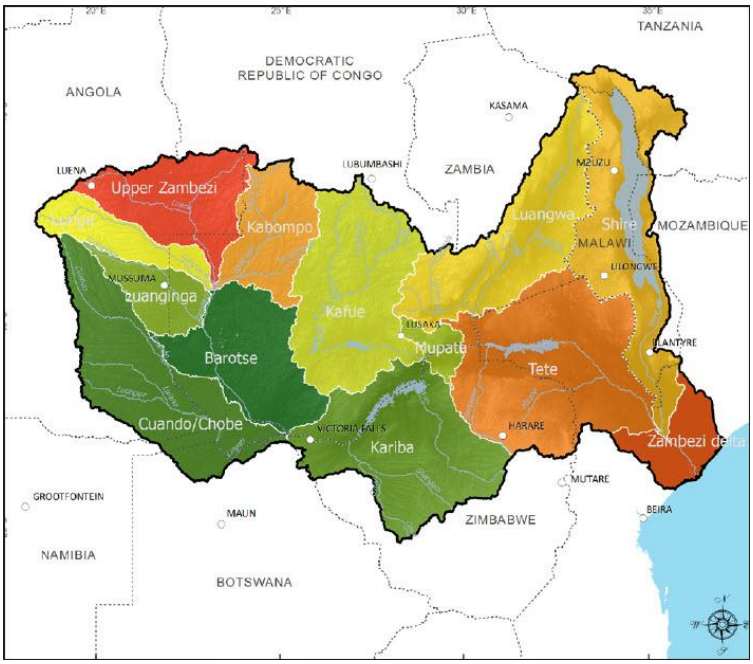

Source: SADC/SARDC and others, 2012

Figure 5.5: Victoria Falls from the Zambian side

a. Dry season (July 2009) b. River before the falls

Source: Sue Walker, 2016

Natural Vegetation

The Zambezi River rises out of a swampy (*dambo*) riparian *miombo* (Brachystegia) shrubland at 1524m North West of Mwinilunga, in the North-western Province of Zambia (UNESCO, 2016) and flows eastwards to the Indian Ocean forming a delta at its mouth at Quelimane in Mozambique. The basin covers an area of 1,390,000 km^2 with its tributaries (Figure 5.4). It is 2,574 km long flowing through eastern Angola, forming the border between eastern Namibia and northern Botswana, then becoming the border between Zambia and Zimbabwe and finally to Mozambique, where it flows through Tete, Sofala and Zambezia provinces to empty into the Indian Ocean (Figure 5.4). At the delta the dominant vegetation, often flooded, is open grassland-dominated savanna including palm, mangrove and dune forests (Hogan, 2012).

The People

The Zambezi basin is home to more than 40 million people, with about 7.5 million residing in the urban centers. This makes up about a third of the total population of the countries (SADC/SARDC and others, 2012). There are a wide range of population densities between countries across the basin, with Malawi being the most densely populated country and Zambia being the least densely populated. There are also large areas that are not inhabited, as they are reserved for wildlife conservation and tourism. As the basin covers most of the land area of Malawi, > 90% of the 14.9 million people live within the basin. For both Zambia (76% of county in basin) and Zimbabwe (55% of county in basin) about 65% of the total population of each country (13.09 million & 12.57 million) lives within the Zambezi Basin, so it is of vital importance to the national economy. The wetlands and lakes (especially Lake Malawi/Nyasa/Niassa, the Zambezi delta/Sofala bank, Cahora Bassa dam, Itezhi-Tezhi, Kafue and Lake Kariba) also play an important role, as fish contributes to the people's source of protein for food security.

In the Zambezi basin, food security is at the heart of the people's livelihoods as there are many smallholder farmers producing food for local consumption mostly under rain-fed farming systems described below. In order to achieve this, a concerted effort needs to be made to intensify the agricultural production using sustainable techniques, while maintaining an agro-ecological perspective that will balance the available natural resources with the crop production requirements (IFAD, 2010).

Agriculture

The main farming systems (Figure 5.6) in the Zambezi Basin are rain-fed mixed maize systems (#9 in Figure 5.6) including livestock (FAO, 2016). These are mostly managed by smallholders who plant maize after ploughing with animal traction after the first rains at the beginning of the summer growing period in October and November (Figures 5.7 and 5.8).

There are also small pockets of commercial agriculture, cereal-root crop mixed systems (#8 in Figure 5.6) and agro-pastoral systems with sorghum and millet (#11 in Figure 5.6). Generally speaking the farming systems follow the latitude and rainfall patterns (Figure 5.7), as the growing season is limited to the rainy season. Thus the main system of mixed maize (#9 in Figure 5.6) stretches from southern Zimbabwe with 475 mm/y and 90-120d growing season through the middle of Zimbabwe and into Zambia where the rainfall is above 700 mm/y and the growing season is longer than 150d (Figures 5.6 and 5.7). Further north towards Lake Malawi where the rainfall can reach 1400 mm/y and the growing season can stretch to more than 180d, mixed maize systems (#9 in Figure 5.6) are still common (FAO, 2016). Agro-pastoral systems (#11 in Figure 5.6) dominate the south-western regions (< 500mm/y) and the steep ravines along the edges of Lake Kariba and Cahora Bassa dam, which are areas also suffering from severe land degradation.

Figure 5.6: Farming systems variation across the Zambezi basin countries

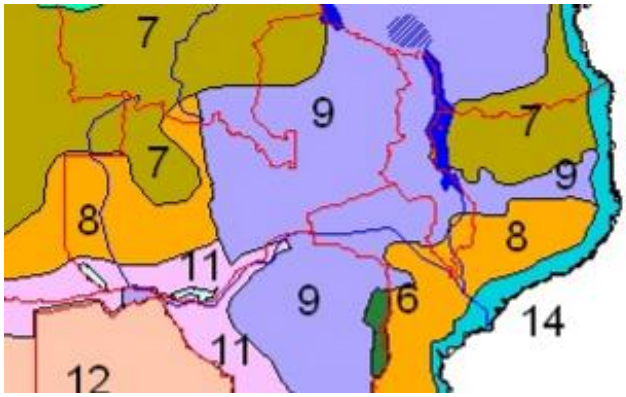

Note: 6 = highland temperate mixed; 7 = root crops: 8 = cereal-root crop mixed; 9 = maize mixed: 11 = agro-pastoral millet/sorghum; 12 = pastoral; 14 = coastal artisanal fishing, (FAO, 2016)

Figure 5.7: Average annual rainfall distribution across the Zambezi basin

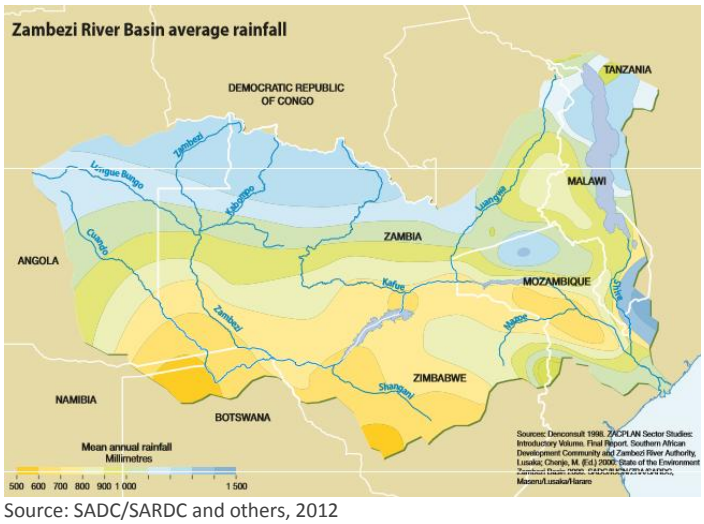

Source: SADC/SARDC and others, 2012

Figure 5.8: Ploughing a field with animal traction ready to plant maize in southern Zambia

Source: Sue Walker, October 2006

Agriculture plays important role in the sustainable economic development in most of the Zambezi basin countries. Although the contribution of agriculture to GDP (Figure 5.10) has been declining over the past decades as the countries have developed, it remains at 33.2% for Malawi, 26.6% for Mozambique, 12.0% for Zimbabwe and 9.6% for Zambia compared to the world average of 3.1% in 2013 (World Bank, 2016). Zimbabwe, Zambia and Malawi together cultivate 86 % of the estimated 5.2 million ha of land in the basin annually (SADC, 2016). The water from the Zambezi has multiple uses as it flows through the basin (Figure 5.9). Besides agriculture and fisheries, the potential for hydropower has also been developed. The hydropower from the Zambezi river generates approximately 5000 MW, with Cahora Bassa (2 075 MW), Kariba (1 470 MW) and Kafue Gorge (990 MW) dams providing the bulk of the basin's hydropower electricity (SADC/SARDC and others, 2012).

Figure 5.9: A young farmer preparing for a simple irrigation system; and goats drinking from a well; both near Monze, Southern Zambia

Source: Sue Walker, October 2006

Figure 5.10: The contribution of agriculture to GDP (Gross Domestic Product) in main countries of Zambezi basin

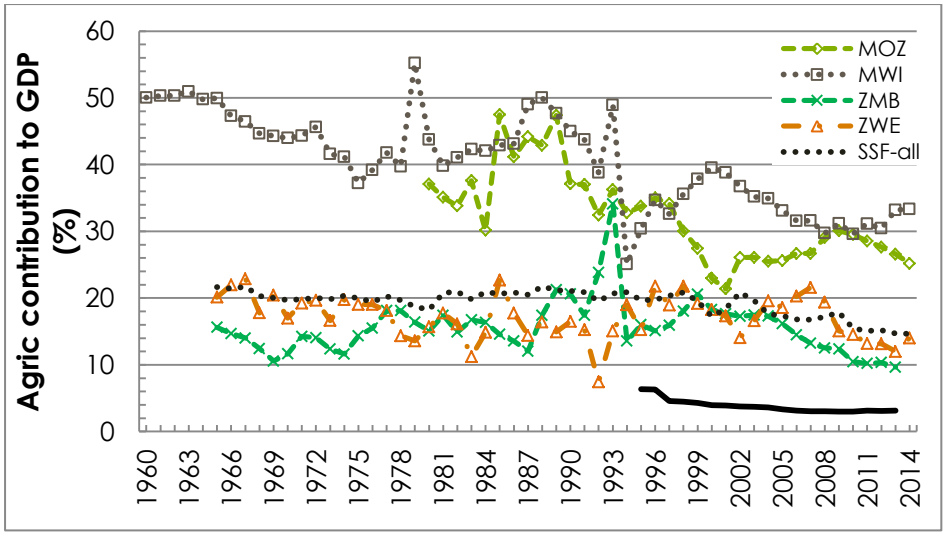

Note: MOZ=Mozambique, MWI=Malawi, ZMB=Zambia, ZWE=Zimbabwe, compared to average from all sub-Saharan African countries (SSF-all) and world mean (World Bank, 2016).

Conservation Areas

There are many areas in the basin that are protected as wildlife parks and forestry areas (Figure 5.11). This includes a number of trans-frontier parks and conservation areas as well as UNESCO declared Biosphere Reserves and two UNESCO World Heritage Sites, namely Mana Pools, and Sapi and Chewore Safari Areas. The trans-frontier parks are (a) Liuwa Plains - Mussuma, (14 464km^2) between Angola and north western Zambia; (b) Kavango - Zambezi where Angola, Botswana, Namibia, Zambia and Zimbabwe converge (approximately 520 000 km^2 including 36 national parks, game reserves, community conservancies and game management areas); (c) Lower Zambezi – Mana Pools (17745 km^2) between Zambia and Zimbabwe; and (d) Malawi - Zambia in the north east. This international recognition is an indication that the Zambezi basin is rich in biological diversity worth preserving. Within its basin are wetlands, aquatic systems, riverine woodlands, Afro-montane forests, dry forests and savannas which are all complex ecosystems which support abundant wildlife and a great diversity of trees and plants; with some species native only to the Zambezi region (ZamSoc, 2016). There are also twenty RAMSAR wetland

sites across these countries, the main ones within the basin being Zambezi Flood Plains in the upper region, Lukanga Swamps and Kafue Falls in central Zambia, and Luangwa Floodplains in the north east (SADC/SARDC and others, 2012).

Figure 5.11: Trans-frontier conservation areas in the Zambezi basin

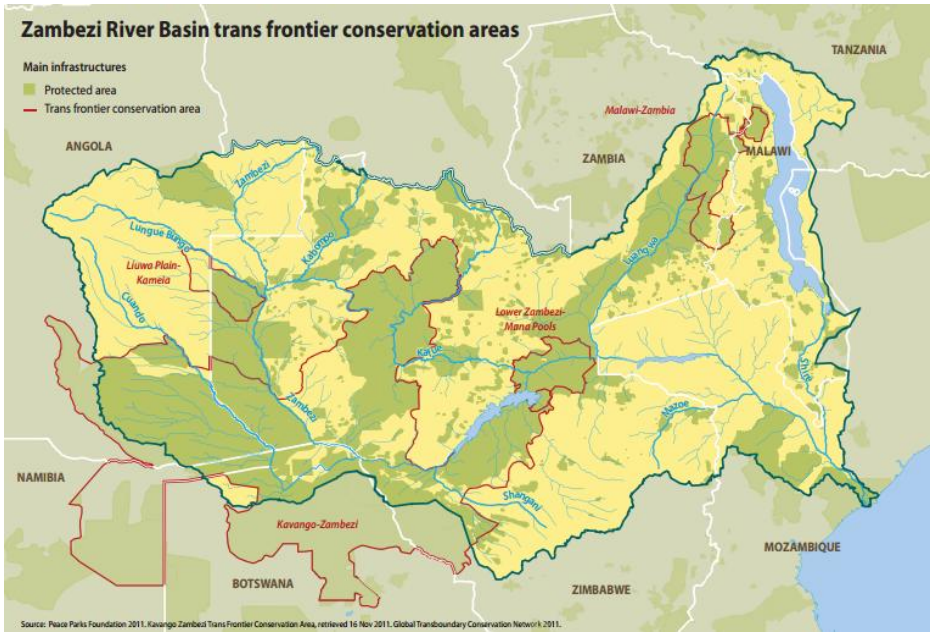

Source: Peace Parks Foundation, 2011

Estimation of Vulnerability

Many people in the Zambezi basin are vulnerable to food insecurity. Causes for their food insecurity include poverty, irregular income and food supply, brought about by limited access to markets (poor infrastructure), as well as the effect of weather variability on food crop production. Variability will be exacerbated by climate change and thus these people can become even more susceptible to food insecurity.

Within the Zambezi Basin, the combination of sensitivity and exposure give highest impact areas in parts of both Zimbabwe and Malawi, followed by parts of Mozambique and Zambia. For the overall vulnerability analysis, areas of Mozambique and Malawi emerged as 'hotspots', with parts of Zimbabwe and Zambia rated as intermediate (Davies et al., 2010). These indices can then also be estimated for future time periods using selected parameters from Global Climate Models, showing that this methodology has promise for application with a range of future scenarios.

Conclusion

From this overview its rich natural and human resources demonstrate the potential for development in the Zambezi basin. Opportunities for development can be based on sustainable environmental development of the water and land resources by their ability to generate income from both farming and tourism. Agricultural development needs to balance the supply of water and demands of the environment with the desires and needs of the people for improved livelihoods using the natural resources available to them. However, attention must be given to transport and marketing infrastructure as well as viable adaptation strategies with intensification of agricultural practices under the variable climatic conditions.

5.4 El Niño

In spite of a declining trend during the current monitoring period, the strong El Niño still persists. CropWatch monitored the following typical climate anomalies associated with El Niño events: positive temperature anomalies in Northeast China and SouthAsia, negative precipitation anomalies in North Australia and maritime Southeast Asia, drought in central and northern South America, positive precipitation anomalies in Argentina and Peru, and especially drought in southern Africa.

Figure 5.12 illustrates the behavior of the Southern Oscillation Index (SOI) of the Australian Bureau of Meteorology (BOM) from January 2015 to December 2015. Sustained negative values of SOI below -7 generally indicate an EI Niño event, while sustained positive values above +7 are typical of La Niña. Values within the range (-7 to +7) indicate neutral conditions. During the current season, SOI has increased to -5.3 in November 2015, indicating a declining trend.

Figure 5.12. Behaviour of the Southern Oscillation Index (SOI) from January-December 2015

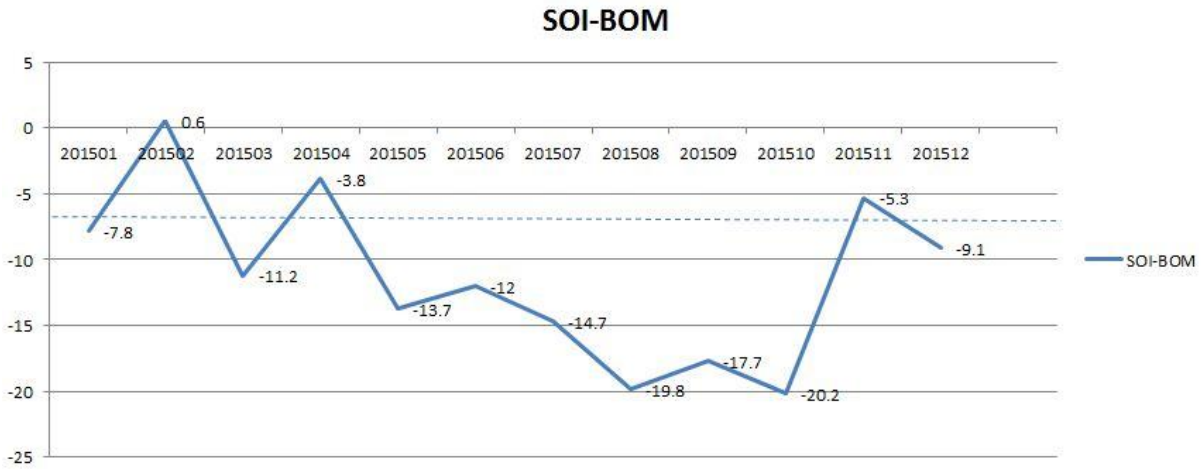

NASA reports the gradual weakening trend of El Niño through spring 2016, and the possible transition to ENSO-neutral conditions during late spring or early summer.

Annex A. Agroclimatic indicators and BIOMSS

Table A.1. October 2015-January 2016 agroclimatic indicators and biomass by global Monitoring and Reporting Unit

	65 Global MRUs	RAIN		TEMP		RADPAR		BIOMSS	
		Current (mm)	14YA dep. (%)	Current (°C)	14YA dep. (°C)	Current (MJ/m^2)	14YA dep. (%)	Current (gDM/m^2)	5YA dep. (%)
1	Equatorial central Africa	443	-8	25.3	0	964	3	1512	-4
2	East African highlands	174	-3	19.8	0.2	987	-3	723	6
3	Gulf of Guinea	249	9	26.4	-0.9	946	1	807	0
4	Horn of Africa	312	13	24.6	-0.3	1024	-4	1107	16
5	Madagascar (main)	476	-10	24.4	-0.5	1104	1	1426	-3
6	Southwest Madagascar	219	-29	24.3	-1.5	1250	3	833	-13
7	North Africa-Mediterranean	74	-53	14.6	0.4	603	2	340	-37
8	Sahel	72	55	27.1	-1	1036	-1	281	38
9	Southern Africa	252	-23	26.3	0.9	1205	7	929	-21
10	Western Cape (South Africa)	36	-68	18.7	0.7	1314	3	196	-60
11	British Columbia to Colorado	264	28	-2.3	0.5	379	-3	582	19
12	Northern Great Plains	200	56	3.2	2	391	-6	755	46
13	Corn Belt	344	14	5.8	2.3	361	-5	998	19
14	Cotton Belt to Mexican Nordeste	484	61	14.5	1.5	521	-9	1241	38
15	Sub-boreal America	128	-2	-3.5	2.9	209	-6	511	15
16	West Coast (North America)	224	-25	8	0.2	448	-3	655	-3
17	Sierra Madre	147	30	15.8	0.3	812	-5	607	55
18	SW U.S. and N. Mexican highlands	128	71	9.2	0.1	624	-5	529	58
19	Northern South and Central America	403	-7	26.5	0.5	789	2	1196	-1
20	Caribbean	371	15	25.6	0.2	774	1	1321	35
21	Central-northern Andes	389	-21	17.9	0.8	973	4	1136	-11
22	Nordeste (Brazil)	172	-9	29	1.2	1188	3	575	-21
23	Central eastern Brazil	598	3	27.2	0.4	1059	4	1703	-4
24	Amazon	426	-32	28.5	0.2	994	8	1424	-26
25	Central-north Argentina	465	38	24.1	-2	946	-11	1431	17
26	Pampas	833	62	21.7	-1.3	971	-14	1899	21
27	Western Patagonia	64	-56	11.9	-0.9	1162	-1	334	-27
28	Semi-arid Southern Cone	135	50	16.4	-2.2	1165	-6	567	49
29	Caucasus	306	36	4.6	-0.2	433	-5	856	17
30	Pamir area	219	102	4.1	0.3	577	-5	591	35
31	Western Asia	148	42	8.6	0.3	527	-5	550	35
32	Gansu-Xinjiang (China)	102	139	-1.1	1.4	464	-5	360	61
33	Hainan (China)	251	-27	23.1	0.8	654	-2	727	-7

	65 Global MRUs	RAIN		TEMP		RADPAR		BIOMSS	
		Current (mm)	14YA dep. (%)	Current (°C)	14YA dep. (°C)	Current (MJ/m^2)	14YA dep. (%)	Current (gDM/ m^2)	5YA dep. (%)
34	Huanghuaihai (China)	114	63	7.2	0	494	-9	514	43
35	Inner Mongolia (China)	94	122	-3.8	0.7	460	-4	421	41
36	Loess region (China)	119	88	3.3	0.8	527	-6	541	58
37	Lower Yangtze (China)	400	110	13	0.4	473	-22	1222	58
38	Northeast China	127	59	-5.4	0.8	395	-3	445	9
39	Qinghai-Tibet (China)	119	31	2.4	0.4	704	0	430	24
40	Southern China	280	93	17	0.2	579	-14	943	51
41	Southwest China	228	69	10.7	0.6	450	-10	789	33
42	Taiwan (China)	109	-34	19.7	0.4	646	-2	538	-26
43	East Asia	133	-29	1.2	1.1	407	-6	545	-10
44	Southern Himalayas	128	3	18.7	0.3	722	-2	457	7
45	Southern Asia	218	0	24.8	0.6	828	-2	572	-15
46	Southern Japan and Korea	309	-13	11.2	1.2	495	0	1084	-9
47	Southern Mongolia	82	272	-6.2	1.8	386	-5	386	105
48	Punjab to Gujarat	15	-37	22.4	0.2	808	0	74	-39
49	Maritime Southeast Asia	725	-24	25.9	-0.1	859	5	1804	-20
50	Mainland Southeast Asia	325	0	25.8	0.3	819	1	903	-2
51	Eastern Siberia	164	10	-8.6	0.2	238	2	365	-6
52	Eastern Central Asia	55	14	-13.4	0.7	303	1	241	8
53	Northern Australia	249	-43	26.9	-0.6	1141	4	840	-42
54	Queensland to Victoria	184	-8	21.3	1.1	1238	1	808	-9
55	Nullarbor to Darling	79	-9	20.1	1.1	1295	0	424	-13
56	New Zealand	92	-65	12.8	-0.3	1083	2	471	-47
57	Boreal Eurasia	219	0	-2.3	0.1	115	1	548	-4
58	Ukraine to Ural mountains	176	4	0.2	0.2	169	-2	667	-1
59	Mediterranean Europe and Turkey	193	-31	10.2	0	449	-1	720	-24
60	W. Europe (non Mediterranean)	234	-4	6.9	0.3	256	-4	893	-7
61	Boreal America	387	60	-4.9	2.9	106	-13	459	24
62	Ural to Altai mountains	161	41	-5.3	0.6	205	-7	459	3
63	Australian desert	108	42	22.3	0.8	1319	0	546	13
64	Sahara to Afghan deserts	71	50	18.4	-0.2	770	-4	269	52
65	Sub-arctic America	96	113	-12.6	4.6	26	10	162	126

Note: Departures are expressed in relative terms (percentage) for all variables, except for temperature, for which absolute departure in degrees Celsius is given. Zero means no change from the average value; relative departures are calculated as (C-R)/R*100, with C=current value and R=reference value, which is the five-year (5YA) or fourteen-year average (14YA) for the same period between April and July.

Table A.2. October 2015-January 2016 agroclimatic indicators and biomass by country

	31 Countries	RAIN		TEMP		RADPAR		BIOMSS	
		Current (mm)	14YA Departure (%)	Current (°C)	14YA Departure (°C)	Current (MJ/m^2)	14YA Departure (%)	Current (gDM/m^2)	5YA Departure (%)

31 Countries		RAIN		TEMP		RADPAR		BIOMSS	
		Current (mm)	14YA Departure (%)	Current (°C)	14YA Departure (°C)	Current (MJ/m^2)	14YA Departure (%)	Current (gDM/m^2)	5YA Departure (%)
[ARG]	Argentina	500	24	21.0	-1.7	1042	-10	1492	13
[AUS]	Australia	176	-11	21.6	0.9	1235	0	741	-11
[BGD]	Bangladesh	137	-38	23.0	-0.2	749	-1	380	-33
[BRA]	Brazil	562	-1	27.1	0.4	1043	3	1535	-9
[CAN]	Canada	165	-15	-1.8	2.4	248	-5	551	13
[CHN]	China	238	85	8.4	0.5	487	-12	683	41
[DEU]	Germany	219	3	7.0	1.7	200	-7	1028	4
[EGY]	Egypt	56	32	19.1	0.3	621	-5	160	15
[ETH]	Ethiopia	142	2	20.6	0.3	986	-3	610	6
[FRA]	France	204	-27	8.9	-0.9	299	0	901	-18
[GBR]	UK	446	48	8.5	-0.7	153	-13	1189	-2
[IDN]	Indonesia	729	-24	26.1	-0.1	876	6	1811	-21
[IND]	India	129	-3	22.7	0.6	811	-1	357	-18
[IRN]	Iran	218	50	8.7	-0.3	598	-5	711	47
[KAZ]	Kazakhstan	153	52	-3.2	1.1	246	-9	518	12
[KHM]	Cambodia	408	23	27.9	0.5	876	3	1036	-3
[MEX]	Mexico	215	21	20.0	0.5	756	-6	682	49
[MMR]	Myanmar	240	6	22.5	-0.4	757	-1	829	12
[NGA]	Nigeria	158	-4	26.6	-0.7	1012	1	456	-13
[PAK]	Pakistan	51	3	15.3	-0.1	714	-2	168	18
[PHL]	Philippines	661	-18	25.8	-0.1	827	10	1313	-32
[POL]	Poland	154	-1	4.5	0.7	193	-4	812	5
[ROU]	Romania	163	-9	4.9	0.9	293	-7	699	-10
[RUS]	Russia	174	16	-3.6	0.3	186	-3	507	0
[THA]	Thailand	284	0	25.9	0.4	827	1	831	-3
[TUR]	Turkey	256	-1	6.6	0.5	490	0	798	-12
[UKR]	Ukraine	149	1	3.0	0.2	234	0	747	4
[USA]	USA	362	47	8.1	1.6	448	-7	927	35
[UZB]	Uzbekistan	189	59	6.7	0.7	439	-9	701	51
[VNM]	Vietnam	380	-8	23.0	0.9	661	-1	1127	13
[ZAF]	South Africa	221	-26	22.1	1.4	1265	9	828	-27

See note table A.1.

Table A.3. Argentina, October 2015-January 2016 agroclimatic indicators and biomass (by province)

	RAIN		TEMP		RADPAR		BIOMSS	
	Current (mm)	14YA Departure (%)	Current (°C)	14YA Departure (°C)	Current (MJ/m^2)	14YA Departure (%)	Current (gDM/m^2)	5YA Departure (%)
Buenos Aires	400	9	18.2	-1.7	1165	-5	1539	14
Chaco	466	7	24.7	-1.3	907	-19	1446	0
Cordoba	396	11	20.4	-2.1	1067	-9	1474	7
Corrientes	989	59	23.1	-1.6	922	-18	2258	32
Entre Rios	559	17	21.1	-1.7	1092	-7	1733	12
La Pampa	482	57	18.9	-2.1	1169	-7	1762	40
Misiones	1291	81	23.4	-0.9	818	-24	2426	27
Santiago Del Estero	383	14	23.9	-1.9	970	-11	1292	5
San Luis	441	40	18.8	-3.1	1057	-12	1494	16
Salta	345	0	23.4	-1.7	943	-7	1096	-6
Santa Fe	478	6	22.1	-1.4	1053	-9	1610	5

See note table A.1.

Table A.4. Australia, October 2015-January 2016 agroclimatic indicators and biomass (by state)

	RAIN		TEMP		RADPAR		BIOMSS	
	Current (mm)	14YA Departure (%)	Current (°C)	14YA Departure (°C)	Current (MJ/m^2)	14YA Departure (%)	Current (gDM/m^2)	5YA Departure (%)
New South Wales	193	-3	21.8	1.1	1240	0	894	-1
South Australia	68	-29	20.2	1.8	1294	4	411	-21
Victoria	94	-45	18.9	2.1	1237	3	530	-37
W. Australia	85	-12	20.8	1.1	1292	0	432	-14

See note table A.1.

Table A.5. Brazil, October 2015-January 2016 agroclimatic indicators and biomass (by state)

	RAIN		TEMP		RADPAR		BIOMSS	
	Current (mm)	14YA Departure (%)	Current (°C)	14YA Departure (°C)	Current (MJ/m^2)	14YA Departure (%)	Current (gDM/m^2)	5YA Departure (%)
Ceara	80	7	28.9	0.3	1186	0	328	-19
Goias	588	-13	27.0	0.6	1093	7	1863	-10
MatoGrosso Do Sul	815	55	26.9	-0.9	1017	-5	2198	26
MatoGrosso	639	-19	28.4	0.6	1066	11	2004	-10

	RAIN		TEMP		RADPAR		BIOMSS	
	Current (mm)	14YA Departure (%)	Current (°C)	14YA Departure (°C)	Current (MJ/m^2)	14YA Departure (%)	Current (gDM/m^2)	5YA Departure (%)
Minas Gerais	583	-12	26.1	1.5	1125	10	1612	-13
Parana	1072	81	23.3	-0.4	857	-17	2378	29
Rio Grande Do Sul	1257	103	21.3	-1.3	867	-21	2245	33
Santa Catarina	1195	84	20.4	-0.5	750	-25	2198	16
Sao Paulo	820	40	25.0	0.3	995	-4	2213	22

See note table A.1.

Table A.6. Canada, October 2015-January 2016 agroclimatic indicators and biomass (by province)

	RAIN		TEMP		RADPAR		BIOMSS	
	Current (mm)	14YA Departure (%)	Current (°C)	14YA Departure (°C)	Current (MJ/m^2)	14YA Departure (%)	Current (gDM/m^2)	5YA Departure (%)
Alberta	73	-17	-3.5	2.1	240	0	420	-5
Manitoba	116	13	-2.1	3.5	241	-10	602	32
Saskatchewan	86	3	-3.0	3.2	247	-6	498	16

See note table A.1.

Table A.7. India, October 2015-January 2016 agroclimatic indicators and biomass (by state)

	RAIN		TEMP		RADPAR		BIOMSS	
	Current (mm)	14YA Departure (%)	Current (°C)	14YA Departure (°C)	Current (MJ/m^2)	14YA Departure (%)	Current (gDM/m^2)	5YA Departure (%)
Arunachal Pradesh	166	-13	16.0	0.1	664	-1	743	11
Andhra Pradesh	277	29	26.0	0.6	853	0	668	-3
Assam	141	-16	22.1	-0.1	696	1	599	26
Bihar	31	-60	22.6	0.1	783	1	143	-54
Chandigarh	n.a.	n.a.	n.a.	n.a.	n.a.	n.a.	n.a.	n.a.
Chhattisgarh	40	-59	23.3	0.8	846	0	193	-57
Daman and Diu	n.a.	n.a.	28.0	2.0	900	1	n.a.	n.a.
Delhi	18	-35	20.5	0.4	757	-1	114	-33
Dadra and Nagar Haveli	75	-20	25.2	0.2	872	0	341	-27
Gujarat	10	-56	25.7	0.5	886	1	65	-64
Goa	173	-11	26.8	0.1	895	-2	570	-19
Himachal Pradesh	55	-34	5.2	1.2	716	-3	257	-27

	RAIN		TEMP		RADPAR		BIOMSS	
	Current (mm)	14YA Departure (%)	Current (°C)	14YA Departure (°C)	Current (MJ/m^2)	14YA Departure (%)	Current (gDM/m^2)	5YA Departure (%)
Haryana	32	25	19.5	0.2	748	-1	155	7
Jharkhand	23	-80	22.1	0.7	809	0	140	-72
Kerala	588	7	26.5	0.2	814	-8	1664	18
Karnataka	223	14	25.1	0.7	878	-2	666	-2
Meghalaya	48	-81	19.3	0.4	741	2	270	-44
Maharashtra	78	-21	25.1	1.0	874	-1	252	-41
Manipur	187	0	16.5	-0.6	727	0	656	13
Madhya Pradesh	32	-39	22.9	0.9	830	-1	155	-42
Mizoram	419	70	19.0	-0.9	747	-2	778	6
Nagaland	189	18	17.1	-0.3	695	0	784	46
Orissa	75	-57	24.1	0.7	816	-1	330	-48
Puducherry	535	21	26.7	0.5	796	-7	1603	28
Punjab	34	2	18.6	0.2	715	-1	156	1
Rajasthan	8	-42	22.3	0.1	818	1	38	-58
Sikkim	69	-50	7.7	0.4	683	-3	333	-28
Tamil Nadu	803	57	26.5	-0.1	759	-6	1646	21
Tripura	260	8	22.2	-0.4	738	-3	632	-8
Uttarakhand	94	37	10.7	1.7	749	0	369	12
Uttar Pradesh	62	33	21.6	0.6	784	0	254	5
West Bengal	46	-73	23.5	0.5	764	-1	223	-58

See note table A.1.

Table A.8. Kazakhstan, October 2015-January 2016 agroclimatic indicators and biomass (by oblast)

	RAIN		TEMP		RADPAR		BIOMSS	
	Current (mm)	14YA Departure (%)	Current (°C)	14YA Departure (°C)	Current (MJ/m^2)	14YA Departure (%)	Current (gDM/m^2)	5YA Departure (%)
Akmolinskaya	136	54	-5.2	0.8	205	-8	459	4
Karagandinskaya	134	61	-4.3	1.5	244	-12	484	13
Kustanayskaya	150	61	-4.9	0.1	204	-4	476	-3
Pavlodarskaya	99	38	-5.2	0.7	199	-9	484	21
Severo	150	63	-6.4	-0.3	172	-5	429	-4
Vostochno	192	50	-4.3	2.7	273	-11	483	18
Zapadno	166	59	-0.3	0.9	211	-11	663	18

See note table A.1.

Table A.9. Russia, October 2015-January 2016 agroclimatic indicators and biomass (by oblast, kray and republic)

	RAIN		TEMP		RADPAR		BIOMSS	
	Current (mm)	14YA Departure (%)	Current (°C)	14YA Departure (°C)	Current MJ/m^2)	14YA Departure (%)	Current (gDM/m^2)	5YA Departure (%)
Bashkortostan	247	58	-4.5	0.2	149	-11	462	-9
Chelyabinskaya	142	39	-6.0	-0.8	166	-8	425	-10
Gorodovikovsk	-999	-999	-999.0	-999.0	-999	-999	-999	-999
Krasnodarskiy	141	-31	-1.4	0.4	234	-2	512	-1
Kurganskaya	146	43	-6.6	-0.8	157	-4	411	-10
Kirovskaya	214	7	-3.7	0.2	105	-5	485	-7
Kurskaya	165	8	0.7	0.0	194	3	723	-1
Lipetskaya	189	22	0.2	0.1	180	-1	689	-3
Mordoviya	232	35	-1.3	0.3	144	-6	602	-6
Novosibirskaya	173	37	-6.8	0.9	152	-7	423	1
Nizhegorodskaya	187	1	-1.7	0.2	127	-2	586	-6
Orenburgskaya	216	70	-3.2	0.4	184	-10	524	-7
Omskaya	152	35	-7.6	-0.3	149	-2	394	-7
Permskaya	250	38	-5.9	-0.2	106	-10	403	-13
Penzenskaya	246	49	-1.2	0.3	158	-8	609	-6
Rostovskaya	155	-14	3.1	0.1	261	2	736	8
Ryazanskaya	178	5	-0.5	0.3	152	0	654	-5
Stavropolskiy	214	32	5.0	0.0	303	1	803	24
Sverdlovskaya	151	25	-7.4	-1.3	126	-7	363	-18
Samarskaya	269	99	-2.0	0.5	157	-13	577	-6
Saratovskaya	217	70	-0.2	0.6	186	-10	669	4
Tambovskaya	203	22	-0.2	0.3	174	-3	663	-5
Tyumenskaya	140	22	-7.7	-0.8	141	-2	376	-12
Tatarstan	245	52	-2.5	0.3	130	-14	543	-6
Ulyanovskaya	258	79	-1.6	0.5	147	-12	590	-4
Udmurtiya	225	25	-4.1	0.2	109	-12	469	-9
Volgogradskaya	196	46	1.5	0.4	220	-5	768	16
Voronezhskaya	188	25	1.0	0.4	205	0	735	2

See note table A.1.

Table A.10. United States, October 2015-January 2016 agroclimatic indicators and biomass (by state)

	RAIN		TEMP		RADPAR		BIOMSS	
	Current (mm)	14YA Departure (%)	Current (°C)	14YA Departure (°C)	Current MJ/m^2)	14YA Departure (%)	Current (gDM/m^2)	5YA Departure (%)
Arkansas	785	88	12.4	1.6	488	-7	1601	27
California	132	-37	8.9	0.1	531	-3	530	-7
Idaho	253	57	-0.6	0.3	393	-5	661	20
Indiana	360	10	8.2	2.4	407	-5	1245	24

	RAIN		TEMP		RADPAR		BIOMSS	
	Current (mm)	14YA Departure (%)	Current (°C)	14YA Departure (°C)	Current (MJ/m^2)	14YA Departure (%)	Current (gDM/m^2)	5YA Departure (%)
Illinois	372	27	8.0	2.4	417	-5	1217	29
Iowa	292	62	5.0	2.2	402	-7	1005	41
Kansas	201	35	7.7	1.5	493	-6	847	53
Michigan	282	9	5.2	2.6	310	-8	980	22
Minnesota	260	76	1.7	3.0	323	-7	810	51
Missouri	532	86	9.0	1.8	449	-6	1307	37
Montana	176	95	-0.3	0.7	362	-4	672	35
Nebraska	196	75	4.5	1.7	443	-8	881	72
North Dakota	159	83	0.0	2.4	327	-7	706	63
Ohio	284	-3	8.3	2.7	392	-4	1176	17
Oklahoma	432	99	10.6	0.6	530	-5	1182	50
Oregon	290	-3	4.4	0.4	358	-4	864	18
South Dakota	192	93	2.7	1.9	394	-6	838	79
Texas	379	78	14.5	0.5	575	-8	1051	69
Washington	340	10	3.6	0.6	293	-5	807	8
Wisconsin	337	59	3.7	2.8	324	-9	924	31

See note table A.1.

Table A.11. China, October 2015-January 2016 agroclimatic indicators and biomass (by province)

	RAIN		TEMP		RADPAR		BIOMSS	
	Current (mm)	14YA Departure (%)	Current (°C)	14YA Departure (°C)	Current (MJ/m^2)	14YA Departure (%)	Current (gDM/m^2)	5YA Departure (%)
Anhui	281	77	10.8	0.0	490	-15	1035	50
Chongqing	181	10	11.0	0.9	375	-12	767	5
Fujian	386	114	15.2	1.2	496	-24	1091	45
Gansu	325	155	18.5	0.5	575	-19	921	62
Guangdong	104	102	2.5	1.2	552	-4	449	66
Guangxi	368	130	16.6	0.1	486	-23	1146	64
Guizhou	379	140	11.8	0.9	379	-18	1134	62
Hebei	70	53	2.2	0.2	476	-8	374	47
Heilongjiang	105	11	8.2	-0.1	503	-11	539	12
Henan	147	91	-7.3	0.9	369	-2	441	14
Hubei	203	25	10.3	0.1	465	-15	815	12
Hunan	416	103	12.2	-0.1	430	-23	1225	45
Jiangsu	128	51	-4.3	0.5	424	-3	498	9
Jiangxi	248	96	10.7	0.3	500	-12	1013	74
Jilin	510	133	13.8	0.5	474	-24	1457	73
Liaoning	85	-3	0.0	0.5	448	-6	457	-6

	RAIN		TEMP		RADPAR		BIOMSS	
	Current (mm)	14YA Departure (%)	Current (°C)	14YA Departure (°C)	Current MJ/m^2)	14YA Departure (%)	Current (gDM/m^2)	5YA Departure (%)
Inner Mongolia	98	139	-6.0	0.8	429	-2	396	36
Ningxia	116	215	1.6	1.1	555	-3	438	74
Shaanxi	122	26	9.7	0.8	466	-6	494	10
Shandong	119	86	7.3	0.2	494	-9	499	35
Shanxi	153	59	5.2	0.8	476	-10	644	44
Sichuan	102	81	1.6	1.2	516	-6	506	61
Yunnan	232	64	12.5	-0.1	619	-3	910	64
Zhejiang	472	112	13.0	1.0	440	-25	1405	59

See note table A.1.

Annex B. 2015-2016 production estimates

Table B.1. Argentina, 2015-2016 wheat production, by province (thousand tons)

	Wheat	
	2015-2016	Δ%
Buenos Aires	6974	11
Córdoba	715	-34
Entre Rios	1072	24
Santa Fe	1206	-14
Sub total	9967	3
Others	708	-71
Argentina	10675	-11

Δ% indicates percentage difference with previous year.

Table B.2. Australia, 2015-2016 wheat production, by state (thousand tons)

	Wheat	
	2015-2016	Δ%
New South Wales	6774	5
South Australia	4094	-7
Victoria	3381	7
Western Australia	10387	-3
Sub total	24636	0
Other states	642	-25
Australia	25278	-1

Δ% indicates percentage difference with 2014.

Table B.3 Brazil, 2015-2016 wheat production, by state (thousand tons)

	Wheat	
	2015-2016	Δ%
Parana	2227	-12
Rio Grande Do Sul	4054	13
Santa Catarina	290	20
Sub total	6572	3
Others	442	25
Brazil	7013	5

Δ% indicates percentage difference with 2014-2015.

Annex C. Quick reference guide to CropWatch indicators, spatial units, and production estimation methodology

The following sections give a brief overview of CropWatch indicators and spatial units, along with a description of the CropWatch production estimation methodology. For more information about CropWatch methodologies, visit CropWatch online at www.cropwatch.com.cn.

CropWatch indicators

The CropWatch indicators are designed to assess the condition of crops and the environment in which they grow and develop; the indicators—RAIN (for rainfall), TEMP (temperature), and RADPAR (photosynthetically active radiation, PAR)—are not identical to the weather variables, but instead are value-added indicators computed only over crop growing areas (thus for example excluding deserts and rangelands) and spatially weighted according to the agricultural production potential, with marginal areas receiving less weight than productive ones. The indicators are expressed using the usual physical units (e.g., mm for rainfall) and were thoroughly tested for their coherence over space and time. CWSU are the CropWatch Spatial Units, including MRUs, MPZ, and countries (including first-level administrative districts in select large countries). For all indicators, high values indicate "good" or "positive."

INDICATOR			
BIOMSS			
Biomass accumulation potential			
Crop/ Ground and satellite	grams dry matter/m^2, pixel or CWSU	An estimate of biomass that could potentially be accumulated over the reference period given the prevailing rainfall and temperature conditions.	Biomass is presented as maps by pixels, maps showing average pixels values over CropWatch spatial units (CWSU), or tables giving average values for the CWSU. Values are compared to the average value for the last five years (2010-14), with departures expressed in percentage.
CALF			
Cropped arable land and cropped arable land fraction			
Crop/ Satellite	[0,1] number, pixel or CWSU average	The area of cropped arable land as fraction of total (cropped and uncropped) arable land. Whether a pixel is cropped or not is decided based on NDVI twice a month. (For each four-month reporting period, each pixel thus has 8 cropped/ uncropped values).	The value shown in tables is the maximum value of the 8 values available for each pixel; maps show an area as cropped if at least one of the 8 observations is categorized as "cropped." Uncropped means that no crops were detected over the whole reporting period. Values are compared to the average value for the last five years (2010-14), with departures expressed in percentage.
CROPPING INTENSITY			
Cropping intensity Index			
Crop/ Satellite	0, 1, 2, or 3; Number of crops growing over a year for each pixel	Cropping intensity index describes the extent to which arable land is used over a year. It is the ratio of the total crop area of all planting seasons in a year to the total area of arable land.	Cropping intensity is presented as maps by pixels or spatial average pixels values for MPZs, 31 countries, and 7 regions for China. Values are compared to the average of the previous five years, with departures expressed in percentage.

INDICATOR			
NDVI			
Normalized Difference Vegetation Index			
Crop/ Satellite	[0.12-0.90] number, pixel or CWSU average	An estimate of the density of living green biomass.	NDVI is shown as average profiles over time at the national level (cropland only) in crop condition development graphs, compared with previous year and recent five-year average (2010-14), and as spatial patterns compared to the average showing the time profiles, where they occur, and the percentage of pixels concerned by each profile.
RADPAR			
CropWatch indicator for Photosynthetically Active Radiation (PAR), based on pixel based PAR			
Weather/Satellite	W/m^2, CWSU	The spatial average (for a CWSU) of PAR accumulation over agricultural pixels, weighted by the production potential.	RADPAR is shown as the percent departure of the RADPAR value for the reporting period compared to the recent fourteen-year average (2001-14), per CWSU. For the MPZs, regular PAR is shown as typical time profiles over the spatial unit, with a map showing where the profiles occur and the percentage of pixels concerned by each profile.
RAIN			
CropWatch indicator for rainfall, based on pixel-based rainfall			
Weather/Ground and satellite	$Liters/m^2$, CWSU	The spatial average (for a CWSU) of rainfall accumulation over agricultural pixels, weighted by the production potential.	RAIN is shown as the percent departure of the RAIN value for the reporting period, compared to the recent fourteen-year average (2001-14), per CWSU. For the MPZs, regular rainfall is shown as typical time profiles over the spatial unit, with a map showing where the profiles occur and the percentage of pixels concerned by each profile.
TEMP			
CropWatch indicator for air temperature, based on pixel-based temperature			
Weather/Ground	°C, CWSU	The spatial average (for a CWSU) of the temperature time average over agricultural pixels, weighted by the production potential.	TEMP is shown as the departure of the average TEMP value (in degrees Centigrade) over the reporting period compared with the average of the recent 14 years (2001-14), per CWSU. For the MPZs, regular temperature is illustrated as typical time profiles over the spatial unit, with a map showing where the profiles occur and the percentage of pixels concerned by each profile.
VCIx			
Maximum vegetation condition index			
Crop/ Satellite	Number, pixel to CWSU	Vegetation condition of the current season compared with historical data. Values usually are [0,1], where 0 is "NDVI as bad as the worst recent year" and 1 is "NDVI as good as the best recent year." Values can exceed the range if the current year is the best or the worst.	VCIx is based on NDVI and two VCI values are computed every month. VCIx is the highest VCI value recorded for every pixel over the reporting period. A low value of VCIx means that no VCI value was high over the reporting period. A high value means that at least one VCI value was high. VCI is shown as pixel-based maps and as average value by CWSU.
VHI			
Vegetation health index			
Crop/ Satellite	Number, pixel to CWSU	The average of VCI and the temperature condition index (TCI), with TCI defined like VCI but for	Low VHI values indicate unusually poor crop condition, but high values, when due to low temperature, may be difficult to interpret. VHI is

INDICATOR			
		temperature. VHI is based on the assumption that "high temperature is bad" (due to moisture stress), but ignores the fact that low temperature may be equally "bad" (crops develop and grow slowly, or even suffer from frost).	shown as typical time profiles over Major Production Zones (MPZ), where they occur, and the percentage of pixels concerned by each profile.
VHIn			
Minimum Vegetation health index			
Crop/ Satellite	Number, pixel to CWSU	VHIn is the lowest VHI value for every pixel over the reporting period. Values usually are [0, 100]. Normally, values lower than 35 indicate poor crop condition.	Low VHIn values indicate the occurrence of water stress in the monitoring period, often combined with lower than average rainfall. The spatial/time resolution of CropWatch VHIn is 16km/week for MPZs and 1km/dekad for China.

Note: Type is either "Weather" or "Crop"; source specifies if the indicator is obtained from ground data, satellite readings, or a combination; units: in the case of ratios, no unit is used; scale is either pixels or large scale CropWatch spatial units (CWSU). Many indicators are computed for pixels but represented in the CropWatch bulletin at the CWSU scale.

CropWatch spatial units (CWSU)

CropWatch analyses are applied to four kinds of CropWatch spatial units (CWSU): Countries, China, Major Production Zones (MPZ), and global crop Monitoring and Reporting Units (MRU). The tables below summarize the key aspects of each spatial unit and show their relation to each other. For more details about these spatial units and their boundaries, see the CropWatch bulletin online resources.

SPATIAL LUNITS	
CHINA	
Overview	*Description*
Seven monitoring regions	The seven regions in China are agro-economic/agro-ecological regions that together cover the bulk of national maize, rice, wheat, and soybean production. Provinces that are entirely or partially included in one of the monitoring regions are indicated in color on the map below.

Countries (and first-level administrative districts, e.g., states and provinces)	
Overview	*Description*
"Thirty plus one" countries to represent main producers/exporters and other key countries.	CropWatch monitored countries together represent more than 80% of the production of maize, rice, wheat and soybean, as well as 80% of exports. Some countries were included in the list based on criteria of proximity to China (Uzbekistan, Cambodia), regional importance, or global geopolitical relevance (e.g., four of five most populous countries in Africa). The total number of countries monitored is "thirty plus one," referring to thirty countries and China itself. For the nine largest countries—, United States, Brazil, Argentina, Russia, Kazakhstan, India, China, and Australia, maps and analyses may also present results for the first-level administrative subdivision. The CropWatch agroclimatic indicators are computed for all countries and included in the analyses when abnormal conditions occur. Background information about the countries' agriculture and trade is available on the CropWatch Website, www.cropwatch.com.cn.

Major Production Zones (MPZ)	
Overview	*Description*
Seven globally important areas of agricultural production	The six MPZs include West Africa, South America, North America, South and Southeast Asia, Western Europe and Central Europe to Western Russia. The MPZs are not necessarily the main production zones for the four crops (maize, rice, soybean, wheat) currently monitored by CropWatch, but they are globally or regionally important areas of agricultural production. The seven zones were identified based mainly on production statistics and distribution of the combined cultivation area of maize, rice, wheat and soybean.

Global Monitoring and Reporting Unit (MRU)	
Overview	*Description*
65 agro-ecological/agro-economic units across the world	MRUs are reasonably homogeneous agro-ecological/agro-economic units spanning the globe, selected to capture major variations in worldwide farming and crops patterns while at the same time providing a manageable (limited) number of spatial units to be used as the basis for the analysis of environmental factors affecting crops. Unit numbers and names are shown in the figure below. A limited number of units (e.g., MRU-63 to 65) are not relevant for the crops currently monitored by CropWatch but are included to allow for more complete coverage of global production. Additional information about the MRUs is provided online under www.cropwatch.com.cn .

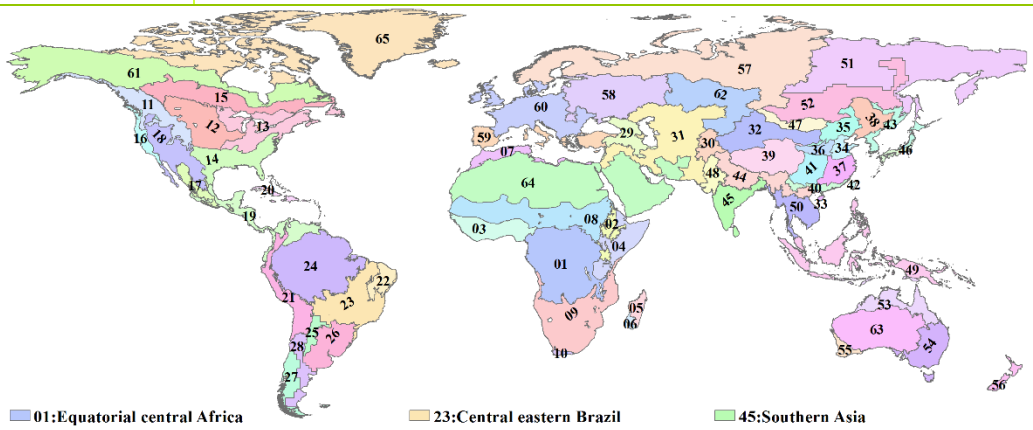

01:Equatorial central Africa
02:East African highlands
03:Gulf of Guinea
04:Horn of Africa
05:Madagascar (main)
06:Southwest Madagascar
07:North Africa Mediterranean
08:Sahel
09:Southern Africa
10:Western Cape (South Africa)
11:British Columbia to Colorado
12:Northern Great Plains
13:Corn Belt
14:Cotton Belt to Mexican Noreste
15:Sub-boreal America
16:West Coast (North America)
17:Sierra Madre
18:Southwest U.S. and north Mexican highlands
19:Northern South and Central America
20:Caribbean
21:Central-northern Andes
22:Nordeste (Brazil)
23:Central eastern Brazil
24:Amazon
25:Central-north Argentina
26:Pampas
27:Western Patagonia
28:Semi-arid Southern Cone
29:Caucasus
30:Pamir area
31:Western Asia
32:Gansu-Xinjiang (China)
33:Hainan (China)
34:Huanghuaihai (China)
35:Inner Mongolia (China)
36:Loess region (China)
37:Lower Yangtze (China)
38:Northeast China
39:Qinghai-Tibet (China)
40:Southern China
41:Southwest China
42:Taiwan (China)
43:East Asia
44:Southern Himalayas
45:Southern Asia
46:Southern Japan and Korea
47:Southern Mongolia
48:Punjab to Gujarat
49:Maritime Southeast Asia
50:Mainland Southeast Asia
51:Eastern Siberia
52:Eastern Central Asia
53:Northern Australia
54:Queensland to Victoria
55:Nullarbor to Darling
56:New Zealand
57:Boreal Eurasia
58:Ukraine to Ural mountains
59:Mediterranean Europe and Turkey
60:W. Europe (non Mediterranean)
61:Boreal America
62:Ural to Altai mountains
63:Australian desert
64:Sahara to Afghan deserts
65:Sub-arctic America

Production estimation methodology

The main concept of the CropWatch methodology for estimating production is the calculation of current year production based on information about last year's production and the variations in crop yield and cultivated area compared with the previous year. The equation for production estimation is as follows:

$$Production_i = Production_{i-1} * (1 + \Delta Yield_i) * (1 + \Delta Area_i)$$

where i is the current year, $\Delta Yield_i$ and $\Delta Area_i$ are the variations in crop yield and cultivated area compared with the previous year; the values of $\Delta Yield_i$ and $\Delta Area_i$ can be above or below zero.

For the 31 countries monitored by CropWatch, yield variation for each crop is calibrated against NDVI time series, using the following equation:

$$\Delta Yield_i = f(NDVI_i, NDVI_{i-1})$$

where $NDVI_i$ and $NDVI_{i-1}$ are taken from the time series of the spatial average of NDVI over the crop specific mask for the current year and the previous year. For NDVI values that correspond to periods after the current monitoring period, average NDVI values of the previous five years are used as an average expectation. $\Delta Yield_i$ is calculated by regression against average or peak NDVI (whichever yields the best regression), considering the crop phenology of each crop for each individual country.

A different method is used for areas. For China, CropWatch combines remote-sensing based estimates of the crop planting proportion (cropped area to arable land) with a crop type proportion (specific type area to total cropped area). The planting proportion is estimated based on an unsupervised classification of high resolution satellite images from HJ-1 CCD and GF-1 images. The crop-type proportion for China is obtained by the GVG instrument from field transects. The area of a specific crop is computed by multiplying farmland area, planting proportion, and crop-type proportion of the crop.

To estimate crop area for wheat, soybean, maize, and rice outside China, CropWatch relies on the regression of crop area against cropped arable land fraction of each individual country (paying due attention to phenology):

$$Area_i = a + b * CALF_i$$

where a and b are the coefficients generated by linear regression with area from FAOSTAT or national sources and CALF the Cropped Arable Land Fraction from CropWatch estimates. $\Delta Area_i$ can then be calculated from the area of current and the previous years.

The production for "other countries" (outside the 31 CropWatch monitored countries) was estimated as the linear trend projection for 2014 of aggregated FAOSTAT data (using aggregated world production minus the sum of production by the 31 CropWatch monitored countries).

Data notes and bibliography

ACAPS, 2016.http://acaps.org/img/documents/a-acaps-crisis-overview-2015-trends-and-risks-2016.pdf

http://www.acaps.org/img/documents/1-160105-start-acaps-ethiopia-drought.pdf

BBC, 2015.http://www.bbc.com/news/world-latin-america-35179103

Collins Thesaurus of the English Language, 2002.http://www.collinsdictionary.com/dictionary/english-thesaurus/livelihood

Cropwatch, 2015.http://www.cropwatch.com.cn/htm/en/files/20151123213525951.pdf

Davies, R.A.G., Midgley, S.J.E. and Chesterman, S., 2010. Climate Risk and Vulnerability Mapping for Southern Africa: Status Quo (2008) and Future (2050). OneWorld Sustainable Investments (Pty) Ltd. Cape Town, South Africa.pp67.

Fang, J.X., 2011. New perspective of price – the law of the spiraling price, China Price, 9: 17-18. (方景新，2011. 价格规律的新发现——价格的螺旋变化规律，中国物价，9：17-18.)

FAO. 1996. Rome Declaration on World Food Security and World Food Summit Plan of Action. World Food Summit 13-17 November 1996. Rome.

FAO, 2016. Farming systems interactive maps. http://www.fao.org/farmingsystems/maps_SSA_en.htm

http://www.fao.org/elearning/course/FI/EN/pdf/trainerresources/learnernotes0764.pdf

Hogan, C. 2012. Zambezi River. http://www.eoearth.org/view/article/174239

IFAD, 2010.Rural Poverty Report – 2011.http://www.ifad.org/rpr2011/report/e/rpr2011.pdf

Munich RE, 2016.http://www.munichre.com/en/media-relations/publications/press-releases/2016/2016-01-04-press-release/index.html

NOAA, 2016.http://www.cpc.ncep.noaa.gov/products/analysis_

NY Times, 2015.http://www.nytimes.com/2015/12/27/world/africa/drought-deepens-south-africas-malaise.html

http://www.nytimes.com/2015/12/31/science/climate-chaos-across-the-map.html

Peace Parks Foundation, 2011.

https://maps.ppf.org.za/sadc/?extent=28.4440,-16.3201,30.7511,-15.0562

SADC, 2016. Water portal, http://www.sadc.int/information-services/water-information-services-portals/

SADC/SARDC and others, 2012.Zambezi River Basin Atlas of the Changing Environment. SADC, SARDC, ZAMCOM, GRID-Arendal, UNEP. Gaborone, Harare and Arendal

UNESCO, 2016. Tentative lists http://whc.unesco.org/en/tentativelists/5427/

UNISDR, 2015.http://www.unisdr.org/archive/46793

http://www.unisdr.org/2015/docs/climatechange/COP21_WeatherDisastersReport_2015_FINAL.pdf

ZamSoc, 2016.Zambezi Society – Conserving Wildlife and Wilderness in the Zambezi Valley.http://www.zamsoc.org/?page_id=636

World Bank, 2016. Data. http://data.worldbank.org/indicator/NV.AGR.TOTL.ZS/countries?page=2

Acknowledgments

This bulletin is produced by the CropWatch research team at the Institute of Remote Sensing and Digital Earth (RADI), at the Chinese Academy of Sciences in Beijing, China. The team gratefully acknowledges the active support of a range of organizations and individuals, both in China and elsewhere.

Financial and programmatic support is provided by the Ministry of Science and Technology of the People's Republic of China, National Natural Science Foundation of China, State Administration of Grain, and the Chinese Academy of Sciences. We specifically would like to acknowledge the financial support through the National High Technology Research and Development Program of China (863 program), Grant No. 2012AA12A307; the International Science & Technology Cooperation Program of China, Grant No. 2011DFG72280; National Natural Scientific Foundations of China, Grant No. 91025007; China Grains Administration Special Fund for Public Interest, Grant No. 201313009-02, 201413003-7; CAS global food production monitoring and customization service, Grant No. KFJ-EW-STS-017; Visiting Professorships for Senior International Scientists, Grant No. 2013T1Z0016; National Natural Science Foundation, Grant No: 41561144013 and RADI funding in the form of the "Global Spatial Information System for Environment and Resources" project, Grant No: Y6SG0300CX.

The following contributions by national organizations and individuals are greatly appreciated: China Center for Resources Satellite Data and Application for providing the HJ-1 CCD data; China Meteorological Satellite Center for providing FY-2/3 data; China Meteorological Data Sharing Service System for providing the agro-meteorological data; and Chia Tai Group (China) for providing GVG (GPS, Video, and GIS) field sampling data.

The following contributions by international organizations and individuals are also recognized: François Kayitakire at FOODSEC/JRC for making available and allowing use of their crop masks; Ferdinando Urbano also at FOODSEC/JRC for his help with data; Herman Eerens, Dominique Haesen, and Antoine Royer at VITO, for providing the JRC/MARS SPIRITS software, Spot Vegetation imagery and growing season masks, together with generous advice; Patrizia Monteduro and Pasquale Steduto for providing technical details on GeoNetwork products; and IIASA and Steffen Fritz for their land use map.

Online resources

This bulletin is only part of the CropWatch resources available. Visit **www.cropwatch.com.cn**for access to additional resources, including the methods behind CropWatch, country profiles, and other CropWatch publications. For additional information or to access specific data or high-resolution graphs, simply contact the CropWatch team at cropwatch@radi.ac.cn.

Online Resources posted on www.cropwatch.com.cn:

- ✓ **Definition of spatial units**
  Adescription of the four spatial levels of analysis: Monitoring and Reporting Units (MRU), Major Production Zones (MPZ), selected countries, and the use of sub-national administrative areas.
- ✓ **Methodology**
  Overview of CropWatch data sources and methods.
- ✓ **Time series of indicators**
  Background data on agroclimatic indicators presented in a series of tables.
- ✓ **Country profiles**
  Short profiles for each of the 30 countries and China highlighting key facts of interest to agriculture.
- ✓ **Country long termtrends**
  Quick overview of average crop area, yield, and production values for maize, rice, soybean, and wheat for recent years, along with long-term (2001-12) trends (basedon FAOSTAT data).

CropWatch bulletins introduce the use of several new and experimental indicators. We would be very interested in receiving feedback about their performance in other countries. With feedback on the contents of this report and the applicability of the new indicators to global areas, please contact:

Professor Bingfang Wu
Institute of Remote Sensing and Digital Earth
Chinese Academy of Sciences, Beijing, China
E-mail: cropwatch@radi.ac.cn, wubf@radi.ac.cn